Tracking Neurophysiological Markers of Auditory Change Detection and Consciousness for Clinical Assessment in Coma

Tracking Neurophysiological Markers of Auditory Change Detection and Consciousness for Clinical Assessment in Coma

By
Adianes Herrera Diaz , M.Sc., B.Sc.

A Thesis Submitted to the School of Graduate Studies in Partial Fulfillment of the Requirements for the Degree of Doctor of Philosophy

McMaster University
Doctor of Philosophy (2022)
Hamilton, Ontario (Neuroscience Graduate Program)

TITLE: Tracking Neurophysiological Markers of Auditory Change Detection and Consciousness for Clinical Assessment in Coma
AUTHOR: Adianes Herrera Diaz
M.Sc. (Cognitive and Systems Neuroscience), Cuban Neuroscience Center, Cuba
B.Sc. (Psychology), University of Havana, Cuba
SUPERVISOR: Dr. John F. Connolly
NUMBER OF PAGES: xvi, 150

Declaration of Academic Achievements

The present dissertation is a "sandwich" thesis as defined by the School of Graduate Studies, McMaster University. This dissertation was conducted within the framework of an ongoing protocol study, in which I have made a significant contribution. I am also the primary author of three main articles contained in this document that are either submitted or in preparation for submission to peer-reviewed journals.

The following outlines the study protocol, each of the three main studies forming chapters 2, 3, and 4 and the role of the co-authors.

The original study protocol was published in *BMJ Open* as: "Connolly, J.F., Reilly, J.P., Fox-Robichaud, A., Britz, P., Blain-Moraes, S., Sonnadara, R., Hamielec, C., **Herrera-Diaz, A.** and Boshra, R., 2019. Development of a point of care system for automated coma prognosis: a prospective cohort study protocol". *BMJ open*, 9(7), e029621".

JFC, JPR and AF-R conceived of the study. JFC, JPR, **AH-D** and RB designed the study protocol. RB and **AH-D** wrote the first draft of the paper. All authors revised the manuscript for relevant scientific content. JPR and RB specifically revised the machine learning design and validation sections of the paper. PB, CH, SB-M and RS provided an advisory role on various aspects of the paper. All authors approved the final version of the manuscript.

Chapter 2 is ready to be submitted to *Frontiers in Neurology* as: "**Herrera-Diaz, A.**, Boshra, R., Tavakoli, P., Lin, CY., Pajankar, N., Baheri, E., Kolesar, R., Fox-Robichaud, A., Hamielec,C., Reilly, J.P and Connolly, J.F. Tracking auditory MMN responses during full conscious state and coma".

JFC, RB, JPR, AF, CH and **AH-D** contributed to the conception of the study. CYL and PT contributed to the organization of the study and recruitment of controls. **AHD** analyzed the data and wrote the first draft of the manuscript. **AH-D**, RB, NP and EB conducted the experiments. All authors reviewed and edited the manuscript.

Chapter 3 was published as a conference paper in *Brain Injury*: "**Herrera-Diaz, A.**, Kolesar, R., Boshra, R., Reilly, J., Tavakoli, P., Pajankar, N., Lin, C.Y., Bagheri, E., Morrison,

H. and Connolly, J.F, 2022. Multivariate Decoding of Auditory Event-Related Potentials to Track Coma Progression. In *BRAIN INJURY* (Vol. 36, pp. 114-114)".

AH-D, RB, JPR and **AH-D** conceived the study. CYL, PT and HM contributed to the organization of the study and recruitment of controls. **AH-D** conceived the multivariate decoding design, analyzed the data and wrote the first draft of the manuscript. **AH-D**, RB, NP and EB collected the ERP data. All authors reviewed and edited the manuscript.

Chapter 4 is a manuscript in preparation to be submitted to *Clinical Neurophysiology* as: "**Herrera-Diaz, A.**, Boshra, R., Kolesar, R., Reilly, J.P and Connolly, J.F. "Functional connectivity in the dying brain: a case study".

Additional Achievements

In addition to what is presented in the chapters, the author is a primary contributor on other five studies closely associated with the topic of this thesis. The first three studies were published as conference papers and the others are in preparation for submission to peer-reviewed journals.

- Kolesar, R.E., **Herrera-Diaz, A.**, Boshra, R. and Connolly, J.F., 2021. General Anesthesia Suppresses Mismatch Negativity During Surgery. In *ANESTHESIA AND ANALGESIA*. (Vol. 132, No. 5 S SUPPL, pp. 537-539).

- Tavakoli, P., **Herrera-Diaz, A.**, Kolesar, R., Reilly, J., Pajankar, N., Boshra, R., Fox-Robichaud, A., Hamielec, C. and Connolly, J., 2022, January. Using Event-related Potentials to Track Fluctuations in Responsiveness in Disorders of Consciousness: A Case Study of Unresponsive Wakefulness Syndrome. In *BRAIN INJURY* (Vol. 36, pp. 118-119).

- Bagheri, E., Reilly, J., Tavakoli, P., **Herrera-Diaz, A.**, Kolesar, R. and Connolly, J., 2022, January. An Improved Machine Learning Based Biomarker for Characterizing Disorders of Consciousness. In *BRAIN INJURY* (Vol. 36, pp. 108-109).

- Bagheri, E., Tavakoli, P., **Herrera-Diaz, A.**, Boshra, R., Kolesar, R., Fox-Robichaud, A., Connolly, J.F and Reilly, J.P. A deep learning structure for characterizing coma. (In preparation for submission to *Journal of Neural Engineering*)

- Tavakoli, P., **Herrera-Diaz, A.**, Boshra, R., A.,Bagheri, E., Reilly, J.P. and Connolly, J.F. Looking for a sensitive and automatic technology for assessing cognitive function in coma. (In preparation for submission to *Lancet Neurology*)

Abstract

The present dissertation expands the utility of EEG-based tools for the clinical assessment of coma. First, auditory mismatch negativity (MMN) responses were recorded in healthy controls and in a case series of comatose patients (over 12 and 24 hours, respectively). The results (Chapter 2) showed that the MMN elicited by deviant sounds, particularly for duration stimuli, is extremely robust in full conscious state over the course of several hours at both the group and single-subject levels. However, preliminary results in three comatose patients provide further evidence that the MMN is present but fluctuates in detectability in coma. These findings highlight that repeated assessments and proper stimuli selection are essential when assessing this ERP component as neurophysiological predictor of coma emergence. Then, a follow-up study (Chapter 3) demonstrated the feasibility of multivariate pattern analysis in our sample as an automatic tool able to discriminate accurately between single-trials responses at single-subject level, providing further evidence of changes in auditory discrimination over time in coma patients. Additionally, a phase-based measure of functional connectivity in response to auditory stimuli and resting state was computed for the first time at both the sensor (electrode) and source levels in a dying comatose patient. This report provided a ML procedure able to discriminate (with perfomance accuracies above 90%) single-trial functional connectivity elicited by deviant sounds between a comatose patient and healthy controls; and showed at least a period of increased synchronized activity during resting state before the end of life in the coma patient. Taken together, our findings showed that the EEG/ERP responses here studied, are highly transient in acute coma over hours and days, suggesting that repeated assessments are crucial for their objective detection and the methods of analyses should be sensitive enough to capture such changes. Overall, this work illustrates the utility of EEG along with machine learning to individualized neurophysiological assessment of comatose patients.

Acknowledgements

I would like to thank my supervisor Dr. John Connolly for his endless support, patience and encouragement during these years. Being part of your lab made my life turn positively around 180 degrees. Thanks to show confidence and faith in my abilities at times when I lacked both.

Thanks to my supervisory committee members (Jim Reilly and Ian Bruce), who have been key contributors to this research and whose guidance on technical aspects of this thesis has been extremely valuable.

I extend my gratitude to Dr. Alison Fox-Robichaud and Dr. Cindy Hamielec, who very generously sponsored my studies in the Hamilton General Hospital and introduced me to a supportive team of excellent nurses and intensivists. I must also give thanks to the patients and families that I met in intensive care. All this work would have been impossible without you.

Many thanks to my lab mates, Dr. Rober Boshra and Dr. Richard Kolesar. I cannot thank you enough for all you help and contribution over these years. Thanks to my dear Chia-Yu. What you have done for me as a colleague and friend is priceless.

I would also like to thank my colleagues and members of the LMB Lab and ARiEAL research centre, past and present, who assisted me with data collection and I had the pleasure to work during this and other related EEG projects: Netri, Gaisha, Nathalee, Kiersten, Hope, Paniz, Melda, Kyle, Fareeha, Gwenyth, Adeba, and the list goes on.

My deepest sense of gratitude goes to my family. I include here, of course, my Cuban-Argentinian-Canadian family (Ginet, Gloria, Servilio, Olivia, Seguí, Giselle, Sergio, Ale, Sofia and Stefan). You made me feel home and are truly the best gift I have ever received from Canada. To my brother and my parents, who are my backbone and whose unconditional love and support kept me afloat and gave me the strength to move forward. Thanks to my aunt, cousins and in-laws for always believing in me. Thanks to my friend Lisbet for her words of encouragement and the virtual coffee breaks that would lifted up my day.

Last, but not least, to my husband, the love of my life and best friend. Your infinite love and patience got me through the most challenging times. Thanks for your unwavering faith in me.

Contents

List of Figures

List of Tables

List of Abbreviations

ABI	**A**cquired **B**rain **I**njury
ANOVA	**A**nalysis **o**f **V**ariance
AUC	**A**rea **U**nder the **C**urve
CMD	**C**ognitive **M**otor **D**issociation
CT	**C**omputed **T**omography
CRS-R	**C**oma **R**ecovery **S**cale -**R**evised
DOC	**D**isorder **o**f **C**onsciousness
EEG	**E**lectroencephalography
ERP	**E**vent **R**elated **P**otential
FC	**F**unctional **C**onnectivity
FOUR	**F**ull **O**utline **o**f **U**nresponsiveness
GCS	**G**lasgow **C**oma **S**cale
fMRI	**F**unctional **M**agnetic **R**esonance **I**maging
ICA	**I**ndependent **C**omponent **A**nalysis
ICU	**I**ntensive **C**are **U**nit
MCS	**M**inimally **C**onscious **S**tate
ML	**M**achine **L**earning
MMN	**M**is**M**atch **N**egativity
MVPA	**M**ultivariate **P**attern **A**nalysis
RS	**R**esting **S**tate
UWS	**U**nresponsive **W**akefulness **S**yndrome
SVM	**S**upport **V**ector **M**achine

Chapter 1

Introduction and Background

Acquired brain injury (ABI) is a serious public health concern and one of the leading causes of death and disability worldwide. This term includes a variety of acute brain lesions of traumatic (i.e., caused by an external force or trauma) and non-traumatic origin (anoxia, stroke, tumors, infections, toxic-metabolic encephalopathy and so forth). According to the Centers for Disease Control and Prevention (CDC), about 150 Americans die from traumatic brain injuries each day, and more than five million children and adults are currently living with long-term disabilities as result of an ABI (Peterson et al., 2019).

A subset of those who survive, are usually encountered in emergency departments and intensive care units (ICUs), remaining either in coma state or transitioning to other disorders of consciousness (DOC), such as minimally conscious state (MCS) or unresponsive wakefulness syndrome (UWS, formerly known as vegetative state). In addition to represent a huge burden for patients and families, the economical cost of long-term clinical management of DOC patients is disproportionately large. The global annual cost of traumatic brain injury is estimated at US $400 billion (Maas et al., 2017).

Despite comatose patients remain unresponsive to their environment, in a persistent sleep-like state of immobility from which they cannot be aroused (Koch et al., 2016), their clinical assessment mostly relies on bedside observations of behavioral signs of consciousness, such as verbal, motor responses and command following. The inability of comatose and DOC patients in general to show unequivocally such behavioral signs, has led to alarming rates of misdiagnosis and thus potentially more serious consequences,

including inefficient allocation of rehabilitation resources and removing individuals with potential for recovery from life support. This explains the important role that current neurophysiological techniques, in particular the electroencephalogram (EEG) and the event-related potentials (ERPs), play in accurately assessing brain function in comatose patients and predicting their outcomes.

The present dissertation constitutes an investigation of coma as the most severe and acute disruption within the spectrum of DOC, building on a substantial body of research that demonstrates the utility of EEG/ERP techniques for diagnosis and prognosis of coma. The following sections from this introductory chapter, will briefly describe the state of the science in coma, including definition, clinical evaluation and a set of diagnostic tools to detect several EEG/ERP markers, known as reliable predictors of coma emergence.

1.1 Defining coma state

According to a traditional but still useful definition, coma is considered an acute and temporary state characterized by the lack of both "wakefulness" (i.e., arousal or vigilance) and "awareness" (i.e., subjective experiences of self and the environment) (Young, 2009). These are multifaceted dimensions of consciousness that have been widely accepted to distinguish coma from other DOC patients, who are awake, but their subjective awareness is supposed to be absent (UWS) or severely disturbed (MCS) (Kotchoubey, 2017).

Clinicians have outlined the features of a comatose patient, including loss of spontaneous or stimulus-induced arousal, absence of sleep-wake cycles on EEG, there is no verbal output, purposeful motor activity (e.g., no localization or reflexive movements) or following commands (Giacino et al., 2014; Wijdicks, 2020). Since the pioneering definition of Plum and Posner, it is commonly accepted in the literature that coma is an eyes-closed state of unresponsiveness (Johnson and Kaplan, 2019). The return of spontaneous eye opening is believed to indicate recovery of consciousness or progression to UWS. However, a recent report showed that some comatose patients can exhibit prolonged eyes-opening and still being in coma (Kondziella and Frontera, 2021). Unlike

UWS, these patients do not regain sleep wake cycles and tend to lose progressively their brainstem reflexes. These recent observations reveal that the classical definition of coma is likely to be updated and modified in the future.

In 2019, the Neurocritical Care Society (NCS) launched the Curing Coma Campaign, bringing together DOC experts from all over the world to identify the current challenges and gaps in definition, diagnosis and management of DOC patients. As part of this campaign, an anonymous, worldwide survey was completed by a total of 258 health care professionals (from 41 countries) caring for patients with coma and DOC (Helbok et al., 2022). Initially, respondents were asked to select cardinal features from a predefined list of 8 items that must be present to define coma. The features were: absence of wakefulness, Glasgow Coma Scale (GCS) score ≤ 8, failure to respond purposefully to visual, verbal or tactile stimuli based on clinical exam, inability to follow commands (excluding aphasic patients), no eye-opening, no visual pursuit of objects, fixation or saccade to stimuli, no evidence of cognitive motor dissociation (i.e., the covert ability to follow commands) based on exam, neurophysiological studies or functional imaging and no intelligible speech or recognizable gesture. Surprisingly, only 15% of respondents selected all these 8 features of coma, revealing the substantial discrepancies in opinions that exist nowadays regarding the clinical definition of coma. Considering some features separately, the eye-opening component was suggested as misleading in coma, since 73% of survey respondents acknowledged treating at least one patient with eye open coma per month. Additionally, while 64% of respondents felt that a GCS ≤ 8 may be necessary for diagnosis, it is possible to have a score less than 8 in patients who are able to localize pain or follow verbal commands. Although a consensual definition of coma was ultimately proposed by an expert panel, the overall level of agreement was 64%. As stated by the authors, these results highlight the need for more education even in academic centers with experienced specialists in the care of comatose patients.

Coma must also be distinguished from brain death, which in addition to the absence of wakefulness and awareness (coma state) encompasses the complete loss of brainstem functions, including respiratory drive (Young et al., 2021). The current tests to confirm brain death are mainly used to document absent intracranial blood flow (e.g, transcranial doppler, CT-angriography, positron emission tomography, etc) or lack of electrical brain activity (e.g., evoked potentials) (Kondziella, 2020).

1.2 Clinical evaluation of coma and other DOC

While clinical examinations are extremely valuable to assess consciousness and determine coma prognosis, they are poorly standardized in critical care and highly reliant on "good" judgments of clinicians (Claassen, 2020). The most used clinical scales for evaluating comatose patients are the GCS and the Full Outline of UnResponsiveness (FOUR) score, with this latter including the assessment of brainstem reflexes and respiratory patters in comparison to the former, and showing potential advantages for the prediction of in-hospital mortality and poor functional outcome (Foo et al., 2019). In addition, the Coma Recovery Scale-Revised (CRS-R)(Giacino et al., 2004) allows the classification of patients emerging from coma into other DOC different states, including UWS, MCS with/without inconsistent command following (MCS-/MCS+), and those who emerge from MCS (EMCS) who usually evidence functional object use and/or functional communication. However, the CRS-R is not widely used in clinical settings. In the recent Curing Coma Campaing survey, only 12% of health care professionals reported using it in the accute setting (Helbok et al., 2022).

As alluded above, the downside of all these scales is ironically their reliance on behavioral responses, which may be essentially biased when it comes to unresponsive patients (Harrison and Connolly, 2013). About 37-40% of clinical assessments of levels of consciousness are inaccurate, that is, a high number of patients with demonstrable evidence of consciousness are diagnosed as post-comatose patients with UWS (Schnakers et al., 2009; Wade, 2018; Schnakers, 2020). As a result, many medical decisions are made on the basis of a high degree of uncertainty or incorrect prognosis, yielding to inappropriate medical decisions (e.g., inadequate pain treatment) and frequent premature withdrawal of life supporting interventions (Giacino et al., 2014). This latter was demonstrated by a Canadian study, which reported that 70% of deaths in six level-one trauma centres were associated to withdrawal of life-sustaining therapies, with half occurring within the first three days of care (Turgeon et al., 2011).

Complementary to clinical evaluation, funtional neuroimaging and EEG techniques have allowed to detect conscious awareness even when rigorous behavioral assessment have suggested absent or low-level responsiveness. A recent meta-analysis suggested that about 15% of patients who were classified as being in chronic UWS were able

to respond to commands (Kondziella et al., 2016), by modifying their brain activity during task-based fMRI or EEG. This clinical syndrome of cover cognition, coined as cognitive motor dissociation (CMD) (Schiff, 2015), is characterized by behavioral unresponsiveness (as seen in patients with coma, UWS or MCS-), along with covert consciousness or volitional brain activity (Luppi et al., 2021). One of the largest study conducted in ICU with 104 DOC patients from diverse traumatic and non-traumatic etiologies (Claassen et al., 2019) revealed similar proportion of CMD detection (15%) reported by the above-mentioned meta-analysis (Kondziella et al., 2016), whose patients were in sub-acute or chronic state. Moreover, Claassen and colleagues, using non-invasive EEG and machine learning algorithms, also demonstrated that the identified CMD patients in ICU had a higher likelihood of functional recovery at 1 year post-injury.

These studies demonstrate that functional brain diagnostic tools should not longer be considered as complimentary, but essential in the clinical evaluation and diagnosis of coma patients. The fact that "absence of CMD", which is typically diagnosed with either fMRI or EEG techniques, was proposed by a global panel of experts as part of an updated definition of coma (Helbok et al., 2022), demonstrates that the access to these technologies in clinical settings is crucial.

1.3 Event-related potentials

For comatose and DOC patients, EEG turns to be the most suitable functional technique among various neuroimaging techniques, since it is less expensive and can be easily set up along the bedside of the patients. Most of the EEG studies related to the assessment of consciousness are based either on resting state and sensory stimulation tasks, which have a huge potential in predicting the recovery of coma patients. EEG at resting state does not require the subject to perform any specific task, providing valuable information about the spontaneous brain activity of patients; while EEG during sensory stimulation entails to evaluate the electrical brain responses elicited by external stimuli or events from different modalities (auditory, visual, olfactory, tactile). ERPs are the most typical and studied time-locked EEG responses to these stimuli.

In the clinical setting, short latency evoked potentials, such as somatosensory evoked responses usually occurring in the 30 ms range, and brainstem auditory potentials (BAEPs) typically observed within 10 ms after stimulus onset, have been useful in confirming the integrity of ascending sensory pathways, showing high prognostic value of poor outcome in comatose patients (Logi et al., 2003)}. Longer-latency ERP responses, are better suited to evaluate cognitive function and conscious awareness in unresponsive patients, since they are mainly associated with higher-order processing and positive coma outcome. In coma research, the most extensively studied ERP components are mismatch negativity (MMN), P300 and N400.

The mismatch negativity (MMN), originally described by Näätänen in 1978, is considered an automatic deviance-specific response linked to a predictive coding process (Garrido et al., 2009). In the auditory domain, it is elicited after the presentation of oddball paradigms, in which a deviant stimulus interrupts a constant sequence of sounds. The MMN is a frontocentral negative response peaking at around 100-250 ms after stimulus onset, and is a extreme popular tool for investigating a wide range of clinical populations. A large body of work have shown that the MMN is one of the most reliable predictors of emergence from coma, probably surpassing other current ERP components (Fischer et al., 1999; Daltrozzo et al., 2007; Morlet and Fischer, 2014). Furthermore, the fact that MMN can be elicited in passive conditions, regardless of whether the subjects are paying attention to the sequence of sounds, makes it ideal for the assessment of comatose patients and other DOC, whose cognitive function are otherwise difficult to access. Therefore, its inclusion in clinical assessments is beneficial, as indicates the patient's ability to process regularities and discriminate changes in the auditory environment.

The P300 is a later positive component (typically >250ms) that can also be elicited by using variants of oddball paradigms, and has been related with several cognitive functions involved in orientation of attention, novelty detection, memory, decision making and so on (Polich, 2007; Duncan et al., 2009). The P300 is considered to include two overlapping subcomponents: P3a and P3b. The P3a has a fronto-central distribution and emerges at about 200-300 ms by novel unpredictable stimuli (e.g., deviant tones, environmental sounds, subject's own name), and is considered to index the reorienting of automatic attention to the deviant or novel stimuli, having been triggered by the

MMN generation (Chennu and Bekinschtein, 2012; Näätänen et al., 2019). In contrast, the later and centro-posterior P3b (peaking after 300 ms) is thought to reflect selective attention to stimuli, working memory and conscious access (Bekinschtein et al., 2009; Dehaene and Changeux, 2011). Like the MMN, the P300 has been reported as a reliable marker of coma emergence (Daltrozzo et al., 2007; Fischer et al., 2008; Morlet and Fischer, 2014).

The N400 component, is an ERP index of semantic and language processing that has also been reported in coma (Kotchoubey and Daltrozzo, 2005; Daltrozzo et al., 2009; Rämä et al., 2010). Although this component was not evaluated in the present dissertation, its potential to determine the recovery of language ability upon emergence from coma is indisputable.

1.3.1 MMN as predictor of coma emergence

From all mentioned ERP components, MMN is probably the one that has received more sustained interest from researchers, as it can be easily targeted in severe-brain injured patient without requiring their cooperation.

The prognostic power of a component, as stated by Morlet and Fischer (2014), is evaluated mainly through sensitivity, specificity, and positive predictive values. Sensitivity for good coma outcome refers to the proportion of patients who exhibit the component and return to consciousness; specificity includes the proportion of patients who do not show the component among the patients with poor outcome or considered as "non-awake" (death or UWS); while the proportion of patients showing good outcome among those exhibiting the component is the positive predictive value (PPV). While the MMN is reported to predict a return to consciousness with good specificity, ranging from 90 to 100% (Kane, 1996; Fischer et al., 1999; Naccache et al., 2005), and a PPV close to 91% (Fischer et al., 1999, 2004); its sensitivity is still low (approximately between 30 and 52%) (Luauté et al., 2005; Naccache et al., 2005), which indicates that a relatively high proportion of coma patients may emerge without having exhibited before the MMN (Connolly, 2020).

Several factors could explain the low sensitivity of MMN found in previous studies, such as the reliance on single assessments and the exclusive use of visual inspection methods to determine the presence of the MMN. The subsequent chapter (2) will deeply investigate the instability of this component in coma as another plausible explanation. As suggested in a pioneer meta-analysis of ERPs in comatose patients (Daltrozzo et al., 2007), MMN should be considered a positive and not a negative early predictor of coma emergence. This means that its presence may reliable reflect a good change of improving or emerging from coma, while its absence does not necessarily predict a poor outcome.

In contrast to seminal studies that investigated the prognostic value of MMN in non-sedated comatose patients (Kane, 1996; Naccache et al., 2005; Fischer et al., 2004), a recent study focused on a cohort of deeply sedated critically ill patients (Azabou et al., 2018). The authors found that the amplitude of MMN elicited by a conventional oddball paradigm was significantly greater in patients who awakened (i.e., eye opening and visual contact occurred within 28 days) compared with those who had not. The authors, however, concluded that traditional visual analysis alone is unreliable to assess MMN in the the ICU environment, and should be systematically completed with individual level statistics.

1.4 Advanced approaches: machine learning for signal decoding and functional connectivity

Advancements in signal processing and machine learning techniques have allowed to recognize and classify EEG/ERP neural responses in comatose and DOC patients that can be difficult to identify even by EEG specialists. Machine learning (ML), essentially is a field of artificial intelligence related with the development of algorithms that allows computer programs to learn from data and make predictions from it.

Multivariate pattern classification analyses, driven by ML algorithms, have considerably improved the sensitivity in extracting brain signals of interest at the single-subject level, by estimating the most discriminative patterns within trials or classes (King et al., 2014; Noirhomme et al., 2017). It has been reported that multivariate analyses of MMN

responses recorded in comatose patients is able to predict their chances of survival (Tzovara et al., 2013), and it is feasible for tracking MMN responses in real-time (Brandmeyer et al., 2013). Using a more sophisticated ML approach, Armanfard and colleagues provided preliminary evidence of waxing and waning cycles of MMN in coma patients over 24 hours. The authors hypothesized that the presence of even short waxing intervals is a salient indicator for coma emergence (Armanfard et al., 2019).

On the other hand, different connectivity methods have also been crucial to distinguish levels of consciousness and evaluate the integration of brain networks in comatose and DOC patients (Höller et al., 2014; Sitt et al., 2014; Chennu et al., 2017). Brain connectivity refers to patterns of anatomical links such as synapses or fiber pathways (known as "structural connectivity"), of statistical dependencies ("functional connectivity") or of causal interactions measured as information flow ("effective connectivity") between distinct units/regions within a nervous system (Friston, 2011). Neuroimaging techniques, such as positron emission tomography (PET) and fMRI, have proven that a set of brain regions or nodes within the fronto-parietal network (FPN) and the default mode network (DMN) are disrupted in DOC, depending of their level of consciousness. For example, Achard and colleagues (Achard et al., 2012), examined functional networks in comatose patients shortly after brain injury and demonstrated a radical reorganization of central hubs in comparison to healthy controls, including the medial parietal cortex (precuneus), which is a key region within the DMN that has been associated with the recovery of consciousness (Laureys et al., 2006). Recent studies have also demonstrated the utility of EEG-based functional connectivity features in the outcome prediction of coma patients, particularly after cardiac arrest (Zubler et al., 2017; Kustermann et al., 2020; Carrasco-Gómez et al., 2021). All these studies have the peculiarity of using ML classifiers to distinguish between different outcome categories.

1.5 Dissertation Overview

This dissertation is developed within the framework of an ongoing large study in which EEG/ERP data in comatose patients are recorded across multiple time points to develop a point of care system for automated coma prognosis. We have conducted several studies,

three of which are included as separated chapters here. Each chapter targets specific hypothesis and questions, but all share two main objectives: one, to determine through different methods and algorithms, whether electrophysiological markers of auditory cortical processing such as the MMN or other neural correlates associated with return of consciousness can be objectively detected in coma over time; and two, demonstrate the transient and dynamic characteristic of such markers in coma at single-subject level. The specific questions along with a brief overview of each chapter is presented below.

1) Does the MMN and subsequent ERP components fluctuate in detectability over time in healthy, fully-conscious state of awareness, or is this a specific feature of coma?

This question is addressed in Chapter 2, which details the first study to continuously track the detectability of auditory MMN responses over an extended period of time (around 12 hours) in healthy controls at both group and single-subject levels. Data from a case series of comatose patients, recorded over the course of 24 hours, provide preliminary evidence that the MMN is present in coma but can be transient (i.e., waxes and wanes) to greater or lesser extent. This chapter highlights the fact that regular and repeated assessments are extremely important when using MMN as a neurophysiological predictor of coma emergence.

2) Can multivariate decoding approaches accurately discriminate between different auditory neural responses, and be feasible to track changes underlying auditory deviance detection in coma?

Chapter 3 constitutes a follow-up analysis to the previous chapter, implementing a multivariate decoding approach to discriminate automatically between auditory neural responses at single-subject level. Methodological aspects that may affect the classification performance, such as the signal amplitude and a reduced number of electrodes, were considered in order to evaluate whether this approach is feasible for the assessment of critically ill patients with severe DOC. Results reveal fluctuations in auditory discrimination over time in coma patients; however a slight improvement in the performance was observed, especially during the second day of recording. Based on our findings, ERP-based decoding performance could be included as part of a neurophysiological monitoring of parameters to follow-up the clinical evolution of these patients.

3) How is the functional connectivity in response to auditory stimuli and resting state during last hours of life in coma after severe brain damage?

This question emerged during the assessment of an acute comatose patient with poor outcome prognosis, who died after a cardiac arrest during our EEG recording session. Chapter 4 is a case report study in which a machine learning procedure is proposed to characterize, for the first time, sensor-and source-level functional connectivity in response to auditory stimuli and resting state in a comatose patient during his last hours of life. Our findings showed high classification performance (>90% accuracy) across all frequency bands when discriminating single-trial FC in response to auditory stimuli between the coma patient and healthy controls, indicating a significant reduction of functional connectivity in coma. On the other hand, when assessing resting state across different time periods in the coma patient at single-subject level, we identified at least one period of hyperconnectivity before death. This latter finding, provides somehow evidence of fluctuating and transient brain activity in coma even within hours before death.

References

Achard, S., Delon-Martin, C., Vértes, P. E., Renard, F., Schenck, M., Schneider, F., Heinrich, C., Kremer, S., and Bullmore, E. T. (2012). Hubs of brain functional networks are radically reorganized in comatose patients. *Proc. Natl. Acad. Sci. U. S. A.*, 109(50):20608–13.

Armanfard, N., Komeili, M., Reilly, J. P., and Connolly, J. F. (2019). A Machine Learning Framework for Automatic and Continuous MMN Detection with Preliminary Results for Coma Outcome Prediction. *IEEE J. Biomed. Heal. Informatics*, 23(4):1794–1804.

Azabou, E., Rohaut, B., Porcher, R., Heming, N., Kandelman, S., Allary, J., Moneger, G., Faugeras, F., Sitt, J. D., Annane, D., Lofaso, F., Chrétien, F., Mantz, J., Naccache, L., and Sharshar, T. (2018). Mismatch negativity to predict subsequent awakening in deeply sedated critically ill patients. *Br. J. Anaesth.*, 121(6):1290–1297.

Bekinschtein, T. A., Dehaene, S., Rohaut, B., Tadel, F., Cohen, L., and Naccache, L. (2009). Neural signature of the conscious processing of auditory regularities. *Proc. Natl. Acad. Sci. U. S. A.*, 106(5):1672–1677.

Brandmeyer, A., Sadakata, M., Spyrou, L., McQueen, J. M., and Desain, P. (2013). Decoding of single-trial auditory mismatch responses for online perceptual monitoring and neurofeedback. *Front. Neurosci.*, 7:265.

Carrasco-Gómez, M., Keijzer, H. M., Ruijter, B. J., Bruña, R., Tjepkema-Cloostermans, M. C., Hofmeijer, J., and van Putten, M. J. (2021). EEG functional connectivity contributes to outcome prediction of postanoxic coma. *Clin. Neurophysiol.*, 132(6):1312–1320.

Chennu, S., Annen, J., Wannez, S., Thibaut, A., Chatelle, C., Cassol, H., Martens, G., Schnakers, C., Gosseries, O., Menon, D., and Laureys, S. (2017). Brain networks predict metabolism, diagnosis and prognosis at the bedside in disorders of consciousness. *Brain*, 140(8):2120–2132.

Chennu, S. and Bekinschtein, T. A. (2012). Arousal modulates auditory attention and awareness: Insights from sleep, sedation, and disorders of consciousness. *Front. Psychol.*, 3:65.

Claassen, J. (2020). Coma science: intensive care as the new frontier. *Intensive Care Med.*, 46(1):97–101.

Claassen, J., Doyle, K., Matory, A., Couch, C., Burger, K. M., Velazquez, A., Okonkwo, J. U., King, J.-R., Park, S., Agarwal, S., Roh, D., Megjhani, M., Eliseyev, A., Connolly, E. S., and Rohaut, B. (2019). Detection of Brain Activation in Unresponsive Patients with Acute Brain Injury. *N. Engl. J. Med.*, 380(26):2497–2505.

Connolly, J. F. (2020). Clinical neurophysiology: Research methods and event-related potential components as assessment tools. In *Handb. Clin. Neurol.*, volume 174, pages 277–287.

Daltrozzo, J., Wioland, N., Mutschler, V., and Kotchoubey, B. (2007). Predicting coma and other low responsive patients outcome using event-related brain potentials: A meta-analysis. *Clin. Neurophysiol.*, 118(3):606–614.

Daltrozzo, J., Wioland, N., Mutschler, V., Lutun, P., Calon, B., Meyer, A., Pottecher, T., Lang, S., Jaeger, A., and Kotchoubey, B. (2009). Cortical information processing in Coma. *Cogn. Behav. Neurol.*, 22(1):53–62.

Dehaene, S. and Changeux, J. P. (2011). Experimental and Theoretical Approaches to Conscious Processing. *Neuron*, 70(2):200–227.

Duncan, C. C., Barry, R. J., Connolly, J. F., Fischer, C., Michie, P. T., Näätänen, R., Polich, J., Reinvang, I., and Van Petten, C. (2009). Event-related potentials in clinical research: Guidelines for eliciting, recording, and quantifying mismatch negativity, P300, and N400. *Clin. Neurophysiol.*, 120(11):1883–1908.

Fischer, C., Dailler, F., and Morlet, D. (2008). Novelty P3 elicited by the subject's own name in comatose patients. *Clin. Neurophysiol.*, 119(10):2224–2230.

Fischer, C., Luauté, J., Adeleine, P., and Morlet, D. (2004). Predictive value of sensory and cognitive evoked potentials for awakening from coma. *Neurology*, 63(4):669–673.

Fischer, C., Morlet, D., Bouchet, P., Luaute, J., Jourdan, C., and Salord, F. (1999). Mismatch negativity and late auditory evoked potentials in comatose patients. *Clin. Neurophysiol.*, 110(9):1601–1610.

Foo, C. C., Loan, J. J., and Brennan, P. M. (2019). The Relationship of the FOUR Score to Patient Outcome: A Systematic Review. *J. Neurotrauma*, 36(17):2469–2483.

Friston, K. J. (2011). Functional and Effective Connectivity: A Review. *Brain Connect.*, 1(1):13–36.

Garrido, M. I., Kilner, J. M., Stephan, K. E., and Friston, K. J. (2009). The mismatch negativity: A review of underlying mechanisms. *Clin. Neurophysiol.*, 120(3):453–463.

Giacino, J. T., Fins, J. J., Laureys, S., and Schiff, N. D. (2014). Disorders of consciousness after acquired brain injury: The state of the science. *Nat. Rev. Neurol.*, 10(2):99–114.

Giacino, J. T., Kalmar, K., and Whyte, J. (2004). The JFK Coma Recovery Scale-Revised: Measurement characteristics and diagnostic utility. *Arch. Phys. Med. Rehabil.*, 85(12):2020–2029.

Harrison, A. H. and Connolly, J. F. (2013). Finding a way in: A review and practical evaluation of fMRI and EEG for detection and assessment in disorders of consciousness. *Neurosci. Biobehav. Rev.*, 37(8):1403–1419.

Helbok, R., Rass, V., Beghi, E., Bodien, Y. G., Citerio, G., Giacino, J. T., Kondziella, D., Mayer, S. A., Menon, D., Sharshar, T., Stevens, R. D., Ulmer, H., Venkatasubba Rao, C. P., Vespa, P., McNett, M., and Frontera, J. (2022). The Curing Coma Campaign International Survey on Coma Epidemiology, Evaluation, and Therapy (COME TOGETHER). *Neurocrit. Care*, pages 1–13.

Höller, Y., Thomschewski, A., Bergmann, J., Kronbichler, M., Crone, J. S., Schmid, E. V., Butz, K., Höller, P., Nardone, R., and Trinka, E. (2014). Connectivity biomarkers

can differentiate patients with different levels of consciousness. *Clin. Neurophysiol.*, 125:1545–1555.

Johnson, E. L. and Kaplan, P. W. (2019). Clinical neurophysiology of altered states of consciousness: Encephalopathy and coma. In *Handb. Clin. Neurol.*, volume 161, pages 73–88. Elsevier B.V.

Kane, N. M. (1996). Event-related potentials - Neurophysiological tools for predicting emergence and early outcome from traumatic coma. *Intensive Care Med.*, 22(1):39–46.

King, J. R., Gramfort, A., Schurger, A., Naccache, L., and Dehaene, S. (2014). Two distinct dynamic modes subtend the detection of unexpected sounds. *PLoS One*, 9(1):e85791.

Koch, C., Massimini, M., Boly, M., and Tononi, G. (2016). Neural correlates of consciousness: progress and problems. *Nat. Rev. Neurosci.*, 17(5):307–321.

Kondziella, D. (2020). The Neurology of Death and the Dying Brain: A Pictorial Essay. *Front. Neurol.*, 11:736.

Kondziella, D., Friberg, C. K., Frokjaer, V. G., Fabricius, M., and Møller, K. (2016). Preserved consciousness in vegetative and minimal conscious states: Systematic review and meta-analysis. *J. Neurol. Neurosurg. Psychiatry*, 87(5):485–492.

Kondziella, D. and Frontera, J. A. (2021). Pearls & Oy-sters: Eyes-Open Coma. *Neurology*, 96(18):864–867.

Kotchoubey, B. (2017). Evoked and event-related potentials in disorders of consciousness: A quantitative review. *Conscious. Cogn.*, 54:155–167.

Kotchoubey, B. and Daltrozzo, J. (2005). Semantic processing in a coma patient. *Grand Rounds*, 5:37–41.

Kustermann, T., Ata Nguepnjo Nguissi, N., Pfeiffer, C., Haenggi, M., Kurmann, R., Zubler, F., Oddo, M., Rossetti, A. O., and De Lucia, M. (2020). Brain functional connectivity during the first day of coma reflects long-term outcome. *NeuroImage Clin.*, 27:102295.

Laureys, S., Boly, M., and Maquet, P. (2006). Tracking the recovery of consciousness from coma. *J. Clin. Invest.*, 116(7):1823.

Logi, F., Fischer, C., Murri, L., and Mauguière, F. (2003). The prognostic value of evoked responses from primary somatosensory and auditory cortex in comatose patients. *Clin. Neurophysiol.*, 114(9):1615–1627.

Luauté, J., Fischer, C., Adeleine, P., Morlet, D., Tell, L., and Boisson, D. (2005). Late auditory and event-related potentials can be useful to predict good functional outcome after coma. *Arch. Phys. Med. Rehabil.*, 86(5):917–923.

Luppi, A. I., Cain, J., Spindler, L. R., Górska, U. J., Toker, D., Hudson, A. E., Brown, E. N., Diringer, M. N., Stevens, R. D., Massimini, M., Monti, M. M., Stamatakis, E. A., and Boly, M. (2021). Mechanisms Underlying Disorders of Consciousness: Bridging Gaps to Move Toward an Integrated Translational Science. *Neurocrit. Care*, 35:37–54.

Maas, A. I., Menon, D. K., Adelson, P. D., Andelic, N., Bell, M. J., Belli, A., Bragge, P., Brazinova, A., Büki, A., Chesnut, R. M., et al. (2017). Traumatic brain injury: integrated approaches to improve prevention, clinical care, and research. *The Lancet Neurology*, 16(12):987–1048.

Morlet, D. and Fischer, C. (2014). MMN and novelty P3 in coma and other altered states of consciousness: A review. *Brain Topogr.*, 27(4):467–479.

Näätänen, R., Kujala, T., and Light, G. (2019). *Mismatch negativity: a window to the brain*. Oxford University Press.

Naccache, L., Puybasset, L., Gaillard, R., Serve, E., and Willer, J. C. (2005). Auditory mismatch negativity is a good predictor of awakening in comatose patients: A fast and reliable procedure [1]. *Clin. Neurophysiol.*, 116(4):988–989.

Noirhomme, Q., Brecheisen, R., Lesenfants, D., Antonopoulos, G., and Laureys, S. (2017). "Look at my classifier's result": Disentangling unresponsive from (minimally) conscious patients. *Neuroimage*, 145:288–303.

Peterson, A. B., Xu, L., Daugherty, J., and Breiding, M. J. (2019). Centers for Disease Control and Prevention. Surveillance report of traumatic brain injury-related emergency department visits, hospitalizations, and deaths, United States, 2014. Technical report.

Polich, J. (2007). Updating P300: An integrative theory of P3a and P3b. *Clin. Neurophysiol.*, 118(10):2128–2148.

Rämä, P., Relander-Syrjänen, K., Öhman, J., Laakso, A., Näätänen, R., and Kujala, T. (2010). Semantic processing in comatose patients with intact temporal lobes as reflected by the N400 event-related potential. *Neurosci. Lett.*, 474(2):88–92.

Schiff, N. D. (2015). Cognitive motor dissociation following severe brain injuries. *JAMA Neurol.*, 72(12):1413–1415.

Schnakers, C. (2020). Update on diagnosis in disorders of consciousness. *Expert Rev. Neurother.*, 20(10):997–1004.

Schnakers, C., Vanhaudenhuyse, A., Giacino, J., Ventura, M., Boly, M., Majerus, S., Moonen, G., and Laureys, S. (2009). Diagnostic accuracy of the vegetative and minimally conscious state: Clinical consensus versus standardized neurobehavioral assessment. *BMC Neurol.*, 9(1):35.

Sitt, J. D., King, J. R., El Karoui, I., Rohaut, B., Faugeras, F., Gramfort, A., Cohen, L., Sigman, M., Dehaene, S., and Naccache, L. (2014). Large scale screening of neural signatures of consciousness in patients in a vegetative or minimally conscious state. *Brain*, 137(8):2258–2270.

Turgeon, A. F., Lauzier, F., Simard, J. F., Scales, D. C., Burns, K. E., Moore, L., Zygun, D. A., Bernard, F., Meade, M. O., Dung, T. C., Ratnapalan, M., Todd, S., Harlock, J., and Fergusson, D. A. (2011). Mortality associated with withdrawal of life-sustaining therapy for patients with severe traumatic brain injury: A Canadian multicentre cohort study. *CMAJ*, 183(14):1581–1588.

Wade, D. T. (2018). How often is the diagnosis of the permanent vegetative state incorrect? A review of the evidence. *Eur. J. Neurol.*, 25(4):619–625.

Wijdicks, E. F. (2020). Predicting the outcome of a comatose patient at the bedside. *Pract. Neurol.*, 20(1):26–33.

Young, G. B. (2009). Coma. *Ann. N. Y. Acad. Sci.*, 1157:32–47.

Young, M. J., Bodien, Y. G., Giacino, J. T., Fins, J. J., Truog, R. D., Hochberg, L. R., and Edlow, B. L. (2021). The neuroethics of disorders of consciousness: A brief history of evolving ideas. *Brain*, 144(11):3291–3310.

Zubler, F., Steimer, A., Kurmann, R., Bandarabadi, M., Novy, J., Gast, H., Oddo, M., Schindler, K., and Rossetti, A. O. (2017). EEG synchronization measures are early outcome predictors in comatose patients after cardiac arrest. *Clin. Neurophysiol.*, 128(4):635–642.

Chapter 2

Tracking auditory MMN responses during full conscious state and coma

Abstract

The mismatch negativity (MMN) is considered the electrophysiological change-detection response of the brain, and therefore a valuable clinical tool for monitoring functional changes associated with return to consciousness after severe brain injury. Using an auditory multi-deviant oddball paradigm, we tracked auditory MMN responses in seventeen healthy controls over a 12-hour period, and in three comatose patients assessed over 24 hours at two time points. We investigated whether the MMN responses show fluctuations in detectability over time in full conscious awareness, or whether such fluctuations are rather a feature of coma. Three methods of analysis were utilized to determine whether the MMN and subsequent event-related potential (ERP) components could be identified: traditional visual analysis, permutation t-test and Bayesian analysis. The results showed that the MMN responses elicited to the duration deviant-stimuli are elicited and reliably detected over the course of several hours in healthy controls, at both the group and single-subject levels. Preliminary findings in three comatose patients provide further evidence that the MMN is often present in coma, varying within a single patient from easily detectable to undetectable at different times. This highlights the fact that regular and repeated assessments are extremely important when using MMN as a neurophysiological predictor of coma emergence.

2.1 Introduction

Coma represents the most severe disruption in wakefulness and awareness, which arises when cortical and brainstem pathways are damaged as a result of a catastrophic brain injury due to traumatic or non-traumatic causes (Johnson and Kaplan, 2019). In comparison to other neurological conditions with impaired consciousness, the coma state usually resolves within days or a few weeks, and eventually evolves towards other states along the spectrum from full recovery to minimally conscious state (MCS), unresponsive wakefulness syndrome (UWS), or death (Giacino et al., 2014). Since there is no assessment technique that can reliably detect any sign of inner awareness in comatose patients, the clinical evaluation typically focuses on detecting the level of functional impairment by using scores from traditional behavioral scales.

Recent guidelines provided by the the American Academy of Neurology (AAN) and the European Academy of Neurology (EAN) recommend that patients in coma or other disorder of consciousness (DOC) should be diagnosed by using a multimodal approach including a comprehensive behavioral assessment along with advanced electroencephalography or functional neuroimaging, particularly in patients without command following abilities (Giacino et al., 2018; Kondziella et al., 2020). Although not available in all hospitals, these techniques seem promising for increasing diagnostic accuracy and refining the current model of assessing consciousness and cognitive function. These neurofunctional tests might therefore help to reduce the approximately 40% misdiagnosis rate found in patients who emerge from coma into other states including MCS or locked-in that are often classified as UWS despite a rigorous clinical assessment (Wannez et al., 2017; Schnakers, 2020).

It is even more challenging to predict how one will progress while still in a coma state. In the acute stage post-injury, the decisions made in intensive care have a major impact on patient survival and outcome (Turgeon et al., 2011, 2013). Critically ill comatose patients may be too unstable clinically to be transferred from the intensive care unit (ICU) for functional neuroimaging assessments (Wijdicks, 2020). The point-of-care aspect of the electroencephalogram (EEG) makes it a suitable tool for bedside assessment. One of the most commonly used approaches when investigating cognitive function and coma outcome are event-related potentials (ERPs), which are electrophysiological time-locked

brain responses elicited typically by auditory, visual or tactile stimuli. Particularly, the mismatch negativity (MMN) has been considered a useful predictor of emergence from coma (Kane et al., 2000; Daltrozzo et al., 2009; Morlet and Fischer, 2014; Armanfard et al., 2019), and a key early biomarker in the information processing hierarchy leading up to conscious perception (Chennu and Bekinschtein, 2012).

The auditory MMN (Näätänen et al., 2019) is a neural response to any discriminable change in a repetitive sequence of otherwise identical sounds. The MMN occurs within the time span of sensory memory and is considered independent of volitional attention and task performance. It is usually recorded within the "auditory oddball paradigm" in which repeated “standard” stimuli are interspersed with infrequent or “deviant” stimuli. The MMN has long been considered as an automatic preattentive ERP component, since it can be elicited in coma, during particular sleep stages and in the absence of behavioral discrimination ability (Fitzgerald and Todd, 2020). This claim has been refuted, however, due to a growing body of research showing systematic modulation of MMN amplitude with attention to the stimuli (see Sussman et al. (2014) for a review). The frontal contribution to the attentional network, of which the MMN is part, results in further processing focused on the deviant stimulus. Accordingly, the MMN is often followed by the P3a component that indexes involuntary attention switch or reorientation to the deviants initiated by the MMN generation (Escera et al., 1998; Atkinson et al., 2017; Näätänen et al., 2019).

A different neurophysiological interpretation has been proposed that raises the question of whether the MMN is an indicator of “partial awareness” in the absence of overt behavior (Dykstra and Gutschalk, 2015; Dykstra et al., 2017). Using a masking experimental task, Dykstra and Gutschalk (2015) demonstrated that the MMN is observed only when listeners were aware of the standard stream prior to the onset of the deviant. This approach better explains the presence of MMNs during states of behavioral unconsciousness such as sleep, coma and other DOC (i.e., MCS and UWS), where a certain level of awareness of sensory stimuli is more likely than the ability to “attend" them. Moreover, the MMN appears to be abolished during deep sedation-induced unconsciousness but returns as patients recover from anesthesia (Heinke et al., 2004; Blain-Moraes et al., 2016). Although dissociating attention from consciousness is extremely difficult, a large body of evidence demonstrates that the MMN is highly correlated with emergence from coma

and recovery of consciousness; and this evidence suggests that the MMN may be one of the earliest indicators of partial awareness in such patients.

A pioneering study found that over 91% of comatose patients exhibiting the MMN returned to consciousness (i.e., indicating a high positive predictive value), and over 90% of those who did not show MMN were considered as non-awake patients [a] (i.e., reflecting high specificity). However, only about 30% of patients who emerged from coma showed a MMN, suggesting poor sensitivity (Fischer et al., 1999). Subsequent studies confirmed the strong specificity and positive predictive value of MMN (Fischer et al., 2004), but the sensitivity rate continued to be low, reaching values of about 56% when functional outcome was assessed one month after MMN recordings (Naccache et al., 2005) and 32% when it was evaluated 12 months after coma onset (Luauté et al., 2005). This low sensitivity constitutes a problem for prognosis; while it is possible to state with some confidence that emergence from coma is highly likely once MMN is present, patients who do not show the response can also emerge. Nevertheless, failure to detect the MMN should be interpreted with caution and not be taken as a definitive "absence of response". It is possible that different analysis methods may be better at detecting the MMN. A recent study using machine learning showed that the MMN waxes and wanes in comatose patients when assessed across 24 hours (Armanfard et al., 2019). This cycling pattern of presence/absence was postulated to be the predominant explanation for the low sensitivity rates reported in previous studies. These findings suggest that the MMN should no longer be sought in single-block recording sessions as has been done traditionally for decades. A testing session should be repeated several times, over the course of hours or longitudinally across different days to increase the chances of detecting the MMN and thus improving its sensitivity and relevance to patient care.

This approach of repeated or extended testing must also apply when evaluating healthy control subjects for comparisons, since there is evidence -albeit to a lesser extent- that not all healthy individuals exhibit the MMN in a single first assessment (Bishop and Hardiman, 2010). Single-subject analyses can indeed provide useful information that is obscured or simply not available in the average responses observed across a group of

[a] Non-awake was operationally defined using Glasgow Outcome Scale (GOS) criteria, with GOS levels of 1 or 2 (death or vegetative state)

control participants. This is particularly important for DOC research, since to interpret patient data accurately in clinical settings, it is crucial to identify reliable ERPs at a single subject-level, but also to design experimental paradigms able to elicit such responses.

In the present study, as part of an ongoing longitudinal study (Connolly et al., 2019), we investigate the auditory MMN responses in healthy controls recorded over a 12-hour period that were then analyzed at both the group and single-subject levels. We also report the results of three cases of coma patients whose MMNs were assessed repeatedly over a 24-hour period at two different time points. We sought to investigate if the MMN exhibits fluctuations over time in healthy, fully-conscious states of awareness, or whether such waxing/waning is a specific feature of coma.

2.2 Materials and Methods

2.2.1 Healthy controls and comatose patients

In order to characterize typical ERP responses across a period of up to 12 hours during full conscious awareness and to obtain a baseline for the experimental paradigm, 17 healthy control participants (14 females) were recruited. Participants were aged between 19 to 56 years old (mean = 29.64, SD = 11.73) and had no history of neuropsychiatric disorders, alcohol/drug abuse, head trauma or known hearing impairment. Participants were paid $15/hour up to a maximum of $180 at the end of the study period.The study was approved by the Hamilton Integrated Research Ethics Board (HiREB; project number 4840).

Continuous EEG/ERP data were collected over the course of 24 hours from three female comatose patients. All were assessed over the course of two days in either the ICU or the neurological Step-Down Unit at the Hamilton General Hospital, and were classified as being in a comatose state with Glasgow Coma Scale (GCS) scores less than 8 at the first day of recording. Patients 1 and 2 had neurosurgical complications as their coma etiology, while Patient 3 had a traumatic brain injury following a road traffic accident (see Table 2.1). Patients were off sedative medications during the EEG recordings. Exclusion criteria included seizure or epileptiform activity, known hearing

impairment, medically induced coma, severe liver and renal failure. The presence of N1 components over continuous testing was also taken into account to discard hearing loss.

2.2.2 Behavioral coma assessments

Diagnosis of coma and outcome were assessed by the GCS and the Glasgow Outcome Scale (GOS) (Jennett and Bond, 1975), respectively. In general, the GCS is usually applied to determine severity of coma and includes 3 aspects of behavioral responsiveness: eye opening, verbal and motor responses. The GOS globally rates the functional outcome for patient states into one of five categories: dead, vegetative state (VS; currently known as UWS), severe disability, moderate disability or good recovery.

In addition, we used the Full Outline of UnResponsiveness score (FOUR). The FOUR includes assessment of eye movements and brainstem reflexes, which are unavailable with the GCS. It reduces misdiagnosis of locked-in syndrome and MCS by including assessment of eye movement, and helps to distinguish between comatose and recovering patients (Kondziella et al., 2020).

2.2.3 Stimuli and Procedure

The MMN was recorded in an auditory 3-deviant oddball paradigm (Todd et al., 2008), as part of a modified implementation of an ongoing study (Connolly et al., 2019). 2400 tones at a regular 450-ms stimulus onset asynchrony (SOA) were recorded. The sequence comprised 82% standard tones (50 ms, 1000 Hz, 80 dB sound pressure level (SPL) and three types of deviant tones (6% each): a duration deviant (125 ms), a frequency deviant (1200 Hz) and an intensity deviant (90 dB SPL). Auditory stimuli were delivered through noise-canceling insert earphones (Etymotic ER-1) using Presentation software (Neurobehavioral Systems, Inc.). This was a passive task that lasted approximately 25 min, with no behavioral responses required.

Healthy control subjects participated in several EEG/ERP tasks, that were repeated for a test day of up to 12 hours. This schedule produced between three and five MMN recording blocks. Sufficient breaks were provided to the control subjects during the day

to minimize movement artifacts and fatigue. Patients were tested in two recording sessions conducted 3 days apart, denoted as day 0 and day 3, respectively. Each recording session lasted up to 24 hours with all testing done at the patient's bedside. Each test day comprised the same EEG/ERP protocol used in controls, including the MMN paradigm with resting state periods (10 minutes each) between each task. Behavioral scales were applied at the beginning of each testing day, before the EEG/ERP recordings. According to our protocol (Connolly et al., 2019), if patients were emerging (i.e., awakening, eyes opening) from coma, only two blocks of the oddball paradigm were recorded.

2.2.4 EEG recording and Preprocessing

EEG was recorded online with a bandpass of 0.01-100Hz and sampled at 512 Hz using the ActiveTwo Biosemi system. For healthy controls and one comatose patient, the electrodes were placed on the scalp according to the extended 10/20 system using a 64-electrode cap. A reduced number of 11 electrodes (F3, Fz, F4, C3, Cz, C4, P3, Pz, P4, T7, T8) were used following the same 10/20 system in two patients (Patient 1 and 2) due to surgical incisions and external ventricular drains (EVD). For all controls and patients, vertical and horizontal electrooculogram (EOG) signals were monitored by electrodes placed above and over the outer canthus of the left eye, and reference electrodes were located bilaterally at the mastoids. Identifying markers were automatically placed in the EEG signal at the onset of each stimulus presentation.

Data pre-processing was conducted offline (Brain Products Inc.). All recordings were filtered with a bandpass of 0.1–30 Hz. Epochs containing non-ocular artifacts (e.g., muscle activity, movements) were removed. Ocular artifacts were corrected using the Independent Component Analysis (ICA) transformation (Makeig et al., 1995). EEG trials were separated and segmented by stimulus type from 100 ms pre-stimulus to 600ms post-stimulus and baseline corrected (-100 to 0ms). These segments were averaged together per condition (i.e., stimulus type) for each block and subject or patient.

2.2.5 Statistical Analysis

In addition to visual identification of the averaged ERP components, two main statistical methods were used to detect the presence of these components for each recorded MMN block at both the group level and the single-subject level in healthy controls.

2.2.5.1 Permutation *t*-test

Permutation testing comes from a classical inference approach that relies on the use of null hypothesis significance testing, featuring the *p*-value as an indication of whether this hypothesis is probably true or false. The *p*-value could be derived from comparison to a Monte Carlo estimate of a permutation distribution, generated by randomly exchanging the trials from different conditions. In comparison to other conventional statistical tests, the permutation test seems to be preferred because its greater statistical power, reliability for small samples and independence of any assumptions related to normal distribution of data and homogeneity of variances that are required when using parametric tests such as *t*-tests and analysis of variance (ANOVA) (Collingridge, 2013).

Here, one-tailed serial permutation *t*-tests were performed over a mean of 6 fronto-central electrodes (F3, Fz, F4, C3, Cz, C4) at each time point to find the intervals where the deviant condition was significantly more negative (e.g., a MMN component) or positive (e.g., a P3a component) compared to the standard condition. For group-level analyses, dependent samples permutation-*t* testing was performed across individual-averaged ERPs for the entire epoch (-100 to 600 ms). Maximum effect sizes (Cohen's *d*) were calculated over 50 and 100 ms periods surrounding the peak latency, which was automatically detected as the most negative or positive peak within each component window of interest respectively (MMN: 80-230ms and P3a: 250-350ms). For single-subject analyses, independent samples permutation *t*-tests were conducted across trials/epochs from each subject. For both analyses, the number of permutations was set to 1000, the *p*-values were corrected using the T_{max} statistic for multiple comparisons.

2.2.5.2 Bayesian analysis

Bayesian hypothesis testing presents an attractive alternative to p-values, which have been criticized extensively in the literature (Sullivan and Feinn, 2012; Wellek, 2017; Kraemer, 2019). This analysis is powerful as it provides weights of evidence for or against both the alternative and null hypotheses. Here, the strength of the evidence in favor of the alternative hypothesis $H1$ (difference between standard and deviants) over null hypothesis $H0$ (no difference), was quantified by Bayes factors (BF_{10}). Maximum Bayes factors were calculated over the previous time periods surrounding the peak latency for each component of interest. Traditional interpretations of cut-offs (Jeffreys, 1961) were modified by (Lee and Wagenmakers, 2013), resulting in the following ranges: 1 to 3 - anecdotal evidence, 3 to 10 - moderate; 10 to 30 - strong ; 30 to 100 - very strong and $>$ 100 - extreme. Analyses were done in Matlab, version R2020a (MathWorks Inc., USA), using a function from the FieldTrip toolbox for electrophysiological data analysis, which supports both unpaired and paired designs and assumes flat priors (Oostenveld et al., 2011).

Additionally, in order to compare the MMN responses elicited by each deviant and determine whether there were habituation effects over time in the control group, we conducted a repeated measures analysis of variance (ANOVA) with deviant type (duration, frequency and intensity) and block (1 to 5 blocks recorded over time) as within-subject factors at a cluster of 6 frontocentral electrodes (described above) with amplitude as the dependent variable. Mean amplitudes were exported in a $\pm$50 ms window surrounding the group average peak: 180-230 ms for duration MMN and 80-130 ms for frequency and intensity MMN. When statistically significant differences were found, a Bonferroni post-hoc test was conducted for multiple comparisons. A Geisser and Greenhouse test for sphericity correction was used when appropriate. This analysis was conducted using JASP software (version 0.14.1).

For the comatose patients, a similar procedure as outlined above (visual inspection, serial permutation t-test and Bayesian analysis) was performed at the single-subject level for every recorded MMN block.

Table 2.1: Demographic and clinical information of patients

.

Patient	Sex	Age	Etiology	Testing Day	State	Days since coma onset	GCS (E,V,M)	FOUR (E,M,B,R)	Blocks recorded	Outcome
1	F	41	Neurosurgery	0	Coma	20	5 (1,1,3)	6 (0,1,4,1)	8	Death
				3	Coma/UWS	23	6 (4,1,1)	8 (3,0,4,1)	10	
2	F	51	Neurosurgery	0	Coma	8	5 (1,1,3)	5 (0,1,4,0)	10	Good recovery
				3	Awakening	11	9 (4,1,4)	9 (3,1,4,1)	2	
3	F	43	Trauma	0	Coma	13	4 (1,1,2)	5 (0,1,4,0)	10	UWS
				3	Coma	16	7 (2,1,4)	5 (0,1,4,0)	6	

GCS: Glasgow Coma Scale, which is the sum of E (Eye opening) + V (Verbal response)+ M (Motor response) scores. FOUR: Full Outline of UnResponsiveness score that has four components - E (Eye response), M (Motor response), B (Brainstem reflexes) and R (Respiration). UWS: Unresponsive wakefulness syndrome.

2.3 Results

2.3.1 MMN in controls: from group-level to single-subject analysis

Figure 2.1 (panel A) shows the grand-average ERPs over a mean of 6 frontocentral electrodes (F3, Fz, F3, C3, Cz, C4), corresponding to standard and deviant stimuli (duration, frequency and intensity) for each block recorded over a 12 hour-period. As can be observed, the waveforms from all blocks were extremely similar. Figure 2.1 (B) displays the ERP waveforms from Block 1 as an example, and its corresponding topographical maps averaged over 80-130 ms, 180-230ms and 250-350 time intervals. Frequency and intensity deviants elicited a negative component peaking between 80 to 130 ms, which represents a spatial-temporal summation of both N1 and MMN components, often called deviant-related negativity(DRN) (Tavakoli et al., 2019). This was followed by a frontocentral positivity (P3a), which peaked later between 180-230 ms. The duration deviant elicited 3 dissociated components: the N1 peaking at 150ms, a MMN with maximum amplitude between 180-230 ms and a P3a component with maximum amplitude between 250 and 350ms.

Figure 2.2 (panel B) summarizes the statistical findings at the group level in healthy controls. As can be observed, both the MMN and the P3a components were observed in all blocks, and reliably detected by using permutations *t*-test ($p < 0.05$) and Bayes factor analysis.

For the MMN component, the Cohen's d computed from the permutation t-tests were averaged across all five blocks, reaching values of 1.28 for the duration deviant, 0.79 for frequency and 1.15 for intensity, indicating a very large, a medium and a large effect size, respectively, according to Sawilowsky (2009). For the P3a, the averaged Cohen's *d* indicated a huge effect size for duration (2.25), and a very large effect size for both frequency (1.39) and intensity (1.51). Maximum Bayes factors computed at the time window of interest for each component mostly revealed very strong to extreme evidence for our hypothesis of significant difference between the deviant and standard stimuli in all blocks (see Cohen's *d* and Bayes factors for each recorded block in Supplementary information I (Table S1).

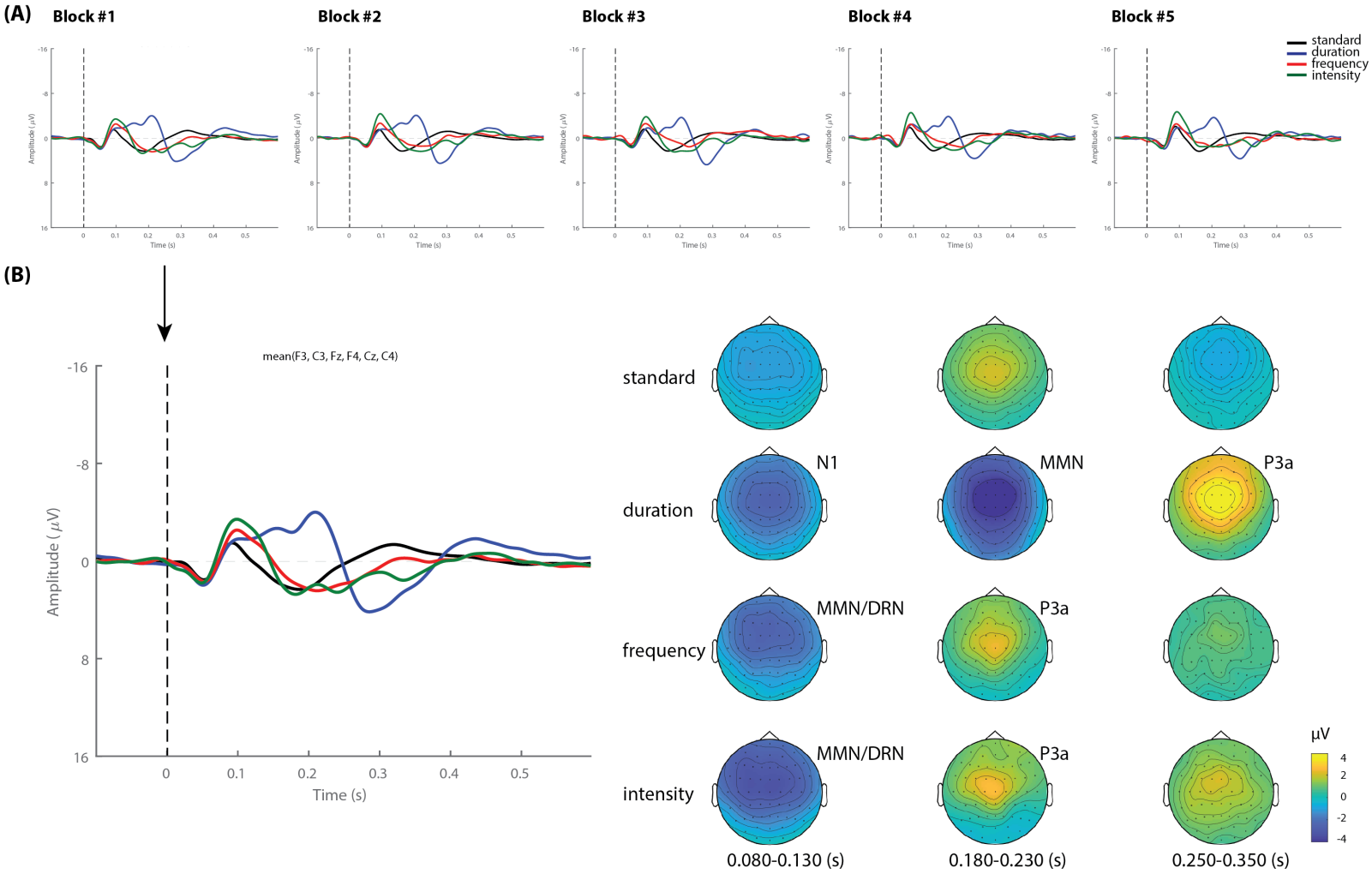

Figure 2.1: Grand-average ERPs and topography in healthy controls. (A) Grand-average ERP for each stimuli (standard, duration, frequency and intensity) across blocks. (B) Example of ERP waveforms and scalp topographical maps of Block 1 averaged over 80-130 ms, 180-230 ms and 250-350 time intervals.

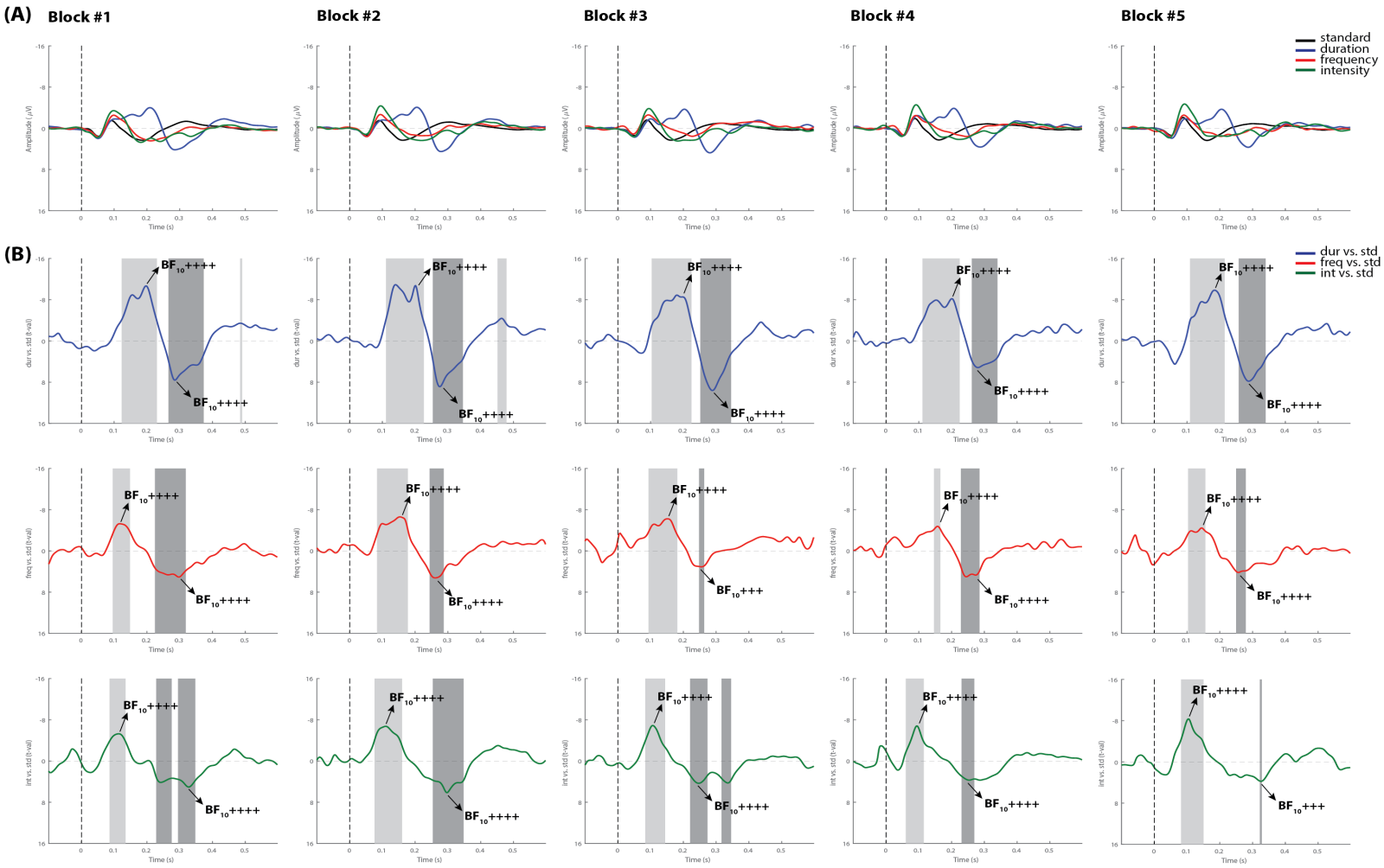

Figure 2.2: Grand-average ERPs and statistical findings in healthy controls. (A) Grand-average ERPs across blocks. (B) Time course of the difference between deviants and standard stimuli expressed in units of *t*-values. Significant intervals for negative components are denoted by a light gray area, and positive components are denoted by a dark gray area. Black arrows show the latency of maximum bayes factors and the strength of evidence for $H1$: + anecdotal; ++ moderate; +++ strong and ++++ very strong to extreme.

When differences between deviants and habituation effects were evaluated within the group, the repeated-measures ANOVA analysis showed a main effect for deviant type ($F(2,24) = 7.13$, $p < 0.05$, $\eta_p^2 = 0.37$). A Bonferroni post-hoc test averaged over the levels of blocks revealed differences between duration and frequency deviants with a mean difference of -1.27μV ($p < 0.05$), and between intensity and frequency with a mean difference of 1.33 μV ($p < 0.01$). No significant main effect was found for block ($F(4,48) = 0.71$, $p = 0.52$, $\eta_p^2 = 0.05$), and the deviant type x block interaction also failed to reach significance ($F(8,96) = 0.84$, $p = 0.47$, $\eta_p^2 = 0.06$). (See Figure 2.3)

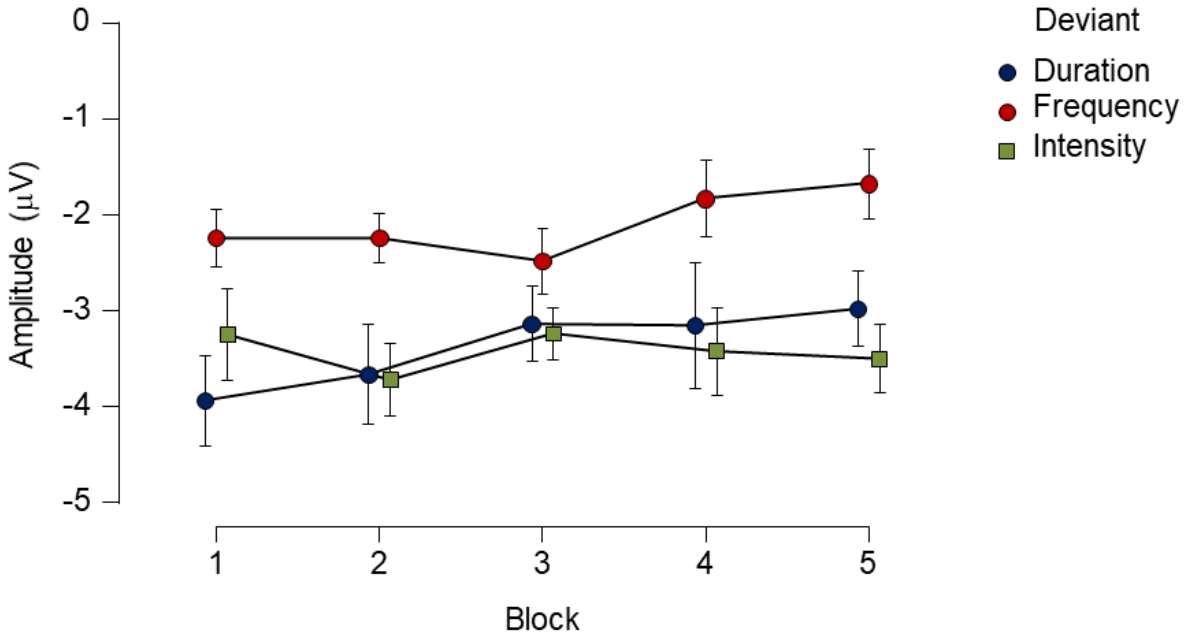

Figure 2.3: Mean amplitude and standard errors (SE) of each deviant type for each block recorded over a 12-hour period in the healthy control group. While there was main effect of deviant type, no reliable main effect of block or interaction was found. Points represent mean amplitude from each deviant type. Vertical extended lines indicate the standard error intervals.

Single-subject analysis showed that both MMN and P3a components elicited by the duration deviant were significantly detected across all blocks in all subjects by using both permutation *t*-test and Bayesian analysis. The serial permutation *t*-test showed that 3 out of 17 subjects did not exhibit significant MMNs to the frequency deviant in any of the recorded blocks, and one subject to the intensity deviant. Bayesian analysis showed evidence in favor of the presence of MMN responses to frequency and intensity deviants

in all subjects in at least one block, confirming the visual inspection. Tables 2.2 and 2.3 summarize the proportion of control subjects exhibiting MMN and P3a responses respectively for each recorded block using the three methods adopted in the present study. Notice (in N column) that not all subjects performed all blocks, but regardless the sample size, the duration deviant still elicited the most reliable responses, as can also be observed in Figure 2.2.

Table 2.2: Proportion of healthy controls showing evidence of MMN in each block.

		DURATION			FREQUENCY			INTENSITY		
Block	**N**	**Visual**	**Perm. test**	**Bayes**	**Visual**	**Perm. test**	**Bayes**	**Visual**	**Perm. test**	**Bayes**
1	17	1.00	1.00	1.00	0.88	0.47	0.65	1.00	0.71	0.82
2	17	1.00	1.00	1.00	0.82	0.53	0.82	0.94	0.76	0.94
3	17	1.00	1.00	1.00	0.88	0.47	0.88	0.88	0.53	0.82
4	14	1.00	1.00	1.00	0.86	0.50	0.71	0.93	0.57	0.93
5	13	1.00	1.00	1.00	0.84	0.31	0.71	1.00	0.46	1.00

Table 2.3: Proportion of healthy controls showing evidence of P3a in each block

		DURATION			FREQUENCY			INTENSITY		
Block	**N**	**Visual**	**Perm. test**	**Bayes**	**Visual**	**Perm. test**	**Bayes**	**Visual**	**Perm. test**	**Bayes**
1	17	1.00	0.82	0.94	0.82	0.47	0.71	0.88	0.71	0.82
2	17	1.00	0.88	1.00	0.53	0.41	0.47	0.88	0.76	0.82
3	17	1.00	0.88	1.00	0.53	0.18	0.53	0.82	0.71	0.76
4	14	1.00	0.79	0.93	0.57	0.21	0.50	0.71	0.71	0.64
5	13	1.00	0.85	1.00	0.54	0.38	0.38	0.69	0.46	0.54

Figures 2.4 and 2.5 display the results from two representative control subjects, showing the highest and lowest ERP detection rates, respectively. As shown in these examples, the first control subject (see Figure 2.4) had the highest ERP detection rate, exhibiting significant MMN intervals for each deviant sound in all recorded blocks when performing all methods of analysis. A reliable P3a response was also found in most of the blocks and deviant conditions, except in the fifth block for the intensity deviant. The second control subject, who had the lowest ERP detection rate (see Figure 2.5) exhibited a significant duration MMN in all recorded blocks with all methods, but the permutation t-test failed to capture a significant MMN in all blocks for the frequency deviant and in fourth blocks for the intensity deviant. The Bayesian analysis confirmed the visual inspection method by showing anecdotal or moderate evidence for the presence of a MMN in 3 blocks for frequency and intensity deviants.

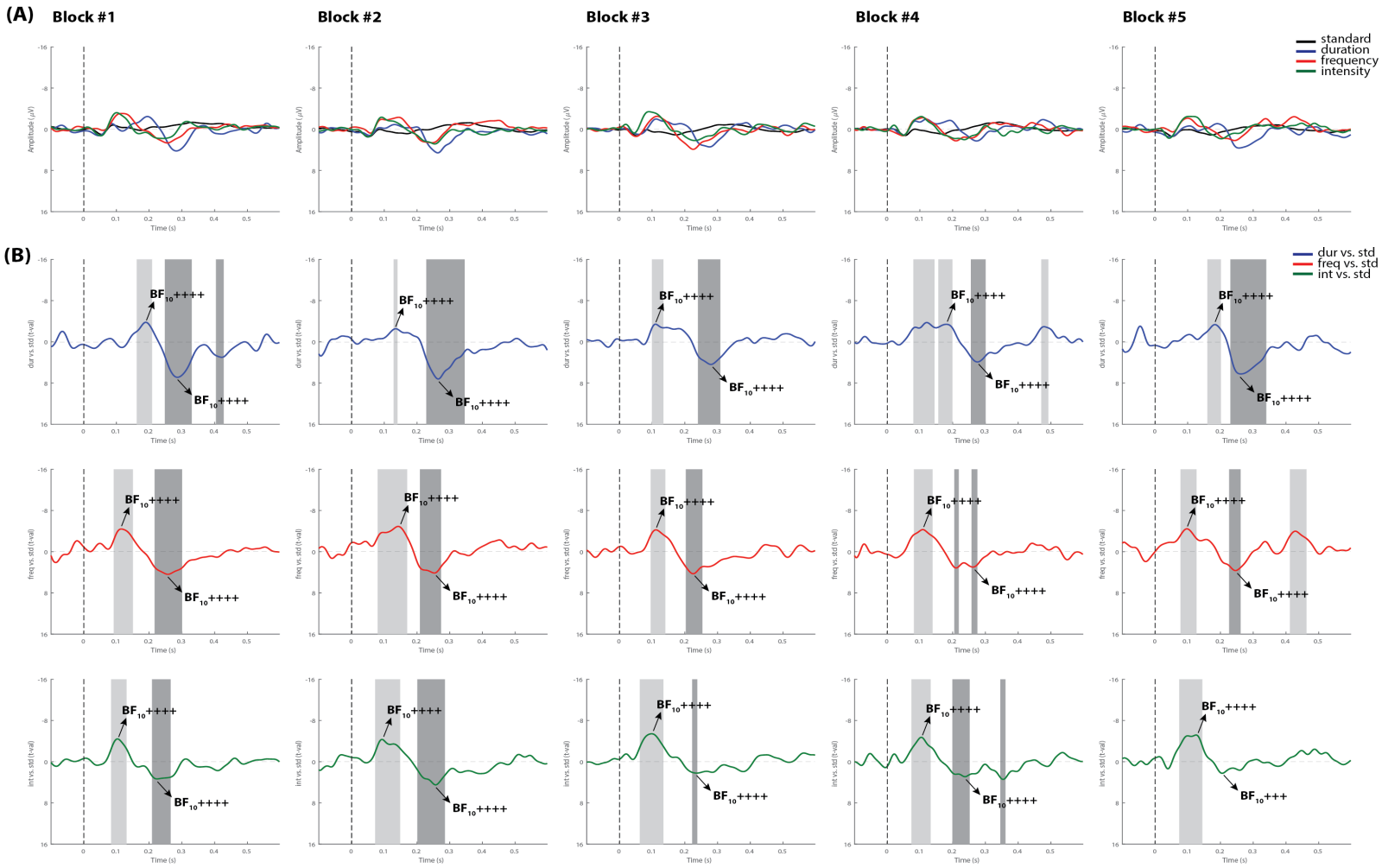

Figure 2.4: Individual ERPs and statistical findings of a representative control subject with the highest MMN detection rate. (A) Individual ERPs across blocks. (B) Time course of the difference between deviants and standard stimuli expressed in units of *t*-values. Significant intervals for negative components are denoted by a light gray area, and those for positive components are denoted by a dark gray area. Black arrows show the latency of maximum bayes factors and the strength of evidence for $H1$: + anecdotal; ++ moderate; +++ strong and ++++ very strong to extreme.

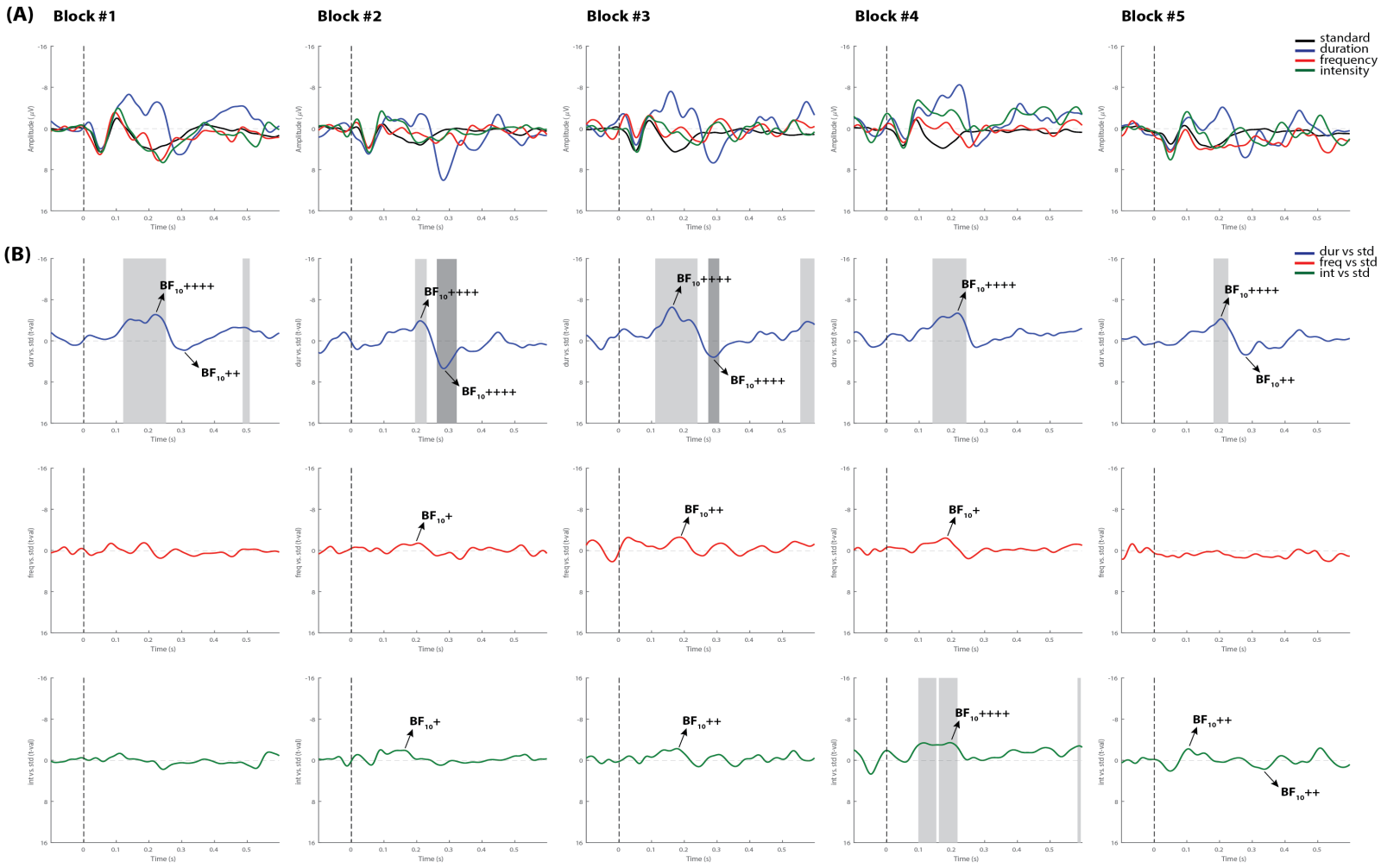

Figure 2.5: Individual ERPs and statistical findings of a representative control subject with the lowest MMN detection rate. (A) Individual ERPs across blocks. (B) Time course of the difference between deviants and standard stimuli expressed in units of *t*-values. Significant intervals for negative components are denoted by a light gray area, and those for positive components are denoted by a dark gray area. Black arrows show the latency of maximum bayes factors and the strength of evidence for $H1$: + anecdotal; ++ moderate; +++ strong and ++++ very strong to extreme.

2.3.2 MMN in coma: case reports

2.3.2.1 Patient 1: from step-down unit to palliative care

Patient 1 was a 41-year-old woman who was admitted to the step-down unit 20 days prior to our assessment. The patient had a history of multiple re-resections of a left frontotemporal oligodendroglioma. She was admitted to the neurosurgery operating room for surgical repair of cerebrospinal fluid (CSF) leak, which required reopening of left frontal subdural craniotomy for a lumbar drain and a subsequent right ventriculoperitoneal (VP) shunt. A right frontal EVD was inserted after a shunt infection and an intracranial abscess resection was performed at the previous surgical site. At the time of the first assessment (day 0), the patient had a GCS score of 5. A summary of the MMN results for this patient are given in Table 2.4. Out of 8 recorded blocks collected on the first day (day 0), a reliable MMN to all deviants was detected in one block (block 4) by using all methods of analysis, and in an additional block (block 6) for the intensity deviant. Also, a significant P3a component was detected in two blocks (blocks 4 and 6) for the intensity deviant (See Table S2) in Supplementary information I for the summary of the P3a results).

On day 3, the patient had spontaneously opened her right eye, which remained persistently halfway open requiring artificial tears or eye pads to prevent corneal abrasions. The patient, however, did not fixate to stimuli or track (see FOUR score in Table 2.1). Confirmed by the three selected analysis methods, the patient had a reliable MMN response in 4 out 10 recorded blocks for the duration deviant (blocks 2,3,8 and 10), in block 8 for frequency and in block 2 for intensity. A P3a component, was also detected in 6 blocks for the intensity deviant (blocks 2, 3, 6, 8, 9 and 10), in 4 blocks for duration (blocks 2, 6, 9 and 10) and in two blocks for the frequency deviant (blocks 6 and 9) (see Table S2 in Supplementary information I).

After a few days of the EEG assessment, the patient's clinical condition worsened. Active care was withdrawn while maintaining comfort measures. The patient subsequently died.

2.3.2.2 Patient 2: from coma to awakening in intensive care

Patient 2 was a 53-year-old woman admitted to the ICU, deeply unconscious after a cystoperitoneal shunt malfunctioning that required neurosurgery. She had a history of meningioma resection from the right posterior cranial fossa, complicated by meningitis, CSF leak and debridement surgeries.

A summary of results for this patient are given in Table 2.5. On day 0, the patient showed a significant MMN in 2 out of 10 recorded blocks (blocks 9 and 10) for the duration deviant according to all selected methods, and in block 10 for the frequency deviant. A significant P3a component was detected in 2 blocks for the intensity deviant.

The second recording, denoted as day 3, included only two blocks of the MMN paradigm, since the patient exhibited behavioral signals of emerging from coma state as shown in GCS and FOUR scales in Table 2.1. The three methods confirmed the presence of a MMN only for the duration deviant in one of the recorded blocks and a P3a response in both blocks. (See summary of the P3a results in Table S3 in Supplementary information I)

This patient was subsequently transferred to the neurosurgery inpatient unit where she was awake, oriented and talking. After a year, the patient had resumed her normal life with minor neurological deficits, which is congruent with a good recovery outcome.

2.3.2.3 Patient 3: coma following multisystem trauma

This was a 43-year-old patient included in the study 13 days post hospital admission for severe multisystem trauma after being involved in a road vehicle accident. On arrival to the ICU, she was intubated and sedated with a GCS of 3. Computed tomography scans revealed bilateral subarachnoid hemorrhage, with no herniation as well as diffuse axonal injury. Her GCS was 4 and 7 during the first and second EEG recordings, respectively (see Table 2.1).

On day 0, the patient showed a MMN confirmed by the three methods in block 8 for the duration deviant and in block 10 for the frequency deviant (block 10). A P3a component was reliably detected for the frequency deviant in block 8 and for the intensity

deviant in the blocks 7 and 8 with all the methods. The presence of this component was confirmed in other blocks by two methods (visual inspection and Bayesian analysis).

On day 3, only a duration MMN was confirmed by visual and Bayesian analysis in 3 blocks (see Table 2.6). A P3a response to duration and frequency deviants was confirmed by all methods in one block (block 2) (see summary of the P3a results in Table S4 in Supplementary information I).

This patient was transferred to another hospital. Based on her records, the patient remained dependent on the ventilator and the tracheotomy by the time of discharge. She was withdrawing and flexing to pain, and would occasionally open her left eye spontaneously, but not to voice or pain and would not track. She then was transferred to chronic care, after being diagnosed as a VS/UWS patient.

All individual ERPs and statistical findings from all comatose patients are displayed in Figures S1 to S10 in Supplementary information I.

Table 2.4: Summary of the MMN results in Patient 1.

DAY 0		DURATION			FREQUENCY			INTENSITY		
Block	**Time**	**Visual**	**Perm. test**	**Bayes**	**Visual**	**Perm.test**	**Bayes**	**Visual**	**Perm.test**	**Bayes**
1	18:35 PM	+	-	+	+	-	-	-	-	-
2	21:10 PM	+	-	+	+	-	+	+	-	+
3	22:49 PM	-	-	-	-	-	-	-	-	-
4	12:47 AM	+	+	++++	+	+	+++	+	+	++++
5	06:26 AM	+	-	+	-	-	-	+	-	++
6	07:58 AM	-	-	-	-	-	-	+	+	++++
7	10:08 AM	+	-	-	+	-	-	+	-	-
8	11:26 AM	+	-	++	+	-	-	+	-	++

DAY 3		DURATION			FREQUENCY			INTENSITY		
Block	**Time**	**Visual**	**Perm.test**	**Bayes**	**Visual**	**Perm.test**	**Bayes**	**Visual**	**Perm.test**	**Bayes**
1	18:20 PM	-	-	-	+	-	-	+	-	-
2	20:29 PM	+	+	++++	+	-	+++	+	+	++++
3	21:15 PM	+	+	+++	-	-	-	-	-	-
4	23:14 PM	+	-	-	-	-	-	-	-	-
5	01:05 AM	+	-	+	+	-	+	-	-	-
6	03:13 AM	+	-	-	-	-	-	-	-	-
7	05:22 AM	-	-	-	-	-	-	-	-	-
8	06:09 AM	+	+	+++	+	+	++	+	-	-
9	07:56 AM	-	-	-	+	-	-	+	-	+
10	10:11 AM	+	+	++	-	-	-	+	-	+

+ indicates a positive result, - a negative result. For Bayes column, + anecdotal evidence; ++ moderate evidence; +++ strong evidence and ++++ very strong to extreme evidence.

Table 2.5: Summary of the MMN results in Patient 2.

DAY 0		DURATION			FREQUENCY			INTENSITY		
Block	**Time**	**Visual**	**Perm. test**	**Bayes**	**Visual**	**Perm. test**	**Bayes**	**Visual**	**Perm. test**	**Bayes**
1	21:15 PM	+	-	-	+	-	-	-	-	-
2	12:14 AM	-	-	-	+	-	+	+	-	-
3	02:24 AM	-	-	-	-	-	-	-	-	-
4	04:51 AM	+	-	+	-	-	-	-	-	-
5	06:50 AM	+	-	-	+	-	++	+	-	+
6	08:00 AM	-	-	-	-	-	-	+	-	-
7	10:09 AM	-	-	-	+	-	-	-	-	-
8	11:48 AM	-	-	-	-	-	-	-	-	-
9	12:28 AM	+	+	++	-	-	-	+	-	+
10	02:37 PM	+	+	+++	+	+	++	-	-	-

DAY 3		DURATION			FREQUENCY			INTENSITY		
Block	**Time**	**Visual**	**Perm. test**	**Bayes**	**Visual**	**Perm. test**	**Bayes**	**Visual**	**Perm. test**	**Bayes**
1	18:34 PM	+	+	++++	+	-	++	+	-	-
2	20:48 PM	+	-	-	+	-	++	+	-	-

+ indicates a positive result, - a negative result. For Bayes column, + anecdotal evidence; ++ moderate evidence; +++ strong evidence and ++++ very strong to extreme evidence.

Table 2.6: Summary of the MMN results in Patient 3.

DAY 0		DURATION			FREQUENCY			INTENSITY		
Block	**Time**	**Visual**	**Perm. test**	**Bayes**	**Visual**	**Perm. test**	**Bayes**	**Visual**	**Perm. test**	**Bayes**
1	14:52 PM	+	-	-	-	-	-	-	-	-
2	16:44 PM	-	-	-	-	-	-	-	-	-
3	18:46 PM	-	-	-	-	-	-	-	-	-
4	20:55 PM	+	-	+	+	-	+++	-	-	-
5	21:36 PM	-	-	-	+	-	+	+	-	+
6	23:25 PM	+	-	+	-	-	-	+	-	-
7	01:34 AM	+	-	+	+	-	+	+	-	+
8	02:50 AM	+	+	++	-	-	-	+	-	+
9	05:24 AM	-	-	-	+	-	-	+	-	-
10	07:09 AM	+	-	-	+	+	+++	+	-	+

DAY 3		DURATION			FREQUENCY			INTENSITY		
Block	**Time**	**Visual**	**Perm. test**	**Bayes**	**Visual**	**Perm. test**	**Bayes**	**Visual**	**Perm. test**	**Bayes**
1	20:46 PM	-	-	-	-	-	-	+	-	-
2	21:45 PM	-	-	-	-	-	-	-	-	-
3	23:29 PM	-	-	-	-	-	-	-	-	-
4	01:38 AM	+	-	+	-	-	-	+	-	+
5	04:33 AM	+	-	+	+	-	-	-	-	-
6	06:21 AM	+	-	+	+	-	-	-	-	-

+ indicates a positive result, - a negative result. For Bayes column, + anecdotal evidence; ++ moderate evidence; +++ strong evidence and ++++ very strong to extreme evidence.

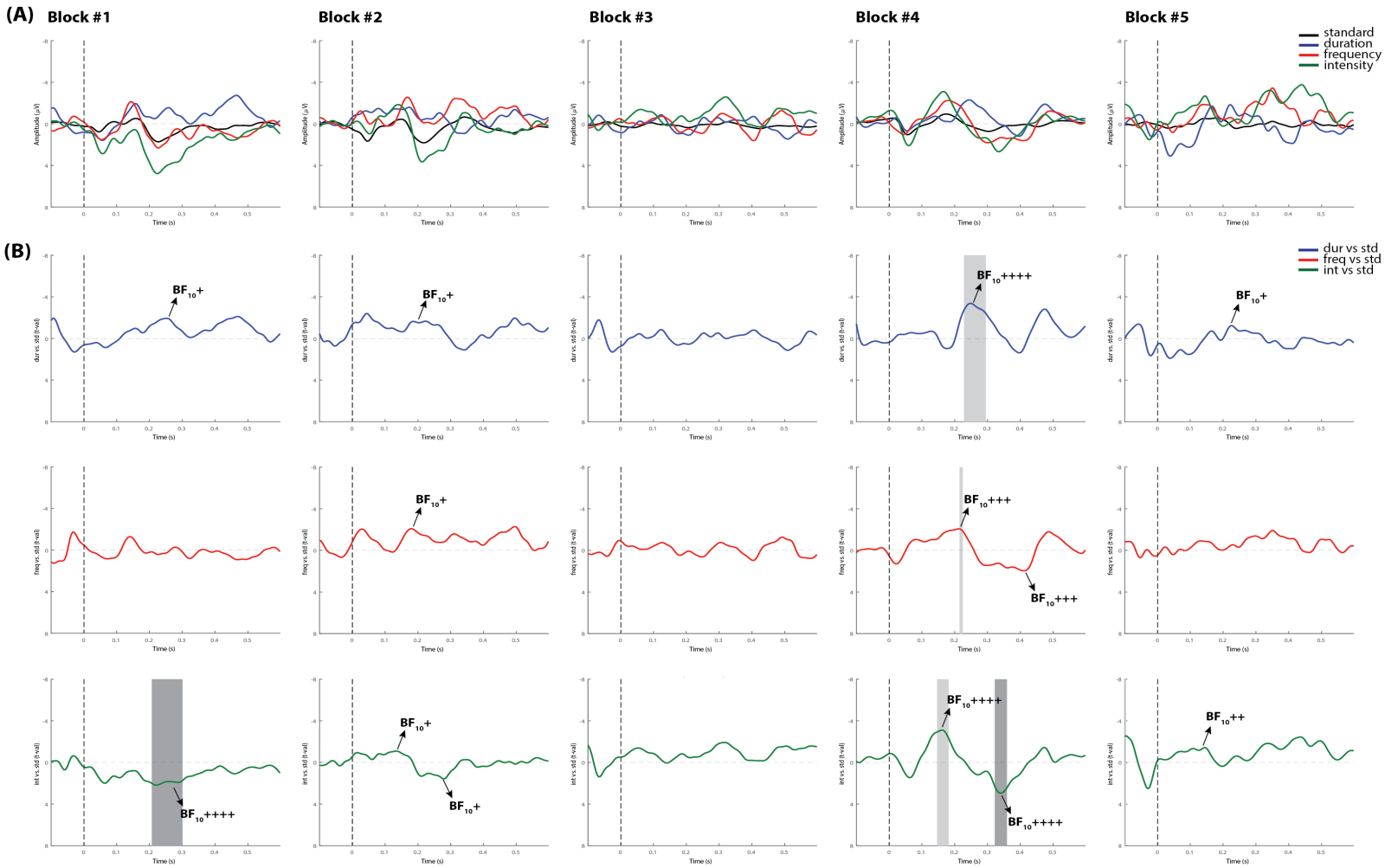

Figure 2.6: Individual ERPs and statistical findings of a coma patient (Patient 1) in the first five blocks on day 0. (B) Time course of the difference between deviants and standard stimuli expressed in units of *t*-values. Significant intervals for negative components are denoted by a light gray area, and those for positive components are denoted by a dark gray area. Black arrows show the latency of maximum bayes factors and the strength of evidence for $H1$: + anecdotal; ++ moderate; +++ strong and ++++ very strong to extreme.

2.4 Discussion

This is the first study to continuously track MMN responses in healthy controls over an extended period of time. In this study we tested controls for a maximum period of 12 hours as part of our ongoing EEG/ERP project to predict coma emergence and eventual functional outcome. The detection rate of the MMN was assessed over time at both the group and single-subject levels using three different methods: traditional visual inspection of the averaged ERPs, permutation *t*-test and Bayesian analysis. We also provided preliminary evidence of the utility of monitoring auditory deviance detection in three comatose patients over a 24 hour-period at two time points to predict coma outcome. We addressed the question of whether short-term fluctuations in MMN detectability may occur during full conscious awareness or is rather a feature of coma state (Armanfard et al., 2019); a finding that would have implications for prognostics of the timing of coma emergence and the clinical state at emergence. In turn, knowledge of the clinical state (i.e., UWS/VS, MCS, Locked-in) would encourage extended assessment of the cognitive state at emergence relevant to future rehabilitation efforts.

2.4.1 Tracking MMN in full conscious awareness

Our results showed that the MMN can be elicited and reliably detected over the course of 12 hours in healthy control subjects at the group level. Serial permutation-*t* tests applied on a within-group design were able to capture significant differences between the three types of deviants (duration, frequency, intensity) and standard stimuli in both MMN and P3a components in all recorded blocks. Bayesian analysis confirmed these findings, by showing "very strong to extreme" evidence. Consistent with the present results, several studies have shown that reliable MMNs can be recorded from session to session in a group of subjects (Pekkonen et al., 1995; Lew et al., 2007; Recasens and Uhlhaas, 2017). In these studies of test-retest reliability, the MMN responses are usually obtained from different sessions or blocks separated by longer time-intervals (i.e., approximately 1 month or more). Using different methods, we found that the MMN can be consistently replicated and detected over intervals of hours in a continuous testing session.

Additionally, while differences in MMN mean amplitude were observed between deviant types within the group, showing smaller MMN responses to frequency deviants, no main effects of blocks recorded over time or interaction were found. In line with prior findings, where this multi-deviant oddball paradigm was first implemented, the duration and intensity MMNs from a group of controls were slightly larger in amplitude than those produced to the frequency deviant tone (Todd et al., 2008). Furthermore, the fact that no habituation effects of the MMN amplitude were found over time (see Figure 2.2), suggests that the detectability of this component is not compromised by the repetition of the oddball paradigm. Its replicability in such short periods of time at group-level highlights the use of appropriate stimuli, and the application of efficient recording procedures as a way to reduce the variability of the recorded responses (Duncan et al., 2009).

On the other hand, the single-subject analysis in this study revealed that fluctuations in MMN detectability may be observed in some control subjects, depending on the deviant type, and the statistical method performed to confirm the presence of the component. As we have demonstrated and as illustrated in Table 2.2, the three methods showed a 100% detection rate of the MMN component for the duration deviant in all recorded blocks. However, the detection rate of subjects showing a reliable MMN response to frequency and intensity deviants at each recorded block was 65-71% and 82-100% respectively with Bayesian analysis, and 31-47% and 46-71% with permutations. This latter test was more conservative, showing that 3 out of 17 subjects did not exhibit significant MMNs to the frequency deviant in any of the recorded blocks, and one subject failed to show any response to the intensity deviant in any block.

Consistent with our findings, another Bayesian approach was recently reported as the most liberal in comparison to other five statistical methods on its ability to detect ERP effects (Kallionpää et al., 2019). This confirmation of neural responses through different statistical methods is especially important for coma research, as the ERPs from patients with brain injury at single-patient level exhibit notable differences in amplitude, latency and scalp distribution in comparison to healthy controls, which makes the visual identification of ERP components extremely challenging. Visual inspection of ERPs remains fairly common practice (Morlet and Fischer, 2014), but as discussed extensively in the literature (Luck and Gaspelin, 2017; Gabriel et al., 2016), it can introduce significant

bias. Besides, reliable visual inspection requires expertise that is not commonly available in the clinical setting (Connolly et al., 2019). Also, the wide availability of statistical methods, revealing large discrepancies among them is a problem for clinicians. Gabriel and colleagues compared six different methods previously used in coma studies to identify the MMN responses, and showed that all six methods confirmed an MMN response in only 4 out of 27 subjects, but at least the combination of two methods confirmed the presence of MMN in all control subjects (Gabriel et al., 2016). One may argue that these methods greatly differ in their mathematical algorithms and answer fundamentally different questions, and therefore should not be expected to provide the same results.

As stated by Naccache et al. (2016), it is an essential prerequisite of any functional brain test to show high sensitivity, especially to evaluate patients with brain injury and determine whether they will regain consciousness. The chosen methods should be able to detect the associated neural responses at the individual level in the vast majority of conscious controls. Otherwise, their use in patient populations could complicate the interpretation of the results. That is, if frequency stimuli elicit robust MMN responses at the group level in all recorded blocks, but such findings are not powerful at the single-subject level, then their use for clinical practice will be limited. Duration deviants, however, have been consistently reported throughout the clinical literature to be more sensitive than frequency deviants to measure neurological changes in various medical conditions (Michie et al., 2000; Chen et al., 2020; O'Reilly and O'Reilly, 2021) and as a consequence promise greater clinical utility.

2.4.2 Tracking MMN in coma

Data from three comatose patients revealed that the MMN component was present in at least one block per recording session by using the three methods of analysis, but fluctuated in detectability over the course of 24 hours. This fluctuation was not observed in healthy controls for the duration deviant, which supports the hypothesis that the MMN responses may be present only transiently in the coma state (Armanfard et al., 2019). As expected, most of the blocks where the MMN was confirmed to be present, corresponded to the duration-deviant condition in two comatose patients (Patient 1 and

2). Multivariate analysis has demonstrated a better discrimination between standard and duration deviants than other types of deviant-stimuli in comatose patients (Tzovara et al., 2015), which is in line with the choice of using duration deviants in previous coma studies (Fischer et al., 1999; Daltrozzo et al., 2009).

Similar to controls, the Bayesian analysis was more sensitive in capturing more blocks with reliable MMN and P3a responses than the permutation *t*-test in the comatose patients in both testing days. As displayed in the example in Figure 2.6, only one block (block 4) out of the first five recorded blocks showed significant MMN responses with all methods. In most cases where the ERP components were significantly detected by permutations, the Bayesian analysis served as a confirmatory test by indicating "moderate", "strong" or "very strong to extreme" evidence of the response. In the opposite direction, where the MMN was not significant by using permutations, but could be judged to be present through visual inspection, the Bayesian test would indicate in most cases weak or "anecdotal" evidence of response.

While the MMN has been reported to be a strong predictor of coma emergence and good functional outcome (Fischer et al., 2004; Luauté et al., 2005; Daltrozzo et al., 2007), we are fully aware that multiple factors might affect the patients' final outcome. For instance, multiple systemic complications mostly associated with infections are very likely to occur in critically ill patients, leading to further deterioration of their clinical status. Patient 1, for example, who showed more reliable MMN responses over time in comparison to the other patients, had the worst clinical outcome (i.e., death) after withdrawal of life support. In one of the first studies of Fischer and colleagues, three patients who had exhibited a MMN response failed to regain consciousness: one developed complications of neurosurgery, the second had organ failure complications and the third died of cardiac failure (Fischer et al., 1999). Using a a different MMN paradigm and a multivariate decoding algorithm, Tzovara's work also demonstrated intact auditory discrimination in comatose patients who eventually died (Tzovara et al., 2013). Consistent with these results, the robust presence of the MMN in Patient 1 is not surprising and could have indicated the patient's chance of emergence prior to unexpected complications.

One could argue that the "spontaneous" opening of the right eye in Patient 1 (without tracking or saccadic eye movements to stimuli) during the second recording (see

Table 2.1), suggests that this patient was probably emerging and transitioning to UWS. Although we cannot rule out this possibility, it was recently claimed that some comatose patients, particularly those with supratentorial, infratentorial or global brain insults, may defy the classical definition of coma (i.e., unarousable unresponsiveness with absent sleep cycles and closed eyes) by showing eye-opening. (Kondziella and Frontera, 2021). Coma with eye opening, according to these authors, differs from the UWS in its clinical trajectory (tendency to worsening rather than stabilization) and absence of sleep-wake cycles. The authors also stated that behavioral scales, such as the Glasgow Coma Scale and the FOUR score, can yield misleading results and overly optimistic outcome estimations for comatose patients with eye opening. Unfortunately, we did not use other more sensitive diagnostic tools (e.g., Coma Recovery Scale-Revised) to confirm whether the patient was in UWS after day 3.

The other two patients in the present study emerged from coma, but exhibited different functional outcomes. Patient 2 emerged three days following the first EEG assessment and after a year showed a positive functional outcome (good recovery). Patient 3, however, was transferred to a different hospital and then to a chronic care facility, with a diagnosis of VS/UWS. Regardless of the functional outcome, the MMN was present in at least a single recording occasion for each patient, which highlights the MMN as a biomarker to predict coma emergence and outcome.

In general, the variability in the presence of the MMN component in these patients may be explained by their brain injuries and fluctuations in responsiveness inherent to DOC. Severe brain damage may alter ERP amplitude and topography, and cause temporal delays and inter-trial variability in comatose patients as result of white matter impairments and cortical dysfunction (Piarulli et al., 2015). Perhaps physiological artifacts (e.g., increased slow wave activity) and the inherent environmental artifacts of the intensive care settings may have added extra noise to the signal for the MMN to be objectively detected across all blocks. More extensive data collection is necessary to clarify the mechanisms behind these fluctuations.

2.4.3 Limitations and ethical implications

Our small sample-size limits the generalization of our findings and requires further replication in future work. Nevertheless, we consider these results relevant and very promising as they can serve as a foundation upon which to develop monitoring techniques for detecting transient periods associated with partial consciousness in patients with severe brain injury. Although it is challenging to run extended EEG studies without frequent interruptions in ICU environments, the recording of multiple blocks of data per day in a larger population would be ideal for tracking the trajectory of patients and identify those with potential for recovery.

Our different analysis methods used non-identical information about the waveforms, such as the selection of the time points. For instance, the permutation *t*-test was applied to the whole ERP time window in order to identify the significant latency windows of the MMN and P3a components, whereas the Bayesian analysis was applied to narrower time windows of interest. This approach of doing Bayesian test post-hoc after convincing results are obtained with permutations seems methodologically unnecessary. However, given that permutation *t*- tests are fairly conservative and showed more evidence in favor of null effects in comatose patients, the Bayesian evidence, even "weak or anecdotal" may still be valuable for this clinical population.

Importantly, the medical team responsible for patient care were blind to our results, which were never used to influence any clinical decision for treatment or the maintenance/withdrawal of life-sustaining therapies. The presence or absence of MMN alone did not impact such decisions. However, in the not too distant future it is apparent that the MMN, in combination with other potential biomarkers, could help critical care teams improve coma prognosis by relying on objective evidence rather than "perceptions of unfavourable prognosis for meaningful neurologic recovery" (Turgeon et al., 2011, p. 01) in making decisions about withdrawal of life-support within days of admission (see also, (Mayer and Kossoff, 1999; Becker et al., 2001; Naidech et al., 2009; Turgeon et al., 2013)).

2.5 Conclusions

The results of the present study demonstrate that the MMN responses elicited by duration deviant stimuli are consistently detected over time in healthy controls, at both the group and single-subject levels. This finding supports the use of the MMN elicited by duration deviants as a promising clinical tool for monitoring functional changes associated with coma awakening and potential return to consciousness. Preliminary findings in three acute coma patients, recorded over 24 hours, provide further evidence that the MMN is present in coma, but can be transient (i.e., waxes and wanes) across hours. This highlights that regular and repeated assessments are extremely important for clinically-appropriate usage of the MMN as a neurophysiological predictor of coma emergence.

Conflict of Interest Statement

The authors declare that the research was conducted in the absence of any commercial or financial relationships that could be construed as a potential conflict of interest.

Funding

This study is funded by the Collaborative Health Research Projects (CHRP) opportunity made possible by the Canadian Institutes of Health Research (CIHR; grant number CPG158287) and the Natural Sciences and Engineering Research Council of Canada (NSERC; grant number CHRP 523461-18) and NSERC Discovery Grant (RGPIN-2016-06633). In-kind support towards equipment, software licences and scientific consultation is provided by Brain Vision Solutions. In-kind support for patient identification and research assessment is provided by Hamilton Health Sciences (HHS). The design, management, analysis and reporting of the study are entirely independent of the funders.

Acknowledgments

The authors are grateful to the nursing staff for supporting with data collection in the Hamilton General Hospital. We would also like to thank Hope Morrison for her coordination, as well as Kiersten Mangold, Gwenyth Lu and Adeba Khogiani as members of the Language, Memory and Brain (LMB) lab, and the ARiEAL Research Center for assisting with the study.

References

Armanfard, N., Komeili, M., Reilly, J. P., and Connolly, J. F. (2019). A Machine Learning Framework for Automatic and Continuous MMN Detection with Preliminary Results for Coma Outcome Prediction. *IEEE J. Biomed. Heal. Informatics*, 23(4):1794–1804.

Atkinson, R. J., Fulham, W. R., Michie, P. T., Ward, P. B., Todd, J., Stain, H., Langdon, R., Thienel, R., Paulik, G., Cooper, G., Anthes, L., Bowen, D., Case, V., Clark, S., Collins-Langworthy, J., Curtis, J., Ehlkes, T., Haddow, T., Lawrence, C., Logan, S., Loneragan, C., Loughland, C., Mathersul, D., O'Donnell, M., Paine, K., Sharp, T., Scott, R., Sculley, A., Seal, M., Thompson, P., Tooney, M., Tooney, P., Treen, L., Whitton, A., Rasser, P., Carr, V., Weickert, T. W., and Schall, U. (2017). Electrophysiological, cognitive and clinical profiles of at-risk mental state: The longitudinal minds in transition (MinT) study. *PLoS One*, 12(2).

Becker, K. J., Baxter, . A. B., Cohen, . W. A., Bybee, . H. M., Tirschwell, . D. L., Newell, . D. W., Winn, . H. R., and Longstreth, W. T. (2001). Withdrawal of support in intracerebral hemorrhage may lead to self-fulfilling prophecies. *Neurology*, 56(6):766–772.

Bishop, D. V. and Hardiman, M. J. (2010). Measurement of mismatch negativity in individuals: A study using single-trial analysis. *Psychophysiology*, 47(4):697–705.

Blain-Moraes, S., Boshra, R., Ma, H. K., Mah, R., Ruiter, K., Avidan, M., Connolly, J. F., and Mashour, G. A. (2016). Normal Brain Response to Propofol in Advance of Recovery from Unresponsive Wakefulness Syndrome. *Front. Hum. Neurosci.*, 10:1–6.

Chen, T. C., Hsieh, M. H., Lin, Y. T., Chan, P. Y. S., and Cheng, C. H. (2020). Mismatch

negativity to different deviant changes in autism spectrum disorders: A meta-analysis. *Clin. Neurophysiol.*, 131(3):766–777.

Chennu, S. and Bekinschtein, T. A. (2012). Arousal modulates auditory attention and awareness: Insights from sleep, sedation, and disorders of consciousness. *Front. Psychol.*, 3:65.

Collingridge, D. S. (2013). A Primer on Quantitized Data Analysis and Permutation Testing. *J. Mix. Methods Res.*, 7(1):81–97.

Connolly, J. F., Reilly, J. P., Fox-Robichaud, A., Britz, P., Blain-Moraes, S., Sonnadara, R., Hamielec, C., Herrera-Díaz, A., and Boshra, R. (2019). Development of a point of care system for automated coma prognosis: a prospective cohort study protocol. *BMJ Open*, 9:29621.

Daltrozzo, J., Wioland, N., Mutschler, V., and Kotchoubey, B. (2007). Predicting coma and other low responsive patients outcome using event-related brain potentials: A meta-analysis. *Clin. Neurophysiol.*, 118(3):606–614.

Daltrozzo, J., Wioland, N., Mutschler, V., Lutun, P., Calon, B., Meyer, A., Pottecher, T., Lang, S., Jaeger, A., and Kotchoubey, B. (2009). Cortical information processing in Coma. *Cogn. Behav. Neurol.*, 22(1):53–62.

Duncan, C. C., Barry, R. J., Connolly, J. F., Fischer, C., Michie, P. T., Näätänen, R., Polich, J., Reinvang, I., and Van Petten, C. (2009). Event-related potentials in clinical research: Guidelines for eliciting, recording, and quantifying mismatch negativity, P300, and N400. *Clin. Neurophysiol.*, 120(11):1883–1908.

Dykstra, A. R., Cariani, P. A., and Gutschalk, A. (2017). A roadmap for the study of conscious audition and its neural basis. *Phil. Trans. R. Soc. B*, 372(1714):20160103.

Dykstra, A. R. and Gutschalk, A. (2015). Does the mismatch negativity operate on a consciously accessible memory trace? *Sci. Adv.*, 1(10):e1500677.

Escera, C., Alho, K., Winkler, I., and Näätänen, R. (1998). Neural mechanisms of involuntary attention to acoustic novelty and change. *J. Cogn. Neurosci.*, 10(5):590–604.

Fischer, C., Luauté, J., Adeleine, P., and Morlet, D. (2004). Predictive value of sensory and cognitive evoked potentials for awakening from coma. *Neurology*, 63(4):669–673.

Fischer, C., Morlet, D., Bouchet, P., Luaute, J., Jourdan, C., and Salord, F. (1999). Mismatch negativity and late auditory evoked potentials in comatose patients. *Clin. Neurophysiol.*, 110(9):1601–1610.

Fitzgerald, K. and Todd, J. (2020). Making Sense of Mismatch Negativity. *Front. Psychiatry*, 11:468.

Gabriel, D., Muzard, E., Henriques, J., Mignot, C., Pazart, L., André-Obadia, N., Ortega, J. P., and Moulin, T. (2016). Replicability and impact of statistics in the detection of neural responses of consciousness. *Brain*, 139(6):e30.

Giacino, J. T., Fins, J. J., Laureys, S., and Schiff, N. D. (2014). Disorders of consciousness after acquired brain injury: The state of the science. *Nat. Rev. Neurol.*, 10(2):99–114.

Giacino, J. T., Katz, D. I., Schiff, N. D., Whyte, J., Ashman, E. J., Ashwal, S., Barbano, R., Hammond, F. M., Laureys, S., Ling, G. S., Nakase-Richardson, R., Seel, R. T., Yablon, S., Getchius, T. S., Gronseth, G. S., and Armstrong, M. J. (2018). Comprehensive Systematic Review Update Summary: Disorders of Consciousness: Report of the Guideline Development, Dissemination, and Implementation Subcommittee of the American Academy of Neurology; the American Congress of Rehabilitation Medicine; and the. In *Arch. Phys. Med. Rehabil.*, volume 99, pages 1710–1719. W.B. Saunders.

Heinke, W., Kenntner, R., Gunter, T. C., Sammler, D., Olthoff, D., and Koelsch, S. (2004). Sequential Effects of Increasing Propofol Sedation on Frontal and Temporal Cortices as Indexed by Auditory Event-related Potentials. In *Anesthesiology*, volume 100, pages 617–625. American Society of Anesthesiologists.

Jeffreys, H. (1961). Theory of probability: Oxford university press. *New York*, page 472.

Jennett, B. and Bond, M. (1975). ASSESSMENT OF OUTCOME AFTER SEVERE BRAIN DAMAGE: A Practical Scale. *Lancet*, 305(7905):480–484.

Johnson, E. L. and Kaplan, P. W. (2019). Clinical neurophysiology of altered states of consciousness: Encephalopathy and coma. In *Handb. Clin. Neurol.*, volume 161, pages 73–88. Elsevier B.V.

Kallionpää, R. E., Pesonen, H., Scheinin, A., Sandman, N., Laitio, R., Scheinin, H., Revonsuo, A., and Valli, K. (2019). Single-subject analysis of N400 event-related potential component with five different methods. *Int. J. Psychophysiol.*, 144:14–24.

Kane, N. M., Butler, S. R., and Simpson, T. (2000). Coma outcome prediction using event-related potentials: P(3) and mismatch negativity. *Audiol. Neurootol.*, 5(3-4):186–91.

Kondziella, D., Bender, A., Diserens, K., van Erp, W., Estraneo, A., Formisano, R., Laureys, S., Naccache, L., Ozturk, S., Rohaut, B., Sitt, J. D., Stender, J., Tiainen, M., Rossetti, A. O., Gosseries, O., and Chatelle, C. (2020). European Academy of Neurology guideline on the diagnosis of coma and other disorders of consciousness. *Eur. J. Neurol.*, 27(5):741–756.

Kondziella, D. and Frontera, J. A. (2021). Pearls & Oy-sters: Eyes-Open Coma. *Neurology*, 96(18):864–867.

Kraemer, H. C. (2019). Is It Time to Ban the P Value? *JAMA Psychiatry*, 76(12):1219–1220.

Lee, M. D. and Wagenmakers, E. J. (2013). *Bayesian cognitive modeling: A practical course*. Cambridge University Press.

Lew, H. L., Gray, M., and Poole, J. H. (2007). Temporal stability of auditory event-related potentials in healthy individuals and patients with traumatic brain injury. *J. Clin. Neurophysiol.*, 24(5):392–397.

Luauté, J., Fischer, C., Adeleine, P., Morlet, D., Tell, L., and Boisson, D. (2005). Late auditory and event-related potentials can be useful to predict good functional outcome after coma. *Arch. Phys. Med. Rehabil.*, 86(5):917–923.

Luck, S. J. and Gaspelin, N. (2017). How to get statistically significant effects in any ERP experiment (and why you shouldn't). *Psychophysiology*, 54(1):146–157.

Makeig, S., Bell, A., Jung, T.-P., and Sejnowski, T. J. (1995). Independent component analysis of electroencephalographic data. *Advances in neural information processing systems*, 8.

Mayer, S. and Kossoff, S. B. (1999). Withdrawal of life support in the neurological intensive care unit. *Neurology*, 52(8):1602–1609.

Michie, P. T., Budd, T. W., Todd, J., Rock, D., Wichmann, H., Box, J., and Jablensky, A. V. (2000). Duration and frequency mismatch negativity in schizophrenia. *Clin. Neurophysiol.*, 111(6):1054–1065.

Morlet, D. and Fischer, C. (2014). MMN and novelty P3 in coma and other altered states of consciousness: A review. *Brain Topogr.*, 27(4):467–479.

Näätänen, R., Kujala, T., and Light, G. (2019). *Mismatch negativity: a window to the brain*. Oxford University Press.

Naccache, L., Puybasset, L., Gaillard, R., Serve, E., and Willer, J. C. (2005). Auditory mismatch negativity is a good predictor of awakening in comatose patients: A fast and reliable procedure [1]. *Clin. Neurophysiol.*, 116(4):988–989.

Naccache, L., Sitt, J., King, J. R., Rohaut, B., Faugeras, F., Chennu, S., Strauss, M., Valente, M., Engemann, D., Raimondo, F., Demertzi, A., Bekinschtein, T., and Dehaene, S. (2016). Reply: Replicability and impact of statistics in the detection of neural responses of consciousness. *Brain*, 139(6):e31.

Naidech, A. M., Bernstein, R. A., Sarice, A. E., Ae, L. B., Garg, R. K., Storm, A. E., Ae, L., Bendok, B. R., Hunt, A. H., Ae, B., and Bleck, T. P. (2009). How Patients Die After Intracerebral Hemorrhage. *Neurocrit. Care*, 11(1):45–49.

Oostenveld, R., Fries, P., Maris, E., and Schoffelen, J. M. (2011). FieldTrip: Open source software for advanced analysis of MEG, EEG, and invasive electrophysiological data. *Comput. Intell. Neurosci.*, 2011.

O'Reilly, J. A. and O'Reilly, A. (2021). A Critical Review of the Deviance Detection Theory of Mismatch Negativity. *NeuroSci*, 2(2):151–165.

Pekkonen, E., Rinne, T., and Näätänen, R. (1995). Variability and replicability of the mismatch negativity. *Electroencephalogr. Clin. Neurophysiol. Evoked Potentials*, 96(6):546–554.

Piarulli, A., Charland-Verville, V., and Laureys, S. (2015). Cognitive auditory evoked potentials in coma: Can you hear me? *Brain*, 138(5):1129–1131.

Recasens, M. and Uhlhaas, P. J. (2017). Test–retest reliability of the magnetic mismatch negativity response to sound duration and omission deviants. *Neuroimage*, 157:184–195.

Sawilowsky, S. S. (2009). Very large and huge effect sizes. *J. Mod. Appl. Stat. Methods*, 8(2):597–599.

Schnakers, C. (2020). Update on diagnosis in disorders of consciousness. *Expert Rev. Neurother.*, 20(10):997–1004.

Sullivan, G. M. and Feinn, R. (2012). Using Effect Size—or Why the P Value Is Not Enough. *J. Grad. Med. Educ.*, 4(3):279–282.

Sussman, E. S., Chen, S., Sussman-Fort, J., and Dinces, E. (2014). The five myths of MMN: Redefining how to Use MMN in basic and clinical research. *Brain Topogr.*, 27(4):553–564.

Tavakoli, P., Dale, A., Boafo, A., and Campbell, K. (2019). Evidence of P3a during sleep, a process associated with intrusions into consciousness in the waking state. *Front. Neurosci.*, 12:1028.

Todd, J., Michie, P. T., Schall, U., Karayanidis, F., Yabe, H., and Näätänen, R. (2008). Deviant Matters: Duration, Frequency, and Intensity Deviants Reveal Different Patterns of Mismatch Negativity Reduction in Early and Late Schizophrenia. *Biol. Psychiatry*, 63(1):58–64.

Turgeon, A. F., Lauzier, F., Burns, K. E., Meade, M. O., Scales, D. C., Zarychanski, R., Moore, L., Zygun, D. A., McIntyre, L. A., Kanji, S., Hébert, P. C., Murat, V., Pagliarello, G., and Fergusson, D. A. (2013). Determination of neurologic prognosis and clinical decision making in adult patients with severe traumatic brain injury: A

survey of canadian intensivists, neurosurgeons, and neurologists. *Crit. Care Med.*, 41(4):1086–1093.

Turgeon, A. F., Lauzier, F., Simard, J. F., Scales, D. C., Burns, K. E., Moore, L., Zygun, D. A., Bernard, F., Meade, M. O., Dung, T. C., Ratnapalan, M., Todd, S., Harlock, J., and Fergusson, D. A. (2011). Mortality associated with withdrawal of life-sustaining therapy for patients with severe traumatic brain injury: A Canadian multicentre cohort study. *CMAJ*, 183(14):1581–1588.

Tzovara, A., Rossetti, A. O., Spierer, L., Grivel, J., Murray, M. M., Oddo, M., and De Lucia, M. (2013). Progression of auditory discrimination based on neural decoding predicts awakening from coma. *Brain*, 136(1):81–89.

Tzovara, A., Simonin, A., Oddo, M., Rossetti, A. O., and De Lucia, M. (2015). Neural detection of complex sound sequences in the absence of consciousness. *Brain*, 138(5):1160–1166.

Wannez, S., Heine, L., Thonnard, M., Gosseries, O., and Laureys, S. (2017). The repetition of behavioral assessments in diagnosis of disorders of consciousness. *Ann. Neurol.*, 81(6):883–889.

Wellek, S. (2017). A critical evaluation of the current "p-value controversy". *Biometrical J.*, 59(5):854–872.

Wijdicks, E. F. (2020). Predicting the outcome of a comatose patient at the bedside. *Pract. Neurol.*, 20(1):26–33.

Chapter 3

Decoding auditory ERPs for neurophysiological monitoring in coma

Preface: This chapter includes a follow-up analysis to the previous study, detailing a machine learning technique known as multivariate pattern analysis to investigate whether single subjects showed differential electrophysiological responses elicited by standard versus deviant sounds. This approach is not focused on detecting specific ERP components, but rather on an automatic way to predict auditory discrimination at single-subject level. We then evaluated whether this methodology is feasible for neurophysiological assessment underlying auditory deviance detection in comatose patients.

Abstract

Multivariate decoding approaches applied to ERP data, and particularly using mismatch negativity paradigms, have been shown to provide valuable information about patient's chances to survive and emerge from coma. Using a 3-deviant oddball paradigm, this study implements multivariate pattern analysis to automatically quantify the neural discrimination between duration deviant and standard sounds at the single-subject level in healthy controls and in three comatose patients. One EEG recording, containing up to five blocks of an oddball paradigm, was performed in control subjects over a 12 hour period. For patients, two EEG recordings were conducted 3 days apart for up to 24 hours,

denoted as day 0 and day 3, respectively. All trials of up to five recording blocks of the oddball paradigm were concatenated in superblocks and analyzed as single subject datasets. Results showed that healthy controls exhibited a classification performance above-chance level (50%) after stimulus onset, during the latency intervals associated with the MMN and the P3 components. While none of the comatose patients exhibited significant decoding results at the first superblock on day 0, two patients showed some intervals with significantly above-chance performance at about the second half of this day, and all of them reflected significant results on day 3. These preliminary findings showed that the implemented multivariate analysis can accurately classify auditory neural responses at single subject level, and provide evidence of a slight improvement in auditory discrimination over time in coma patients. Further research is needed, using a greater number of patients to determine whether these improvements can predict emergence from coma and recovery of consciousness.

3.1 Introduction

Brain decoding approaches that incorporate machine learning tools on EEG/ERP data have been increasingly embraced by cognitive neuroscience, and are potentially valuable in determining how the representation of information differs between clinical and non clinical populations. The recent advances of these methods have enabled researchers to conduct data-driven investigation where complex neural patterns in large datasets can be identified automatically, without relying on specialist expertise.

Multivariate pattern analysis (MVPA), also referred as multivariate decoding, is a technique mainly used to distinguish between experimental conditions based on the observed patterns of brain responses. It derives from the fields of pattern recognition and supervised machine learning and is useful to track the temporal sequence of various levels of information processing, from sensory to high-level cognitive processes (Fahrenfort et al., 2018; Carlson et al., 2019). The ERP research, which also seeks differences between conditions, uses traditional statistical methods such as *t*-test and analysis of variance (ANOVA) that follow a univariate approach (i.e., taking information from single-recording channels separately or from averaged signals across multiple channels).

In contrast, MVPA allows the exploitation of the multivariate and high-dimensional nature of EEG by taking into account the distribution of activity from multiple channels simultaneously.

In the context of brain-injured patients with disorders of consciousness, various auditory ERP components such as the MMN and P300, which are considered useful predictors of emergence from coma (Daltrozzo et al., 2009; Morlet and Fischer, 2014; Rodriguez et al., 2014), are often absent or challenging to detect at their classical scalp locations and time intervals (Piarulli et al., 2015). Also, the recognition of the presence or absence of these components is particularly difficult in intensive care patients due to the many sources of artifacts (e.g., the array of equipment at each ICU bed) and/or the drastic reduction in the amplitude of brain signals, make them difficult to isolate. This has encouraged the use of MVPA to provide a global measure of the information present in the signal rather than assessing for specific brain areas. It has been reported that multivariate decoding analysis can predict survival rates in comatose patients (Tzovara et al., 2013, 2015; Pfeiffer et al., 2018), and automatically classify the patients' level of consciousness (Sitt et al., 2014).

One of the major advantages of MVPA is its sensitivity in detecting subtle changes in the patterns of neural activity that may not be picked up by more traditional ERP analysis. The use of some classifiers trained to identify specific features in the data (e.g., EEG samples at specific channels and time points) can deal better with noise and artifacts in data. For example, a malfunctioning or very low impedance electrode would be removed or interpolated during a typical ERP preprocessing to assure data quality. Given that the classifiers in MVPA assign weights to each sensor, if the noisy electrode is not informative for the prediction, they can assign it a low weight and cancel its effect (Carlson et al., 2019). (Carlson et al., 2019). This methodology provides a single-time curve of classification, which helps to overcome the inherent issues of statistical correction for multiple comparisons across channels, and therefore provides scientists with a rapid interpretable signal at the whole-brain level with high temporal precision.

Another interesting metric derived from MVPA was introduced by King and Dehaene (2014) to characterize the temporal stability of the neural representations underlying different cognitive processes. Under this procedure, a classifier trained at a given time point of the trial, can also be tested at all available time points to determine whether

specific activation patterns (e.g., associated with the generation of the MMN and P300 components) persist or reoccur across time. The authors discussed in a comprehensive study the results of this so-called "temporal generalization method", and described different generalization patterns that can be distinguished across time (e.g., isolated, sustained, chain, reactivated patterns, and so on).

Here, we proposed the use of multivariate pattern analyses to discriminate the neural representations encoded in single-trial ERPs associated with auditory deviance detection in healthy controls, and showed evidence of its applicability in three comatose patients. Using the MMN dataset described in Chapter 2, we focused on a binary classification problem in order to predict whether a specific single-trial ERP measurement represents a standard or deviant trial. Methodological aspects that influence classification performance, such as the signal amplitude and the number of electrodes, were also considered in order to evaluate the feasibility of this decoding approach for the assessment of brain activity underlying auditory deviance detection in comatose patients.

3.2 Data collection and decoding analysis

EEG/ERP data were collected from 17 healthy controls (one 12-hour recording each) and 3 comatose patients (up to 24-hour recording each) as part of an ongoing coma study (Connolly et al., 2019). For patients, two recordings were conducted 3 days apart, denoted as day 0 and day 3, respectively. For the purposes of this study, only the recording blocks of an auditory oddball paradigm outlined in Chapter 2 (section 2.2.3) were analyzed. Demographic and information of controls and patients are available in section 2.2).

MVPA was implemented to quantify the differences in neural responses to standard vs duration deviants in control subjects and comatose patients. The analyses that are presented here were performed using custom written-MATLAB scripts (MathWorks Inc., USA) based on functions from the MVPA-Light toolbox (Treder, 2020) integrated in Fieldtrip (Oostenveld et al., 2011).

Given the large amount of data, all trials of up to five recording blocks of the oddball paradigm were concatenated to form a "superblock" per subject, which was then analyzed as a single subject dataset. Every healthy control had one superblock, while the comatose patients had two superblocks on day 0 and at least one superblock on day 3. In case of Patient 3, the resulting superblock on day 3 contained six recording blocks in total. This approach of concatenating a large number of trials was carried out to reduce trial-to-trial variability within subjects, and provide a global characterization of individual differences between the auditory responses within a long period of time.

3.2.1 Classification across time

Since oddball tasks designs are often unbalanced, we first re-balanced the model's design by applying undersampling correction (i.e., removing trials belonging to the standard condition as the overrepresented class). The methods of under or oversampling has been shown to prevent bias in classification, and improve the area under the curve (AUC), which is a widely-used quantitative measure of classification performance, calculated from the receiver operating characteristic (ROC) (Xue and Hall, 2015)

MVPA was then performed to discriminate between standard and deviant responses on 11 electrodes (F3, Fz, F4, C3, Cz, C4, P3, Pz, P4, T7, T8) as features for every time point separately, using a support-vector machine (SVM) classifier and the area under the curve (AUC) as a performance metric. These 11 electrodes were the minimum number of channels shared in common for all controls and patients. The input to the model was a 3-D [trials x features x time points] matrix, and a vector of class labels (i.e., standard and deviants).

Preprocessing included a "z-scoring" followed by a "sample-averaging" procedure as nested operations within a cross-validation analysis. A nested preprocessing essentially applies operations to the training and test sets separately. For instance, a nested z-scoring operation, as described in Treder (2020), implies that on the training data the means and standard deviations are computed, and therefore the train data are z-scored (normalized) accordingly. For the test data, the same mean and standard deviation are used to center and scale the data. As result of a "sample-averaging" operation, trials from the same

class are split into multiple groups and subsequently the dataset is replaced by the group means as a way to create new observations. Groups of 5 averaged trials were implemented for consistency across all subjects and patients, as increasing the number of trials improved slightly the classification performance, but led to a larger variability. A 5-fold cross-validation with 10 repetitions was implemented to get a more realistic estimate of the classification performance in discriminating the two classes of auditory responses.

Lastly, a non-parametric permutation test was computed to assess whether the classifier performance (AUC) was significantly above-chance level (50%). An AUC of 50% is uninformative and implies random guessing whereas a score of 100% amounts to perfect classification. The permutation test creates a null distribution by shuffling the class labels (i.e., standard and deviants) and repeating the multivariate decoding analysis multiple times. This permutation test was based on 100 random permutations, using the T_{max} statistic to correct for multiple comparisons.

3.2.2 Generalization across time

An extension of the MVPA called "temporal generalization" was performed to explore whether the classifier performance can be generalized to time periods with shared representations. (Cichy et al., 2014; King and Dehaene, 2014). That is, instead of training and testing the SVM classifier on data at each time point t, as described above, this one is tested across all possible time points t'. For example, if the classifier is trained to discriminate two activation patterns (e.g., standard versus duration deviants trials) at 200 ms, and is able to successfully classify such patterns at 250 ms, one may infer that there is similar underlying neural representation (or cognitive processing) at those time periods. This analysis yields a 2-D temporal generalization matrix of cross-validated metrics. Conventionally, these matrices are depicted with the y-axis denoting training time, and the x-axis denoting testing time or generalization. In each cell of the matrix, the AUC scores are summarized. Classifier trained and tested at the same time corresponds to the diagonal of the matrix, which is referred to as "diagonal decoding" and closely corresponds to the outcome computed in the previous analysis (subsection 3.2.1). In

contrast, if a matrix shows an off-diagonal pattern, it may indicate that the representation is stable (similar) over time or becomes reactivated at different times.

Additionally, a classification analysis across time (outlined above in section 3.2.1) was run on each single recording block collected for each patient in order to identify fluctuations in decoding performance during the day. Since the number of trials is more reduced in the single recording blocks compared to the superblocks, the sample averaging operation included a group of two averaged trials in the preprocessing.

3.2.3 Effects of data features on decoding performance

To evaluate whether the MVPA procedure is actually feasible to be used in coma patients, we investigated the effects of the signal amplitude, as well as the selected number of the electrodes on classification performance in the control group.

Firstly, the mean amplitudes of each individual superblock were computed over 50 and 100 ms periods surrounding the peak latency of each component of interest respectively (MMN: 80-230ms and P300: 250-350ms), and correlated with the maximum AUC scores found within those latency intervals.

Secondly, in order to assess whether the implemented decoding procedure (using 11 electrodes) preserved its predictive value for clinical purposes, we computed the proposed multivariate procedure using 64 electrodes, and compared the maximum AUC scores when reducing the number of electrodes from 64 to 11 using a paired-samples *t*-test.

Finally, a "searchlight" approach with 5-k fold cross-validation as detailed in (Treder, 2020), using a maximum of five ERPs (averaged responses) from each control subject, was carried out to identify which electrodes discriminated better between conditions across subjects. We hypothesized that the selected 11 electrodes contained sufficient discriminative information for the classification. This approach was implemented at the baseline (ranging from -100 to 0 ms), and in 50-ms intervals after stimulus onset (from 50 to 550 ms).

3.3 Results

3.3.1 Single-trial decoding in control subjects

All control subjects exhibited significantly above-chance performance after stimulus onset, peaking within the latency intervals associated with the MMN (150-230 ms) and the P3a components (250-350 ms). Maximum AUC scores when discriminating duration deviants versus standard tones ranged from 80% to 94%. A summary of the individual results is shown in Table 3.1. Notice that seven subjects exhibited maximum scores within the P3a interval.

Table 3.1: Summary of maximum AUC scores for each individual control subject, including the standard deviation (SD), latency and the associated ERP components.

Subjects	AUC (%)	SD (%)	Latency (s)	ERP
1	0.94	0.03	0.294	P3a
2	0.82	0.04	0.156	MMN
3	0.81	0.06	0.154	MMN
4	0.86	0.05	0.162	MMN
5	0.90	0.03	0.269	P3a
6	0.89	0.05	0.255	P3a
7	0.88	0.04	0.271	P3a
8	0.80	0.06	0.212	MMN
9	0.85	0.85	0.267	P3a
10	0.87	0.05	0.222	MMN
11	0.89	0.03	0.195	MMN
12	0.91	0.05	0.212	MMN
13	0.89	0.06	0.208	MMN
14	0.80	0.07	0.199	MMN
15	0.92	0.06	0.267	P3a
16	0.85	0.06	0.271	P3a
17	0.81	0.11	0.201	MMN

The multivariate decoding results from a representative control subject are displayed in Figure 3.1. Classification performance was significant after stimulus onset at the latency intervals associated with the MMN, the P3a, and to lesser extent at time intervals preceding and following these components (see panel A). The diagonal of the temporal

generalization matrix (in panel B) indicated a succession of processing stages, analogous to the classification performance curve (shown in panel A).

Given the variability across trials within each subject, transient generalization patterns off-diagonal (yellow patches) were observed, but two of them were consistently present in most of the subjects. As illustrated in the example (see Figure 3.1B), the SVM classifier trained from 100 to 250 ms (corresponding to the time window of the MMN) generalized data at a later time, between 400 and 600 ms. Similarly, the training time points from 0 to 100 ms generalized around 250-300 ms.

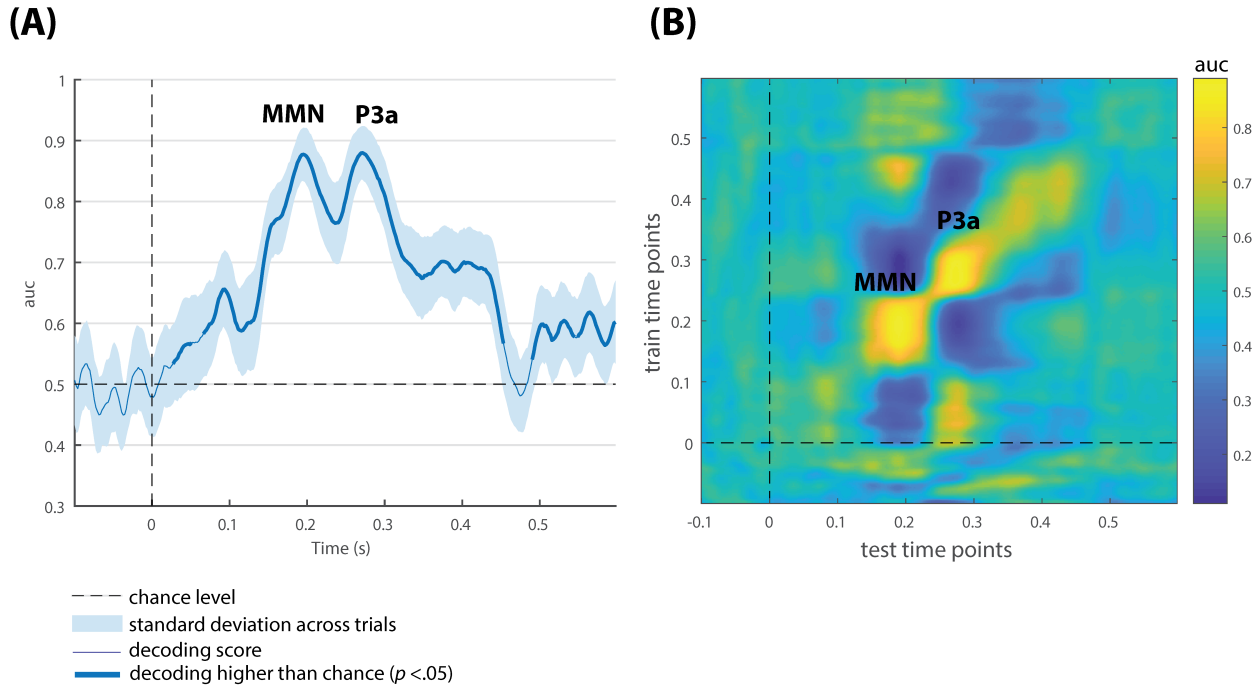

Figure 3.1: Multivariate decoding results of a representative control subject for duration deviant versus standard comparison. (A) Classification performance across time. The shaded area is the standard deviation across trials. The thick line indicates the time points where decoding is significantly higher than chance level. (B) Temporal generalization plot of decoding performance. Color bar indicates AUC scores.

3.3.2 Effects of amplitude and electrodes on decoding performance

Using a Pearson correlation test, the classification performance was found to be strongly correlated with the amplitude of both MMN ($r(15) = -0.668$, $p < 0.01$) and P3a components ($r(15) = 0.843$, $p < 0.01$) (see Figure 3.2).

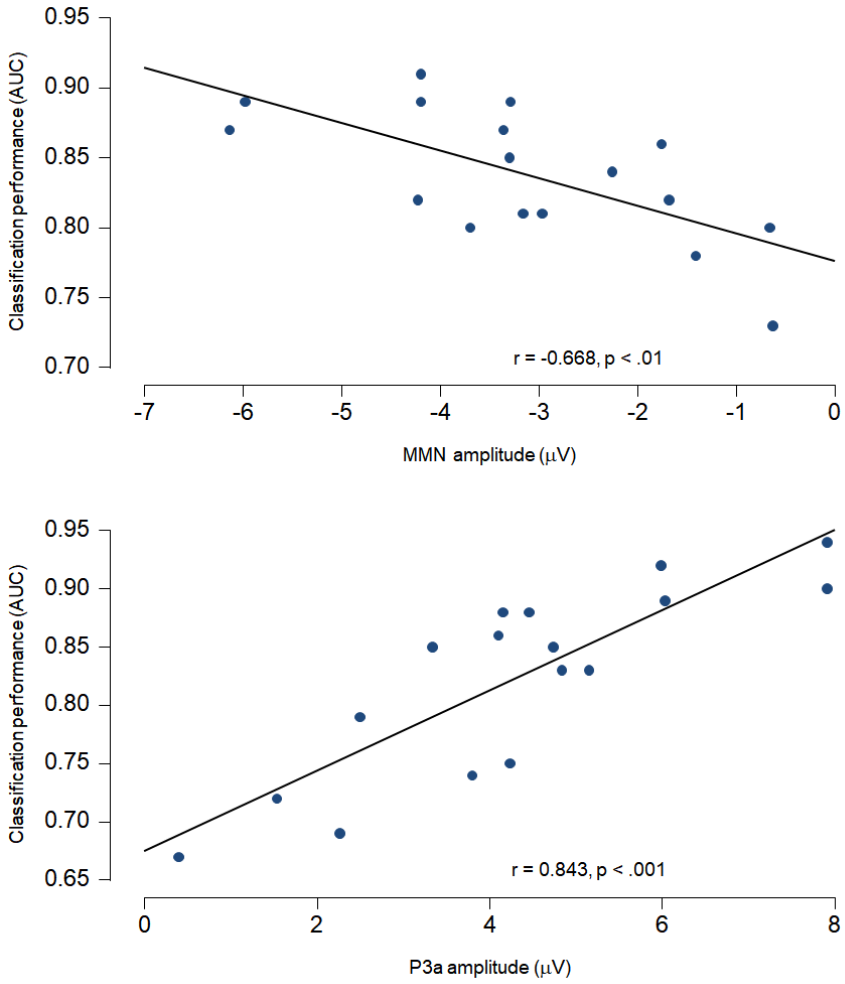

Figure 3.2: Correlation analysis of the individual classification performance with the ERP component amplitude were significant for both the MMN and P3a components.

The effect of reducing the number of electrodes from 64 to 11 on the classification performance is shown in Figure 3.3. After confirming assumptions of normality were met (Shapiro-Wilk test = 0.908, $p > 0.05$), the paired-sample t-test (panel A) showed no significant differences ($t(16)=1.49$, $p > 0.05$), which suggests that the selected electrodes

used in the present study were sufficient to provide discriminative information between conditions.

Figure 3.3 (panel B) showed the results of applying a searchlight MVPA across subjects. Topographic maps showed high decoding performance during the time intervals associated with the MMN/P3a complex (150-250 ms; 250-350 ms), with maximum values at frontocentral electrodes. Notice that the selected 11 electrodes are spatially distributed on the regions showing the highest AUC scores.

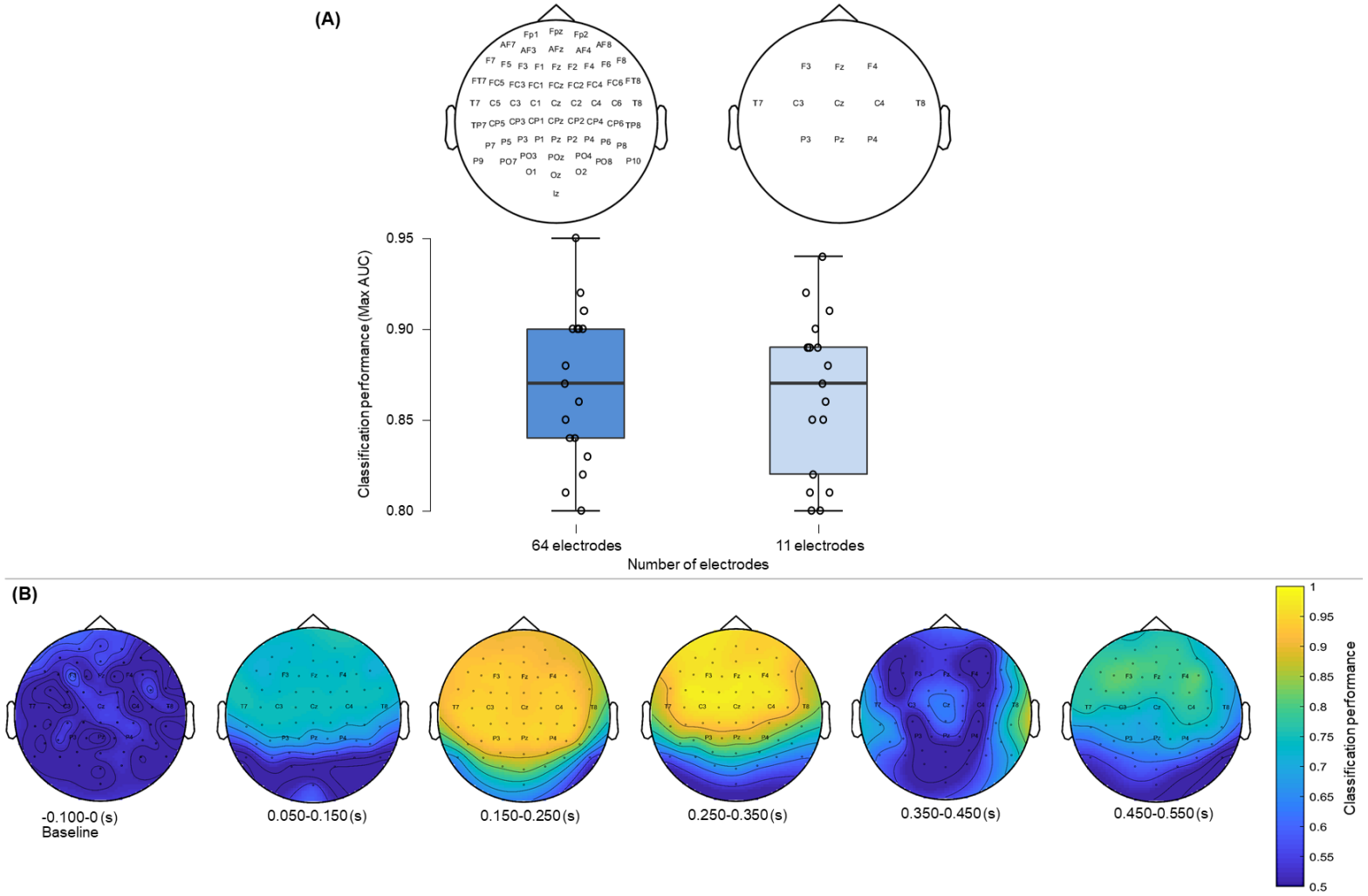

Figure 3.3: Effect of reduced number of electrodes on classification performance and searchlight analysis across subjects. (A) Paired-sample *t*-test revealed no significant differences in classification performance using 64 electrodes in comparison to 11 electrodes. (B) Searchlight MVPA computed over the baseline and 50 ms-time intervals after stimulus onset showed the electrodes that better discriminate between conditions.

3.3.3 Single-trial decoding in coma

The decoding results of the three comatose patients on each recording day are displayed in Figures 3.4 to 3.6. While none of the comatose patients exhibited significant results at the first superblock on day 0, the patients 2 and 3 displayed some intervals with significantly above-chance performance after stimulus onset at about the second half of day 0 (second superblock). Despite being reduced in comparison to controls, the classification performance was significantly above-chance on day 3 in all patients.

Patient 1 displayed significant decoding results in the two superblocks on day 3 (Figure 3.4). The first superblock showed maximum AUC scores around 65%, peaking at 205 ms, within the time window of the MMN component. The second superblock showed two consecutive intervals with above-chance performance (AUC scores around 59% and 62% respectively), suggesting the presence of the MMN/P3a complex. The temporal generalization matrices (on the right) displayed consistently these dynamical patterns of decoding performance on the diagonal.

Patient 2 who had shown reduced performance, but slightly higher than chance in the first recording session on day 0 (AUC scores$\sim$56%), increased the classification performance on day 3 up to 68 and 70% in intervals associated with the MMN and P3a components respectively (see Figure 3.5). A later AUC peak at 71% was also observed around 460 ms. During that day, this patient had showed behavioral signals of emergence from coma state: spontaneous eyes opening and withdrawal from pain as reflected in a GCS score of 9. Based on the study protocol, only a superblock consisting of two recording sessions were performed in patients emerging from coma. The temporal decoding matrix corresponding to the day 3 showed several activation patterns on the diagonal, suggesting the presence of the MMN/P3a complex followed by a late pattern of discrimination between 400 and 600 ms. Transient generalization patterns (off-diagonal yellow patches), were also observed at time points above and below the diagonal, suggesting that brain generators might be reactivated at a later time.

Patient 3 displayed maximum AUC of 63% around 120 ms at the second superblock on day 0, and AUC of 60% at an early time interval, close to 100 ms on day 3 (see Figure 3.6). The time generalization decoding matrices revealed early decoding, limited to the diagonal either associated with the latency of the MMN or the DRN component (i.e., a

deviant-related negativity, which represents a spatial-temporal summation of both N1 and MMN components) as described in Tavakoli et al. (2019).

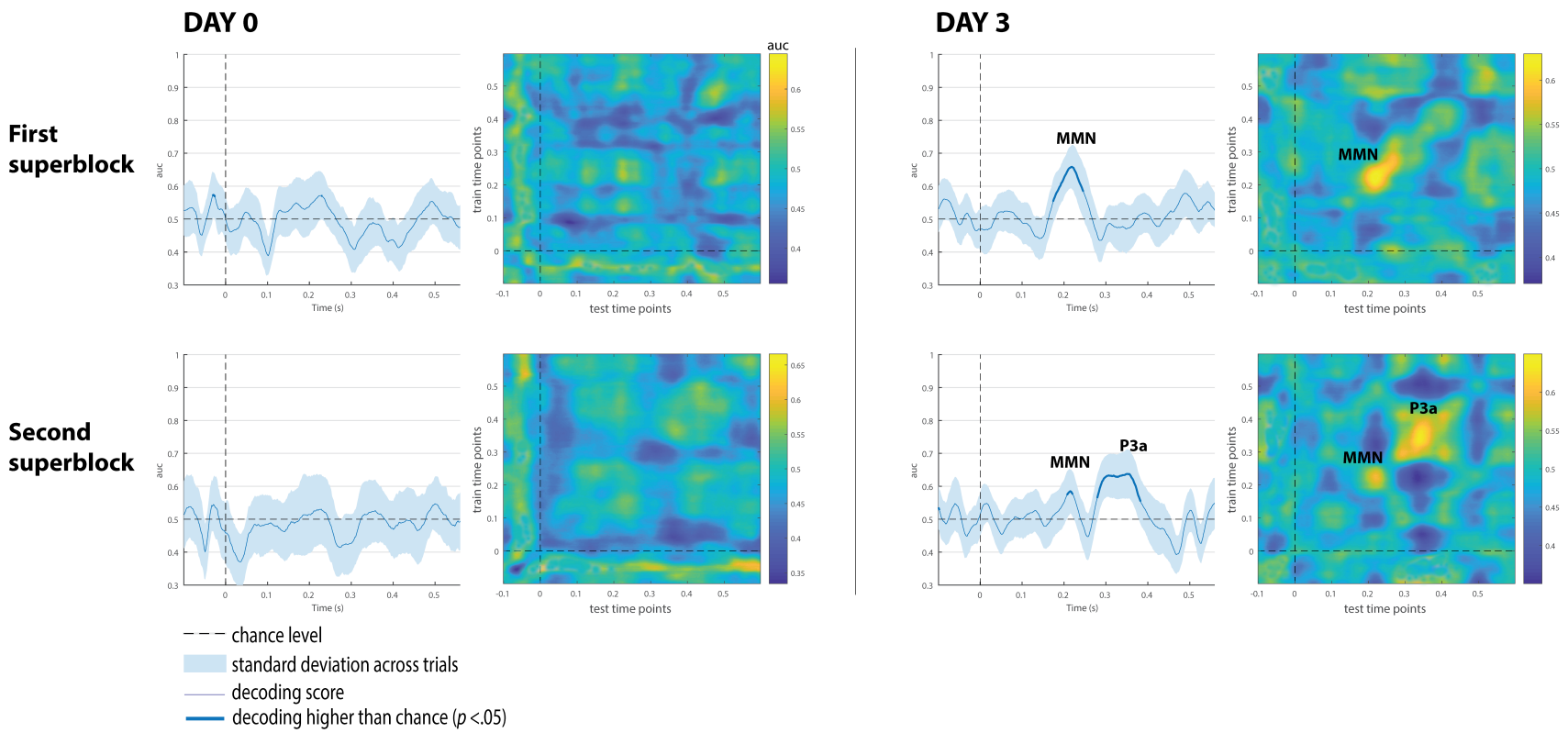

Figure 3.4: Multivariate decoding results of Patient 1 on day 0 and day 3. Color bar in the temporal generalization matrices (second and fourth column) indicates AUC scores.

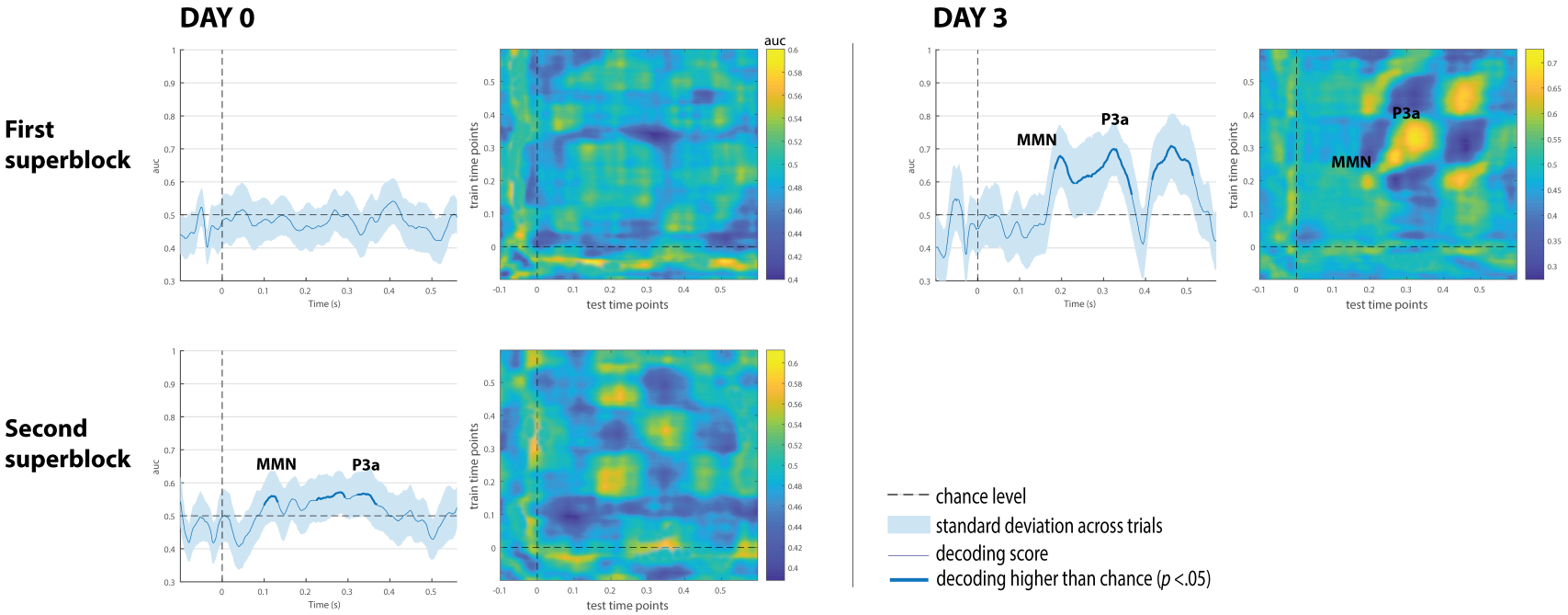

Figure 3.5: Multivariate decoding results of Patient 2 on day 0 and day 3. Color bar in the temporal generalization matrices (second and fourth column) indicates AUC scores.

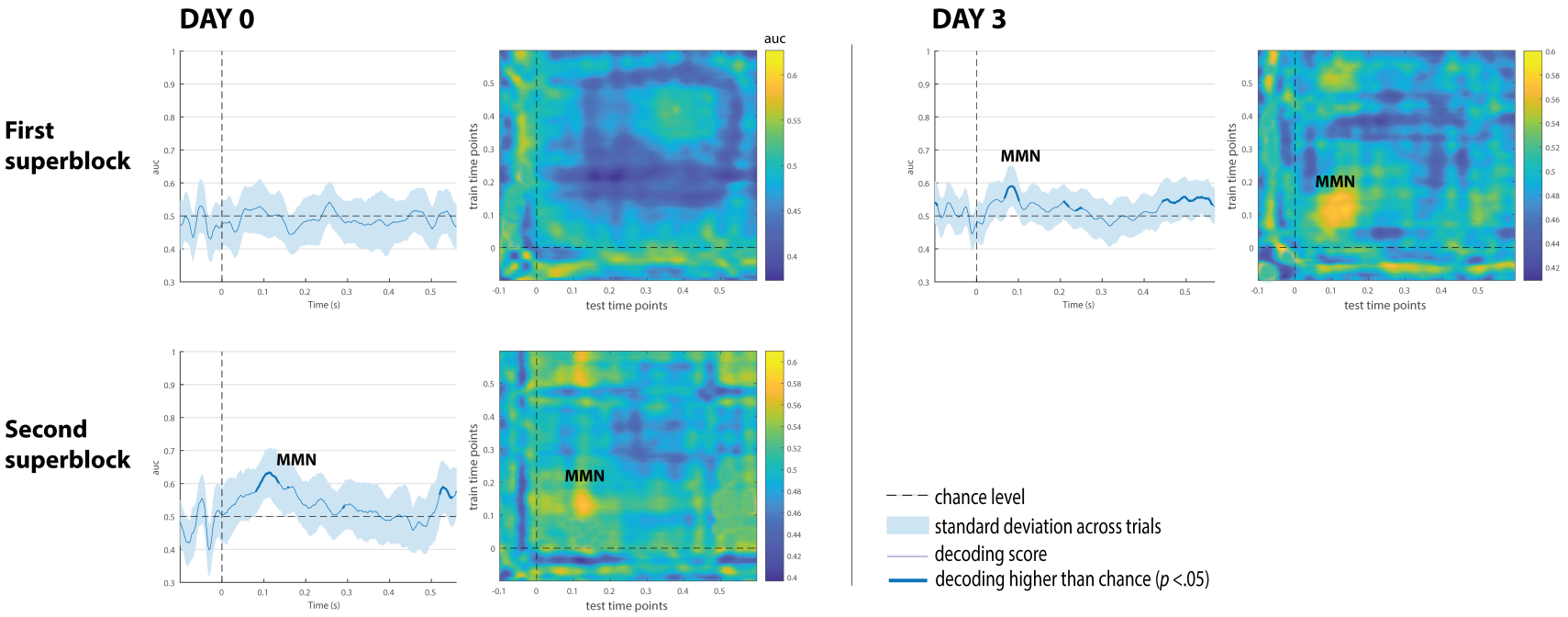

Figure 3.6: Multivariate decoding results of Patient 3 on day 0 and day 3. Color bar in the temporal generalization matrices (second and fourth column) indicates AUC scores.

3.3.4 Tracking decoding performance at each single block in coma

For patients, the classification analysis across time was also computed at each single recording block to track decoding fluctuations over time, and explore which single blocks contributed more to the global responses observed at each superblock.

As displayed in the figures 3.7 to 3.9, all patients showed significantly above-chance performance (with AUC scores ranging from 62 to 65%) only in one block (block 4) out of the five single blocks that were used to form the first superblock on day 0.

Patient 1 had the highest number of single blocks with significantly above-chance performance on day 3, particularly in the last five blocks (blocks 6 to 10), which explains why the second superblock on day 3 showed higher AUC scores.

Patient 2 exhibited significant results in four single blocks at about the second half of day 0 (included in the second superblock). This patient showed signals of awakening from coma on day 3, and therefore only two single recording blocks were collected. Interestingly, these single recordings exhibited the highest AUC scores of 80 and 70% respectively in latency intervals associated with the P3a component (see Figure 3.8).

In Patient 3, three blocks (7, 8 and 10) with significant results on day 0, and three blocks (2, 4 and 6) on day 3 were observed. Considering the proportion of blocks per patient, the classification performance on discriminating duration deviants vs standard sounds was fluctuating across blocks in all patients, particularly in Patient 3 (see Figure 3.9).

3.3.5 Patient outcomes

The three patients showed a slight behavioral improvement on Day 3 as reflected by the clinical scales (see clinical scales in Chapter 2, Table 2.1). Despite the improvement in behavioral scales and decoding performance, Patient 1 passed away after withdrawal of life support. Patient 2, who awakened from coma on day 3, had good recovery after a year. Patient 3 was discharged to a different hospital, remaining dependent on the

ventilator, and subsequently transferred to a chronic care facility where was diagnosed as UWS.

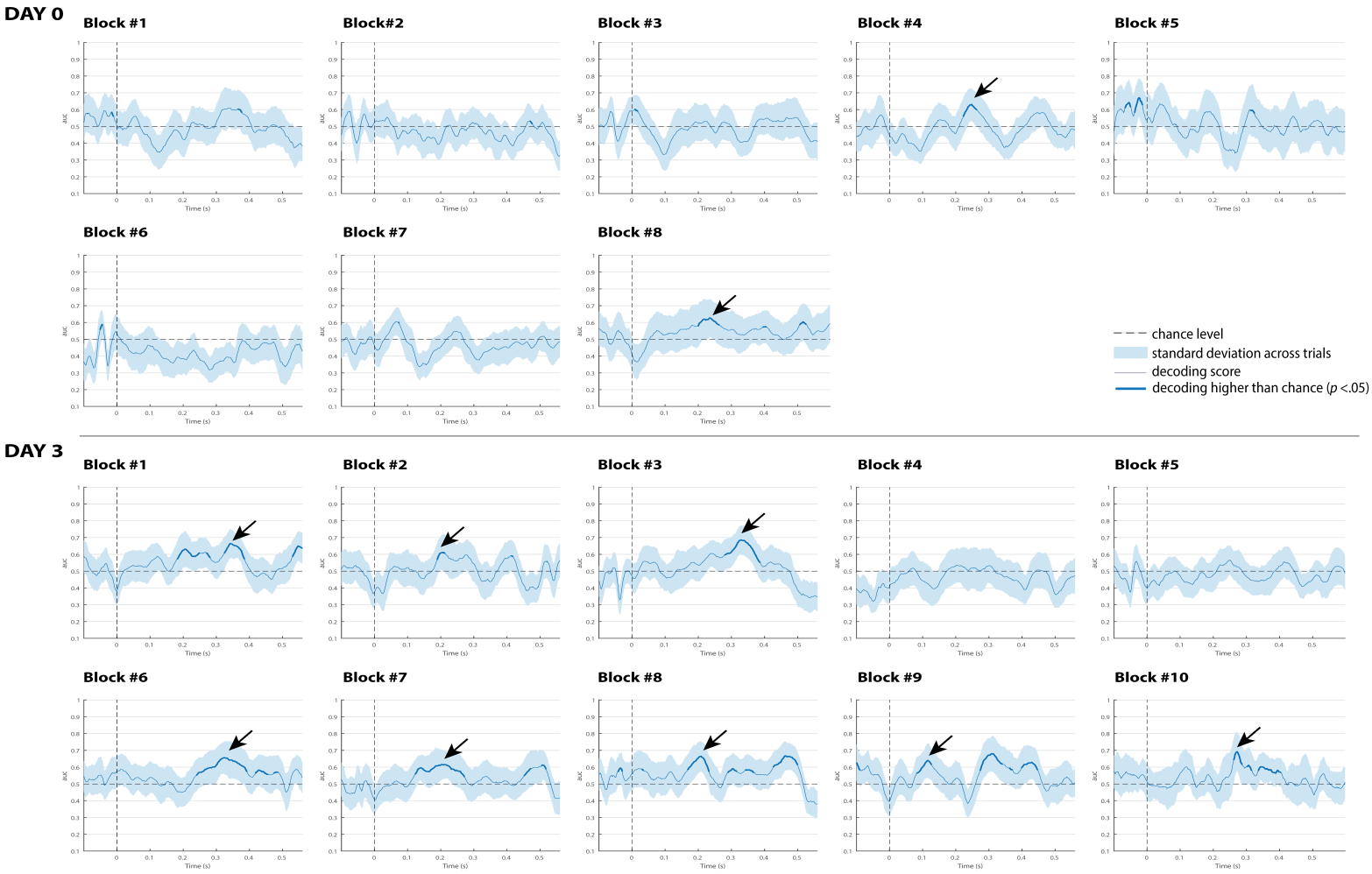

Figure 3.7: Classification performance of Patient 1 at each single block on day 0 and day 3. Black arrows indicate the blocks with above-chance performance.

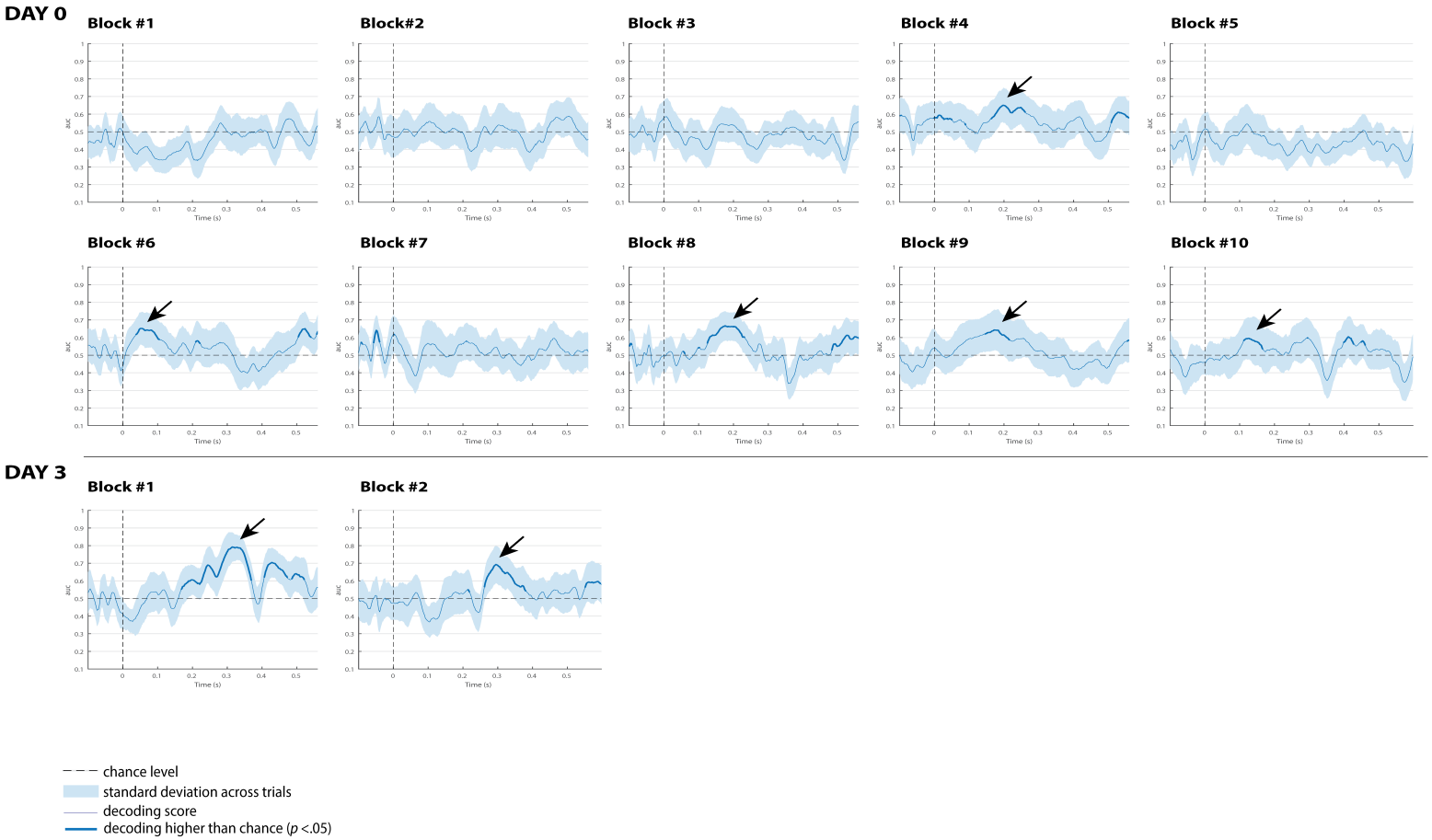

Figure 3.8: Classification performance of Patient 2 at each single block on day 0 and day 3. Black arrows indicate the blocks with above-chance performance.

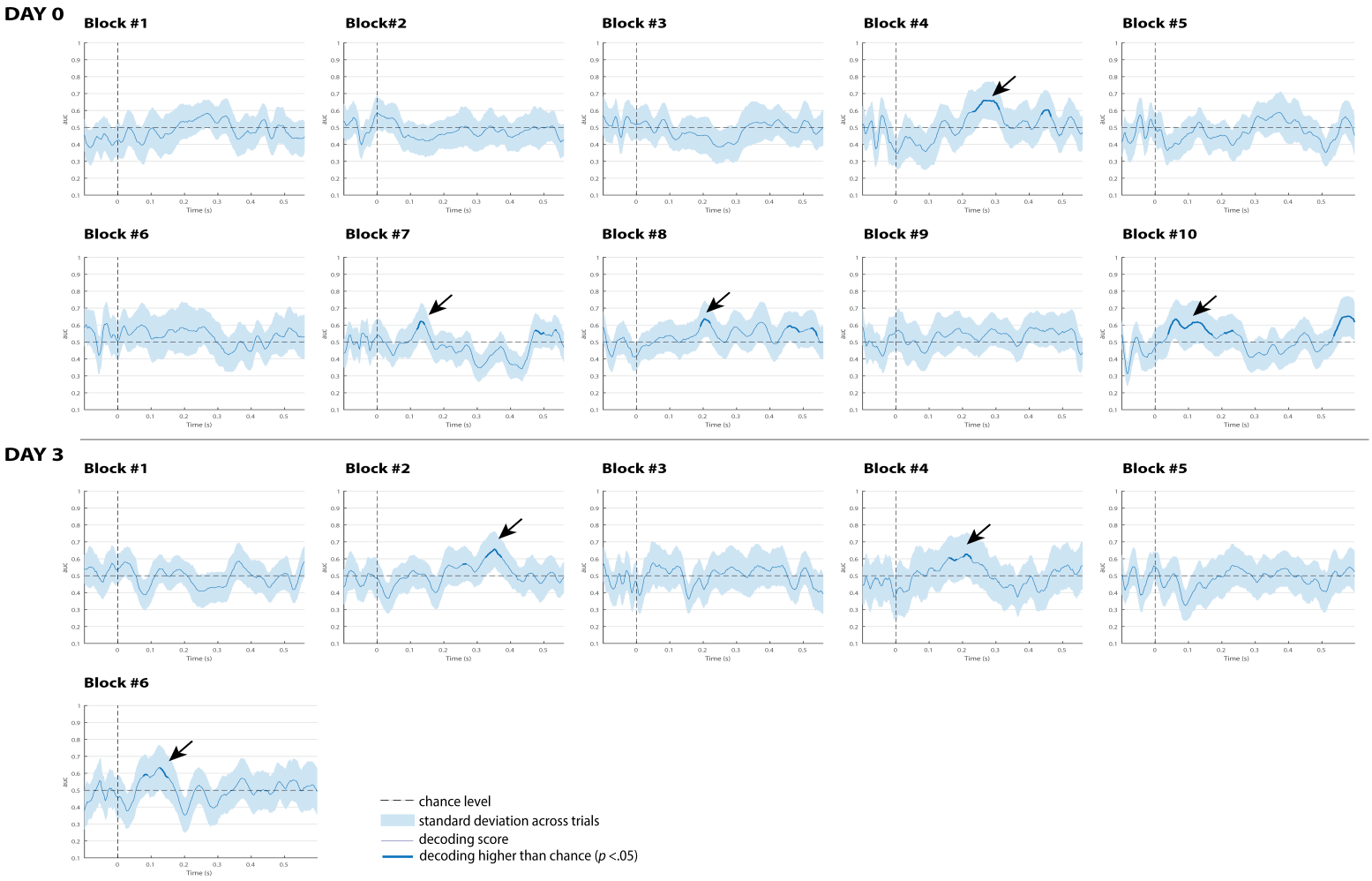

Figure 3.9: Classification performance of Patient 2 at each single block on day 0 and day 3. Black arrows indicate the blocks with above-chance performance.

3.4 Discussion

This study demonstrates that multivariate approaches are well suited to decode single-trial ERP responses that have been typically associated with coma emergence and positive functional outcome. Our results showed high decoding performance in all control subjects, with maximum AUC scores ranging from 80 to 94% corresponding to the MMN and P3a intervals. In some subjects (7/17), the AUC peaks were observed in the associated P3a intervals, a finding that has been previously reported and associated with an automatic attentional shift towards the deviant sounds (Brandmeyer et al., 2013).

Here, we followed a similar approach to that used by Tzovara and collaborators, who applied a multivariate procedure in postanoxic coma patients to decode the differences between deviant and standard trials elicited during a classic oddball paradigm (Tzovara et al., 2013). In contrast to these authors, who modeled the distribution of single-trial ERP responses using a mixture of Gaussian assumptions, we used a linear support vector machine (SVM) classifier, and included nested operations, such as averaging trials within a cross-validation analysis. This latter seeks to reduce data dimensionality and increase the signal-to-noise ratio (SNR), which is known to improve the decoding performance (Grootswagers et al., 2017; Treder, 2020). Taken together, these methodological differences may explain why our approach achieved greater classification scores in healthy controls (mean AUC= 86%) in comparison to Tzovara's findings (mean AUC=72%) when decoding EEG responses to standard versus duration deviants.

In a different context and using other active experimental tasks that required sufficient engagement and attention from the participants, King and colleagues found that single-trial classification with SVM leads to AUCs between 73% and 90% depending on the type of recording (EEG, intracranial EEG or magnetoelectroencephalography(MEEG), reaching mean AUC scores of 77.8% when recorded with high-density EEG (King et al., 2013). Our findings confirm that the implemented decoding algorithm is robust and can automatically distinguish single-trial neural responses, but in passive listening conditions. While active paradigms are supported in the literature for their obvious benefits, they can also underrate the degree of consciousness in DOC patients. As reported in a meta-analysis, passive paradigms using fMRI or EEG suggested preserved

consciousness more often than active paradigms in patients who emerged from coma as VS/UWS or MCS (Kondziella et al., 2016)

Additionally, the exploratory analysis of the temporal generalization matrices confirmed the presence of a serial chain of activation patterns associated with the presence of the MMN and the following P3a component that arises automatically shortly after the MMN. The authors of this method (King and Dehaene, 2014), used MEG recordings while conducting an elegant variant of the classic oddball task, the so-called local-global paradigm (Bekinschtein et al., 2009). In this paradigm two levels of regularity can be violated: one local that implies a change of sound within each single trial, which is postulated to elicit the MMN/P3a complex, and one global (i.e., a change of sound sequence across trials) that generates the P3b component, which is thought to depend on working memory and conscious access. The activation patterns found in our sample, plotted in Figure 3.1B, are equivalent to the local effects found in previous research (King and Dehaene, 2014; King et al., 2014), in which the decoding of local-standard versus local-deviants led to the mismatch and the sequential recruitment of patterns of brain activity, as reflected in a diagonally shaped pattern of temporal generalization. Although there was considerable variability across trials within subjects, short off-diagonal patterns were also observed, but there were two of them consistently seen in healthy controls. The classifier trained around 100-250 ms (the same time window of the MMN component) generalized data between 400 to 600 ms, and the training time points corresponding to 0-100 ms generalized over the latency related with the P3a component. Based on the main types of dynamics postulated by King and Dehaene, this phenomenon may indicate that similar generators associated with early processing stages could be reactivated at a later time, sharing common neural representations (King and Dehaene, 2014). Future research, using source localization methods, could help to identify the brain generators of these ERP responses and confirm whether they are reactivated.

3.4.1 Clinical value for coma research

Decoding auditory ERP responses at the single-subject level promises to be of great value in clinical applications for coma patients. Consistent with previous evidence

(Brandmeyer et al., 2013), the classification performance in our study was found to be strongly related to both the MMN and P3a amplitudes (Figure 3.8), suggesting that the analyses successfully capture relevant single-trial features in the data. In this regard, ERP-based decoding performance (AUC) could also be used as a neurophysiological tool for tracking amplitude fluctuations of brain activity.

Another important aspect to take into account when implementing automatic decoding procedures, is to determine the optimal number of electrodes to achieve high classification performance. Previous studies conducted in patients with acute coma state and other disorders of consciousness, have implemented similar approaches using different EEG configurations, from 19 (Tzovara et al., 2013, 2015; Cossy et al., 2014; Rossetti et al., 2014) to 128 electrodes (King et al., 2013). While a high number of EEG electrodes raises computational and experimental costs, and might deteriorate the decoding performance because of the larger number of features involved, it has been found that reducing the number of EEG channels decreases the classification performance (Brandmeyer et al., 2013). However, an important study conducted by Engemann and his team demonstrated that multivariate analysis utilized to discriminate between levels of consciousness is robust across different EEG configurations (Engemann et al., 2018). The authors found that discrimination performance increased with the number of electrodes and epochs, but was already strong with 16 electrodes from a 10-20 montage. In the current study, reducing all available 64 electrodes to 11 had no effect on the classification performance (Figure 3.3), which suggests that a few electrodes, located over the central-middle line and temporal regions, captures sufficient discriminative information of the auditory responses. Providing a robust decoding performance with such reduced number of EEG channels is extremely useful for clinical applications in intensive care, since severe brain injuries and neurosurgical procedures in some comatose patients may limit the placement of a high-density EEG montage on the scalp.

3.4.2 Decoding single-trial ERP responses in comatose patients

Having demonstrated the feasibility of the decoding procedure to distinguish between single-trial ERP responses in healthy controls, we applied it in three coma patients. The results revealed that while none of the patients exhibited significant results at

the first superblock on day 0, two patients (Patients 2 and 3) showed some intervals with significantly above-chance performance at about the second half on this day (i.e., second superblock). All of them exhibited maximum AUC scores of 65%, 70% and 60% in time windows associated with either the MMN or the P3a component on day 3. These findings are in line with previous work (Tzovara et al., 2013, 2016; Rossetti et al., 2014), which demonstrated intact auditory discrimination in acute coma state, as well as important improvements in classification performance over time.

In contrast to these studies, none of the patients here underwent any therapeutic hypothermia treatment that could explain their improvement in auditory discrimination on day 3. We believe that the patients might have reflected positive neurophysiological changes after three days of intensive care, as illustrated in the slight increase of their behavioral scores (GCS and FOUR scores, in Table 2.1). This indicates that decoding performance may predict the patient's clinical course. In fact, the patient with the highest decoding performance (Patient 2; AUC=70%) showed behavioral signals related with coma awakening on day 3, and a positive outcome after a year of rehabilitation (i.e., good recovery). Similar to controls, the temporal dynamical activation patterns in this patient were observed in chain (although slightly isolated) on the diagonal of the temporal matrix, with transient generalization patterns (off-diagonal). Additionally, the multivariate analysis applied to the single-recording blocks showed a maximum AUC score of 80% on day 3 (Figure 3.8). Such increase of decoding performance in a brain-injured patient in comparison to other single blocks, provides further evidence of the waxing-waning pattern underlying conscious state (not necessarily awareness) in coma (Armanfard et al., 2019). It also highlights the potential use of this decoding technique to track progression of auditory discrimination and complement other available tests and behavioral assement to predict coma emergence. As stated by Morlet and Fischer in a comprehensive review (see Morlet and Fischer (2014)), multivariate algorithms like those implemented in Tzovara and King's studies (Tzovara et al., 2013; King et al., 2013) can provide assessment of sensory and mismatch processes without traditional ERP recognition. Such methods provide each patient's decoding accuracy/performance with no a priori hypothesis about MMN or other responses.

The other two patients have different outcomes: one passed away after withdrawal of life support (Patient 1), and the other (Patient 3) survived in the ICU, but was eventually

declared to be in VS/UWS and transferred to a chronic care facility. These results are also coherent with Tzovara's findings that showed evidence that both survivors and non-survivors patients exhibited accurate auditory discrimination during acute coma state, and only their positive or negative progression of sound discrimination over time was the major predictor of their chance of survival and outcomes (Tzovara et al., 2013, 2015). Based on this scenario, we cannot discard the possibility that Patient 1 would have survived and had a different outcome if the critical care was not withdrawn, especially after showing consistent improvement of auditory discrimination on day 3. In Canada, withdrawal of life supporting interventions is a common cause of death in 70% patients with DOC, and some decisions are made too early for accurate prognostication (Turgeon et al., 2011). Those family and medical decisions are based, to some extent, on the recognition that many survivors of severe brain injuries, who emerge from coma, never recover consciousness (Edlow et al., 2021), remaining in a persistent VS/UWS or MCS with physical and cognitive disabilities for decades or the rest of their lives. However, our preliminary results could encourage the use of neurophysiological measures to support the provision of life-sustaining therapies, particularly when there is clinical uncertainty of coma emergence.

3.5 Conclusions

A multivariate decoding approach revealed that the neurophysiological responses elicited by duration deviants and standard sounds during an oddball paradigm can be robustly discriminated in healthy controls. The same approach applied to a small sample of comatose patients showed lower decoding performance in comparison to controls, but still above-chance level mainly during the second recording day. If assessed in larger patient cohorts, our findings may have potentially important clinical implications, because they could provide clinicians with an automatic tool to monitor neurophysiological changes over time and improve prediction of coma outcome.

References

Armanfard, N., Komeili, M., Reilly, J. P., and Connolly, J. F. (2019). A Machine Learning Framework for Automatic and Continuous MMN Detection with Preliminary Results for Coma Outcome Prediction. *IEEE J. Biomed. Heal. Informatics*, 23(4):1794–1804.

Bekinschtein, T. A., Dehaene, S., Rohaut, B., Tadel, F., Cohen, L., and Naccache, L. (2009). Neural signature of the conscious processing of auditory regularities. *Proc. Natl. Acad. Sci. U. S. A.*, 106(5):1672–1677.

Brandmeyer, A., Sadakata, M., Spyrou, L., McQueen, J. M., and Desain, P. (2013). Decoding of single-trial auditory mismatch responses for online perceptual monitoring and neurofeedback. *Front. Neurosci.*, 7:265.

Carlson, T. A., Grootswagers, T., and Robinson, A. K. (2019). An introduction to time-resolved decoding analysis for M/EEG. *arXiv prepr. arXiv1905.04820*.

Cichy, R. M., Pantazis, D., and Oliva, A. (2014). Resolving human object recognition in space and time. *Nat. Neurosci.*, 17(3):455–462.

Connolly, J. F., Reilly, J. P., Fox-Robichaud, A., Britz, P., Blain-Moraes, S., Sonnadara, R., Hamielec, C., Herrera-Díaz, A., and Boshra, R. (2019). Development of a point of care system for automated coma prognosis: a prospective cohort study protocol. *BMJ Open*, 9:29621.

Cossy, N., Tzovara, A., Simonin, A., Rossetti, A. O., and De Lucia, M. (2014). Robust discrimination between EEG responses to categories of environmental sounds in early coma. *Front. Psychol.*, 5(FEB):155.

Daltrozzo, J., Wioland, N., Mutschler, V., Lutun, P., Calon, B., Meyer, A., Pottecher, T., Lang, S., Jaeger, A., and Kotchoubey, B. (2009). Cortical information processing in Coma. *Cogn. Behav. Neurol.*, 22(1):53–62.

Edlow, B. L., Claassen, J., Schiff, N. D., and Greer, D. M. (2021). Recovery from disorders of consciousness: mechanisms, prognosis and emerging therapies. *Nat. Rev. Neurol.*, 17(3):135–156.

Engemann, D. A., Raimondo, F., King, J.-R. R., Rohaut, B., Louppe, G., Faugeras, F., Annen, J., Cassol, H., Gosseries, O., Fernandez-Slezak, D., Laureys, S., Naccache, L., Dehaene, S., and Sitt, J. D. (2018). Robust EEG-based cross-site and cross-protocol classification of states of consciousness. *Brain*, 141(11):3179–3192.

Fahrenfort, J. J., van Driel, J., van Gaal, S., and Olivers, C. N. (2018). From ERPs to MVPA using the Amsterdam Decoding and Modeling toolbox (ADAM). *Front. Neurosci.*, 12(JUL):368.

Grootswagers, T., Wardle, S. G., and Carlson, T. A. (2017). Decoding dynamic brain patterns from evoked responses: A tutorial on multivariate pattern analysis applied to time series neuroimaging data. *J. Cogn. Neurosci.*, 29(4):677–697.

King, J. R. and Dehaene, S. (2014). Characterizing the dynamics of mental representations: The temporal generalization method. *Trends Cogn. Sci.*, 18(4):203–210.

King, J. R., Faugeras, F., Gramfort, A., Schurger, A., El Karoui, I., Sitt, J. D., Rohaut, B., Wacongne, C., Labyt, E., Bekinschtein, T., Cohen, L., Naccache, L., and Dehaene, S. (2013). Single-trial decoding of auditory novelty responses facilitates the detection of residual consciousness. *Neuroimage*, 83:726–738.

King, J. R., Gramfort, A., Schurger, A., Naccache, L., and Dehaene, S. (2014). Two distinct dynamic modes subtend the detection of unexpected sounds. *PLoS One*, 9(1):e85791.

Kondziella, D., Friberg, C. K., Frokjaer, V. G., Fabricius, M., and Møller, K. (2016). Preserved consciousness in vegetative and minimal conscious states: Systematic review and meta-analysis. *J. Neurol. Neurosurg. Psychiatry*, 87(5):485–492.

Morlet, D. and Fischer, C. (2014). MMN and novelty P3 in coma and other altered states of consciousness: A review. *Brain Topogr.*, 27(4):467–479.

Oostenveld, R., Fries, P., Maris, E., and Schoffelen, J. M. (2011). FieldTrip: Open source software for advanced analysis of MEG, EEG, and invasive electrophysiological data. *Comput. Intell. Neurosci.*, 2011.

Pfeiffer, C., Nguissi, N. A. N., Chytiris, M., Bidlingmeyer, P., Haenggi, M., Kurmann, R., Zubler, F., Accolla, E., Viceic, D., Rusca, M., Oddo, M., Rossetti, A. O., and De Lucia, M. (2018). Somatosensory and auditory deviance detection for outcome prediction during postanoxic coma. *Ann. Clin. Transl. Neurol.*, 5(9):1016–1024.

Piarulli, A., Charland-Verville, V., and Laureys, S. (2015). Cognitive auditory evoked potentials in coma: Can you hear me? *Brain*, 138(5):1129–1131.

Rodriguez, R. A., Bussière, M., Froeschl, M., and Nathan, H. J. (2014). Auditory-evoked potentials during coma: Do they improve our prediction of awakening in comatose patients? *J. Crit. Care*, 29(1):93–100.

Rossetti, A. O., Tzovara, A., Murray, M. M., De Lucia, M., and Oddo, M. (2014). Automated auditory mismatch negativity paradigm improves coma prognostic accuracy after cardiac arrest and therapeutic hypothermia. *J. Clin. Neurophysiol.*, 31(4):356–361.

Sitt, J. D., King, J. R., El Karoui, I., Rohaut, B., Faugeras, F., Gramfort, A., Cohen, L., Sigman, M., Dehaene, S., and Naccache, L. (2014). Large scale screening of neural signatures of consciousness in patients in a vegetative or minimally conscious state. *Brain*, 137(8):2258–2270.

Tavakoli, P., Dale, A., Boafo, A., and Campbell, K. (2019). Evidence of P3a during sleep, a process associated with intrusions into consciousness in the waking state. *Front. Neurosci.*, 12:1028.

Treder, M. S. (2020). MVPA-Light: A Classification and Regression Toolbox for Multi-Dimensional Data. *Front. Neurosci.*, 14:289.

Turgeon, A. F., Lauzier, F., Simard, J. F., Scales, D. C., Burns, K. E., Moore, L., Zygun, D. A., Bernard, F., Meade, M. O., Dung, T. C., Ratnapalan, M., Todd, S., Harlock, J., and Fergusson, D. A. (2011). Mortality associated with withdrawal of life-sustaining

therapy for patients with severe traumatic brain injury: A Canadian multicentre cohort study. *CMAJ*, 183(14):1581–1588.

Tzovara, A., Rossetti, A. O., Juan, E., Suys, T., Viceic, D., Rusca, M., Oddo, M., and Lucia, M. D. (2016). Prediction of awakening from hypothermic postanoxic coma based on auditory discrimination. *Ann. Neurol.*, 79(5):748–757.

Tzovara, A., Rossetti, A. O., Spierer, L., Grivel, J., Murray, M. M., Oddo, M., and De Lucia, M. (2013). Progression of auditory discrimination based on neural decoding predicts awakening from coma. *Brain*, 136(1):81–89.

Tzovara, A., Simonin, A., Oddo, M., Rossetti, A. O., and De Lucia, M. (2015). Neural detection of complex sound sequences in the absence of consciousness. *Brain*, 138(5):1160–1166.

Xue, J. H. and Hall, P. (2015). Why does rebalancing class-unbalanced data improve AUC for linear discriminant analysis? *IEEE Trans. Pattern Anal. Mach. Intell.*, 37(5):1109–1112.

Chapter 4

Functional connectivity in the dying brain: a case study

Preface: In this chapter, we propose a machine learning procedure to characterize EEG functional connectivity in response to auditory stimuli and resting state in a single-comatose patient during his last hours of life. This report, is to our knowledge, the first to compute EEG functional connectivity at both the sensor and source levels in a dying coma patient. We believe that our procedure could be used to gain better understanding of the neurophysiological mechanisms that may occur in coma and other unresponsive patients at the end of life.

Abstract

Functional connectivity (FC) applied to electroencephalogram/event-related potential (EEG/ERP) data has gained considerable traction in the clinical field, as it can be used as a valuable tool to make outcome predictions in coma and other disorders of consciousness (DOC). Here, we computed FC in response to auditory stimuli and during resting state in a coma patient, who unexpectedly died during an EEG recording session. Using a machine learning approach, we found high classification performance (>90%) across all frequency bands when discriminating single-trial FC in response to auditory stimuli between the coma patient and five healthy controls. This translates to decrease FC in response to auditory stimulation in coma. Paradoxically, we observed FC changes

in resting state over time, with periods of hyperconnectivity close to the point of death. If these preliminary findings are replicated in a larger sample, the proposed approach could potentially be translated into a clinical care setting for the EEG monitoring and outcome prediction in coma and other unresponsive patients.

4.1 Introduction

Electroencephalography (EEG) has proven to be a powerful tool for the clinical diagnosis and prognoses of several clinical populations. Among the main advantages of EEG technology is its ability to measure neural activity directly instead of indirect blood flow or metabolic signals, its non-invasiveness, ease of use and accessibility. In general, applications in severe brain injured patients have focused on the spectral analysis of EEG-resting state and event-related potentials (ERP) for the classification of the patient's clinical state. More recently, the study of the neural bases of consciousness and their disorders has greatly benefited from the application of modern and sophisticated connectivity analyses. Indeed, several theoretical proposals of how consciousness arises often refer to aspects of brain activity as a network of interacting brain regions that requires synchronized communication of information (Dehaene and Changeux, 2011; Tononi et al., 2016).

In particular, FC is defined as the non-directed statistical interdependence among spatially distant neurophysiological regions (Friston, 2011), and it is usually quantified by cross-correlation, coherence, phase synchronization, information theory-based metrics and so on. During EEG-resting state, FC seems to be drastically altered in coma and other disorders of consciousness (DOC), showing potential to distinguish different levels of consciousness and predict clinical outcomes (Höller et al., 2014; Sitt et al., 2014; Chennu et al., 2014, 2017; Zubler et al., 2017; Carrasco-Gómez et al., 2021). However, what still remains under-investigated are the disturbed connectivity features in response to deviant or environmental stimuli during cognitive experimental tasks. Only a few studies have so far investigated FC under auditory neural processing, revealing that phase synchronization-based measures such as phase locking value (PLV) could be an

additional neurophysiological tool to measure levels of dysfunction in DOC (Binder et al., 2017) and predict coma awakening (Lechinger et al., 2016; Alnes et al., 2021).

Another element to consider, is that most of the EEG connectivity studies in coma research have been performed at the sensor or electrode level, which may not exactly reflect the true neural linkages among brain areas. That is, the biological interpretations of the identified networks are not straightforward, since EEG signals from scalp can be strongly corrupted by the volume conduction effects as a result of the electrical conduction properties of the head, and that multiple scalp electrodes may pick up the activity arising from the same electrical sources in the brain (Schoffelen and Gross, 2009; Brunner et al., 2016; Hassan and Wendling, 2018). Several studies have reported the limitations of computing connectivity analyses at the sensor level (Schoffelen and Gross, 2009; Hassan and Wendling, 2018; Van de Steen et al., 2019; He et al., 2019). A potential solution, still under development and not without its pitfalls, is using EEG source connectivity methods. These methods seem to reduce the volume conduction problem and permit the identification of meaningful connectivity patterns at the cortical level with a high time-space resolution (Hassan et al., 2014, 2015).

Very recent studies have integrated EEG source localization methods to study FC networks in DOC (Rizkallah et al., 2019) and palliative patients at the end of life (Blundon et al., 2022). The investigation conducted by Blundon and colleagues showed that some hospice patients, who became unresponsive during the last hours of life, evidenced activation of a well-characterized network (DMN: default mode network) that includes medial fronto-parietal regions, and it is usually activated when no explicit task is performed (Blundon et al., 2022).

For this report, we studied an acute coma patient who unexpectedly died during an EEG recording protocol. First, a phase-based measure of FC to auditory stimuli and resting state (RS) was quantified at both the sensor and source levels. Then, we used a machine learning (ML) approach following two main objectives: 1) identify the main single-trial FC features to auditory deviant stimuli that better discriminate a dying coma patient from healthy controls, and 2) determine whether there are RS connectivity changes across time in coma at the single-subject level during the last hours of life.

4.2 Methods

4.2.1 Case study and healthy controls

A 19-year-old man was found comatose (GCS=3) after sustaining an electrocution injury at the workplace. Upon emergency medical services arrival, the patient received cardiopulmonary resuscitation (CPR) and was transported to the Hamilton General Hospital, where he had three episodes of cardiac arrest in the emergency room. Once stabilized, the patient was taken to the ICU. A computed tomography (CT) raised the possibility for an early anoxic brain injury, and a repeated CT done 3 days later showed diffuse hypoxic ischemic injury. Glasgow Coma Scale (GCS) remained 3 throughout his stay in the ICU, and the EEG revealed generalized suppressed activity. The medical team declared a poor outcome prognosis for this patient, and organ donation after cardiac death was discussed and consented by the family. Informed consent for the EEG study was obtained from the substitute decision maker.

Five healthy subjects (mean age: 23 ± 5 years; 3 males) were recruited from the local community and had no reported medical history related to central nervous system (CNS) function or known hearing impairment. The study was approved by the Hamilton Integrated Research Ethics Board (HiREB).

The flow chart of our procedure is summarized in Figure 4.1 depicting the following steps:

a) EEG recording and preprocessing of auditory ERP and resting state paradigms;

b) Computation of FC connectivity at both the sensor and source levels;

c) Implementation of a ML procedure to accomplish two main objectives: identify discriminating FC features in response to deviant stimuli between the coma patient and healthy controls; and explore whether there are RS connectivity changes in the coma patient before death.

Details of each step is explained in the following sections.

4.2.2 EEG recording and preprocessing

EEG/ERP data were acquired from an original study protocol, in which 10 min-RS periods interspersed within several ERP tasks, including the MMN paradigm described above (Chapter 2, section 2.2.3). The EEG recording lasted approximately 2 hours, and was terminated when the patient died as result of a cardiac arrest. For the purposes of this study, we analyzed two datasets: one containing a single-recording block of the MMN paradigm, and the second one, which included three RS-time periods recorded in the comatose patient and healthy controls. The first RS period in the coma patient (denoted as RS01) was recorded approximately 1 hour and 50 min before death declaration, while the second (RS02) and third (RS03) periods were recorded 1 hour and 35 minutes respectively before death.

For healthy controls and the comatose patient, EEG data were recorded with a sample rate of 512 Hz (bandpass between 0.01 and 100Hz) using a 64-channel Biosemi ActiveTwo system (Amsterdam, The Netherlands). Electrodes were placed on the scalp according to the extended 10/20 system using a 64-electrode cap. Data preprocessing was conducted offline (Brain Products Inc.), with bandpass filters of 1-30 Hz. Electroculogram (EOC) signals were monitored by electrodes placed above and over the outer canthus of the left eye and reference electrodes were recorded from mastoids. Ocular artifacts were corrected by using ICA transformation. All EEG trials from the MMN paradigm were segmented from 100 ms pre-stimulus to 600 ms post-stimulus and baseline corrected (-100 to 0 ms), while the RS recordings were segmented in epochs of 3 seconds. All EEG trials and RS epochs were free of eye-movements, blinks, excessive muscle activity, signs of drowsiness (in controls) and electrocardigram (EKG) artifacts.

4.2.3 Functional connectivity to auditory stimuli and resting state

After preprocessing, 70 single-trial ERP responses corresponding to the duration deviant (0-600 ms), and 136 epochs (3 sec each) for each RS time period were the inputs to

compute the FC analyses[a]. These two datasets (auditory ERP responses and resting state conditions) were analyzed separately.

Once the time series were bandpass filtered at the following frequency bands: delta (1-4 Hz), theta (5-7.5 Hz), alpha (8-12 Hz) and beta (13-29 Hz), the phase locking value (PLV) was computed as a FC measure between each electrode pair (i.e., sensor level) and each source-reconstructed region (i.e., source level). The assumption underlying PLV is that if two brain regions are functionally connected, then the difference between the instantaneous phase of the signals from these regions should be more or less constant (Lachaux et al., 1999). Instantaneous phases of each EEG channel were extracted via Hilbert transform, a standard way to transform the real signals into a complex representation. The PLV ranges from 0 (indicating non-phase synchronization) to 1 (implying high synchronization or minimal phase variability over the trials or epochs). All the analyses were done in Matlab, version R2021b (MathWorks Inc., USA), by using the Brainstorm software (Tadel et al., 2011) in combination with custom-written Matlab scripts.

Sensor-level connectivity: A symmetric FC matrix (M) of Ne x Ne (64 x 64)- where Ne is the sensor number- is obtained for each ERP trial or RS epoch and frequency band. Each element Mij of M matrix contains the PLV values between EEG sensors 'i' and 'j'. Given the matrix M is symmetric, the self-connections Mii were excluded, implying zeros in the diagonal of the M matrix. This results in $Ne \times (Ne-1)/2 = 64 \times 63/2 = 2016$ PLV pairs of sensors for each frequency band.

Source-level connectivity: The FC between source brain regions was computed following two main steps as previously suggested by Hassan and colleagues (Hassan et al., 2015): 1) the reconstruction of temporal dynamics of the cortical sources, and 2) the measurement of FC (i.e., PLV) between the reconstructed time series.

[a]The rationale for selecting only the single-trials responses elicited by duration deviants is based on previous findings (see Chapter 2) that showed high detectability of MMN responses to duration deviant types at both the group and single-subject levels

First, a head model, based on the anatomy derived from the ICBM 152 brain template[b], was created using a symmetric boundary element method (BEM) by using the Open-MEEG package, available in Brainstorm software. The BEM includes realistic-shaped shells that represent the brain, scalp and skull, and it is known to integrate correctly their conductivity and anisotropic properties (Gramfort et al., 2010). With regard to physical constraints, a cortical mesh of 15,000 vertices (in which the position of each source is a vertex on the cortical mesh) was used to compute the lead field matrix, which determines how the electrical activity at a certain electrode is related to the activity of the different sources in the brain. The orientation of each source was set up normal (perpendicular) to the cortical surface for each vertex, given the main contributors of EEG signal are the postsynaptic currents from the pyramidal cells, which are organized in macro-assemblies with their dendrites normally oriented to the local cortical surface (Baillet et al., 2001). Then, using an identity matrix as noise covariance, we applied the method Weighted Minimum Norm Estimator (wMNE), which is a mathematical constraint to reconstruct the cortical sources. The source (S) estimated by wMNE is expressed as:

$$\hat{S}(\text{wMNE}) = (L^T W_E L + \lambda C)^{-1} L W_E E \tag{4.1}$$

where W_E is the weighted matrix that is classically a diagonal matrix built from the lead field matrix L. Here, λ denotes a regularization parameter (set at 0.1) and C is the noise covariance matrix. The weighted matrix algorithm compensates for the tendency of the classical MNE methods to favour weak and surface sources (Michel et al., 2004). In order to reduce the number of estimates, the source-reconstructed-time series were projected onto 68 parcelled regions of interest (ROIs), extracted from the MRI template and defined by the Desikan-Killiany atlas. The time series for voxels within each ROI were averaged. Once the PLV values are computed, an adjacency connectivity matrix is generated for each ERP trial or RS epoch across subjects, in which each element Sij of the connectivity matrix (S) contains the PLV values between each ROI. This results in $Ne \times (Ne-1)/2 = 68 \times 67/2 = 2278$ PLV pairs of ROIs for each frequency band.

[b]The ICBM 152 template is an unbiased non-linear average of MRIs of 152 adult human subjects.

4.2.4 Machine learning procedure

The ML procedure contains the following steps: feature extraction, feature selection, classifier training and validation.

Feature extraction and selection: For the auditory ERP task, we extracted a set of most relevant FC features to discriminate single-trials responses of coma versus healthy controls for each separated frequency band. The candidate features are the number of FC pairs (2016 pairs of sensors or 2178 pairs of ROI sources) for each single trial with their corresponding class labels (0 for the 70 deviant single-trials in the coma patient, and 1 for 100 single-trials[c] in healthy controls. These features were then passed tfrough a minimum redundancy maximum relevance (mRMR) feature selection algorithm, which uses a mutual information criterion to quantify statistical dependence (redundancy) and simultaneously maximum statistical dependence (relevance) to yield a set of most salient features that maximize the difference between the classes. The mRMR, developed by Peng et al. (2005), is a popular method that yields better performance, and has been used in several studies for characterization of schizophrenia, (Masychev et al., 2021), mild traumatic brain injury (Cao et al., 2008) and coma (Armanfard et al., 2016). We observed that the best number of salient features for each separated frequency band was 10. (See an example of the mRMR output for alpha frequency band in Supplementary information II, Figure S1).

For the RS condition, the mRMR method and subsequent ML steps were conducted to determine differences among 3 classes (RS01, RS02 and RS03) within each subject and patient. Here, the number of best candidate features varied between 5 and 10 per subject, so we used 10 features to be consistent across the entire study.

Classifier training and validation: For the ERP dataset, we performed a binary classification to determinate differences between duration deviant responses of the comatose patient and those from each individual healthy control. For each comparison (e.g., coma vs. control 1, coma vs. control 2 and so on), we made sure to use a balanced

[c]This number (100) was obtained by extracting 20 trials of each individual healthy control

design, with matrices of dimensionality T x F, where T is the number of single trials (70 for coma and 70 for each individual control), and F is the number of the most salient FC features (i.e., 10 PLV pairs) with their corresponding class labels. For the RS dataset, a multiclass classification was run within the coma patient and each healthy control at the single-subject level to determine differences across time (RS01 vs RS02 vs RS02), where T in the constructed matrices represents the number of RS epochs (136 for each RS period).

We used five widely known classifiers: support vector machine(SVM), linear discriminant analysis (LDA), K-nearest neighbor (KNN), Naive Bayes (NB) and decision trees (Trees). A 5-fold cross-validation was implemented to get a more realistic estimate of the classification performance. This latter involves splitting the data into k mutually exclusive folds. Then K-1 folds are used as the training set, with the remaining fold as the testing set. These methods were implemented using the Statistics and Machine Learning Toolbox in Matlab, version R2021b (MathWorks Inc., USA).

Statistical analysis: Finally, we averaged the PLV over the subset of FC features (i.e., 10 pair of sensors or ROIs), resulting in a single measure of mean FC per single trial within each subject. Then, differences of FC values between the comatose patient and each individual control were assessed with an independent-sample *t*-test. This analysis was done over single trials or epochs, as multiple observations/samples are required to make statistical inferences about the means. Similarly, for each RS period, a single measure of FC was obtained per epoch within each subject. Here, a one-way analysis of variance (ANOVA) at single-subject level was run to determine whether there were mean differences in FC across RS periods in the coma patient. These latter statistical analyses were conducted using JASP software (version 0.14.1).

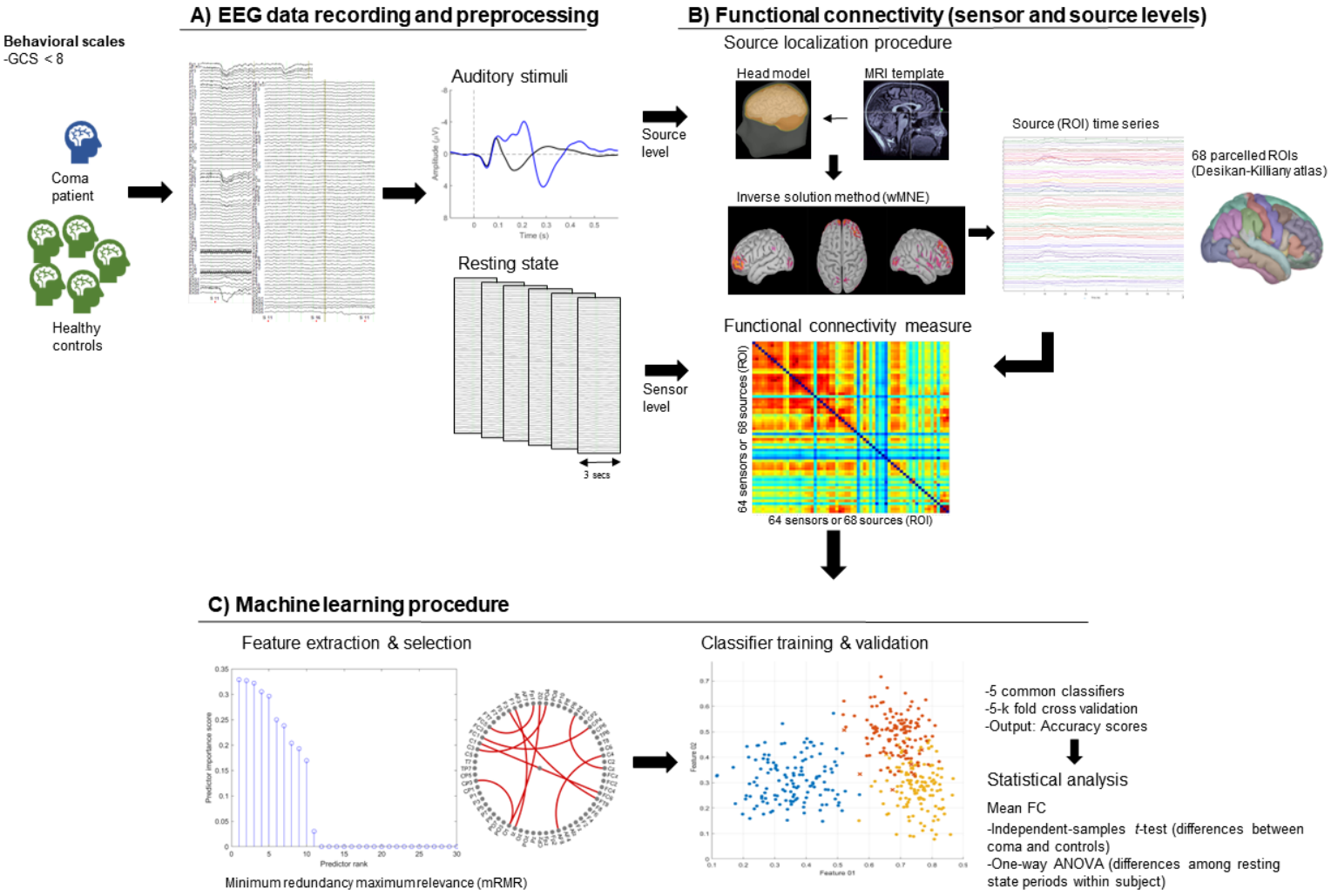

Figure 4.1: Steps to compute FC at both the sensor and source levels, and ML procedure. A) EEG data during an auditory ERP paradigm and three resting-state time periods were recorded in a dying coma patient and five healthy controls. After EEG preprocessing, the single-trial ERP responses to duration deviants (0-600ms) and the resting state epochs (3 sec each) from each period were the inputs to the source reconstruction method. B) Functional connectivity (FC), quantified by phase locking value (PLV) is computed directly from sensors/electrodes or from estimated brain sources using a source localization procedure. This procedure requires a head model (volume conductor) and the position of electrodes. Using a segmented MRI template (e.g., ICBM152), the source distribution is constrained to a field of current dipoles homogeneously distributed over the cortex and normal to the cortical surface. Then, an inverse solution method is computed (wMNE) to estimate the source time series. A source space with defined 68 regions of interest (ROIs), extracted from the Desikan-Killiany atlas was used. C) A ML procedure, following the steps of feature extraction and selection, classification and validation, was performed to discriminate single-trial FC to auditory deviants from the coma patient and healthy controls, and determinate changes across RS periods in coma at single-subject level. Finally, some statistical analyses were conducted to corroborate the ML results.

4.3 Results

4.3.1 Functional connectivity to auditory deviant stimuli

Table 4.1 summarizes the classification performance of five classifiers discriminating single-trial FC to auditory deviant stimuli in a coma patient vs. five healthy controls, and mean FC differences at both sensor and source levels for each frequency band. High classification performance was found across all frequency bands, with maximum accuracies in alpha and beta bands at both the sensor and source levels (acuracies $\geq 90\%$ are displayed in bold). The SVM classifier seems to perform better than other classifiers, showing the highest accuracies for each individual comparison. Notice a slight increase of classification performance as the frequency increases, reaching up to 100% in beta frequency when comparing with most of the controls.

The independent-sample *t*-tests confirmed these results, by showing significant differences of mean FC values between the coma patient and each individual control in all frequency bands. Cohen's d according to Sawilowsky (2009) indicated a small or medium effect size ($d = 0.2$ and 0.5, respectively) in the delta band; and either a large, very large or huge effect size ($d = 0.8$, 1.2 and 2.0 respectively) in the other frequency bands.

Figure 4.2 summarizes the results of computing FC in beta band at both the sensor and source levels. Panel A shows the most discriminative FC features between the comatose patient and controls for the beta frequency band, while panel B displays a scatter plot projecting the first two main FC features for a linear SVM model prediction, indicating a perfect and almost perfect separation of classes (coma vs controls) for connectivity at the sensor and source levels, respectively. Notice the mean FC differences between the comatose patient and each healthy control (in panel C).

The main FC features that better discriminate single-trial responses to deviant stimuli in coma and controls, varied for each frequency band. Overall, the sensor-level FC features (i.e., electrode pairs) were mainly located in frontocentral and frontoparietal regions. The source-level FC features included a large variety of brain regions connecting prefrontal, frontal, centrotemporal, limbic and posterior regions. Rostral anterior,

caudalanterior and posterior cingulate, postcentral gyrus, insula, cuneus, precuneus, superiotemporal and parahippocampal cortex were involved in all frequency bands. (See the full list of both sensor and source-FC features in Supplementary information II, Tables S1 and S2).

Table 4.1: Classification performance of several classifiers discriminating single-trial FC of a coma patient from five healthy subjects, and mean differences at both the sensor and source levels for each frequency band.

		Patient vs Control 1				Patient vs Control 2				Patient vs Control 3				Patient vs Control 4				Patient vs Control 5			
	Classifiers	Delta	Theta	Alpha	Beta	Delta	Theta	Alpha	Beta	Delta	Theta	Alpha	Beta	Delta	Theta	Alpha	Beta	Delta	Theta	Alpha	Beta
SENSOR	SVM	**92.3**	**95.8**	**97.2**	**100**	**91.5**	**96.8**	**97.3**	**100**	**92.3**	**95.1**	**95.8**	**100**	**93.0**	**94.4**	**97.9**	**100**	**90.0**	**90.1**	**97.2**	**99.3**
	LDA	86.0	**90.1**	**95.8**	**99.3**	88.0	**90.1**	**97.2**	**100**	89.4	**92.3**	**94.4**	**100**	**90.8**	**91.5**	**94.4**	**99.3**	83.8	87.3	**96.5**	**98.6**
	NB	88.0	**92.3**	**95.1**	**98.6**	89.4	**90.1**	**97.9**	**99.3**	88.7	**93.0**	**95.8**	**100**	85.9	**91.5**	**93.0**	**100**	87.3	88.0	**95.1**	**98.6**
	KNN	88.7	**90.1**	**93.3**	**99.3**	89.4	**90.8**	**95.8**	**95.8**	86.6	**95.1**	**93.0**	**99.3**	84.5	**93.7**	**95.1**	**97.2**	85.9	88.7	**94.4**	**97.3**
	Tree	83.8	**90.8**	**94.4**	**97.9**	85.9	**91.5**	**90.1**	**96.5**	80.3	85.2	89.4	98.6	86.6	**92.3**	**94.4**	**97.2**	83.3	84.5	87.3	**96.5**
	Patient mean	0.74	0.69	0.60	0.39	0.74	0.69	0.60	0.39	0.74	0.69	0.60	0.39	0.74	0.69	0.60	0.39	0.74	0.69	0.60	0.39
	Control mean	0.78	0.83	0.71	0.48	0.79	0.85	0.73	0.48	0.78	0.84	0.71	0.48	0.77	0.83	0.70	0.49	0.79	0.82	0.73	0.48
	t-value	-3.08	-10.2	-7.9	-9.31	-3.45	-12.1	-9.28	-9.64	-2.55	-11.5	-7.62	-9.60	-2.13	-10.8	-7.93	-10.1	-3.42	-8.55	-8.40	-9.31
	p-value	< .05	< .001	< .001	< .001	< .001	< .001	< .001	< .001	< .05	< .001	< .001	< .001	< .05	< .001	< .001	< .001	< .001	< .001	< .001	< .001
	Cohen's d	0.52	1.71	1.32	1.56	0.58	2.03	1.56	1.62	0.43	1.93	1.28	1.61	0.36	1.81	1.33	1.70	0.57	1.42	1.41	1.56
	Effect size	Med	Vlarge	Vlarge	VLarge	Med	Huge	Vlarge	VLarge	Small	Vlarge	Vlarge	Vlarge	Small	Vlarge	VLarge	Vlarge	Med	Vlarge	Vlarge	Vlarge
SOURCE	SVM	89.4	**92.8**	**96.0**	**96.6**	85.6	89.8	**95.8**	**98.0**	**90.8**	89.4	**96.5**	**98.6**	88.7	86.6	**94.3**	**98.6**	88.0	89.2	**95.8**	**98.6**
	LDA	81.7	83.1	**93.0**	**98.6**	84.9	78.2	**93.7**	**95.8**	**90.1**	78.2	**94.4**	**98.6**	85.9	83.8	**90.8**	**98.6**	87.3	81.7	**91.5**	**97.9**
	NB	78.9	88.7	**92.3**	**98.6**	84.5	81.0	**95.1**	**97.2**	89.5	89.4	**96.5**	**98.6**	85.9	82.4	**91.5**	**98.0**	88.0	83.1	**90.8**	**98.6**
	KNN	81.0	80.3	**91.5**	**98.6**	83.8	73.9	**95.8**	**95.8**	88.6	68.3	**95.8**	**97.3**	86.6	83.8	**90.8**	**97.2**	86.6	83.1	**90.8**	**98.6**
	Tree	73.9	83.8	81.7	88.0	73.9	76.8	85.2	**93.7**	76.1	86.6	81.0	**90.8**	81.7	73.2	88.0	**93.7**	78.2	81.0	77.5	**93.0**
	Patient mean	0.63	0.70	0.49	0.40	0.63	0.70	0.49	0.40	0.63	0.70	0.49	0.40	0.63	0.70	0.49	0.40	0.63	0.70	0.49	0.40
	Control mean	0.69	0.78	0.66	0.48	0.66	0.76	0.68	0.46	0.66	0.78	0.67	0.47	0.67	0.78	0.67	0.46	0.66	0.76	0.64	0.46
	t-value	-3.71	-6.58	-15.3	-8.05	-2.14	-5.06	-16.7	-6.61	-2.21	-6.66	-14.8	-6.68	-3.05	-6.78	-14.3	-6.48	-2.31	-5.03	-12.2	-5.90
	p-value	< .001	< .001	< .001	< .001	< .05	< .001	< .001	< .001	< .05	< .001	< .001	< .001	< .05	< .001	< .001	< .001	< .05	< .001	< .001	< .001
	Cohen's d	0.62	1.04	2.57	1.35	0.36	0.85	2.81	1.11	0.37	1.12	2.48	1.12	0.51	1.14	2.40	1.09	0.39	0.84	2.05	0.99
	Effect size	Med	Large	Huge	Vlarge	Small	Large	Huge	Large	Small	Large	Vlarge	Large	Med	Large	Huge	Large	Small	Large	Huge	Large

SVM: Support Vector Machine; LDA: Linear discriminant analysis; NB: Naive Bayes; KNN: K-nearest neighbors; Tree: Decision trees; Med: Medium effect size, Vlarge: Very large effect size. Accuracies $\geq$ 90% are displayed in bold.

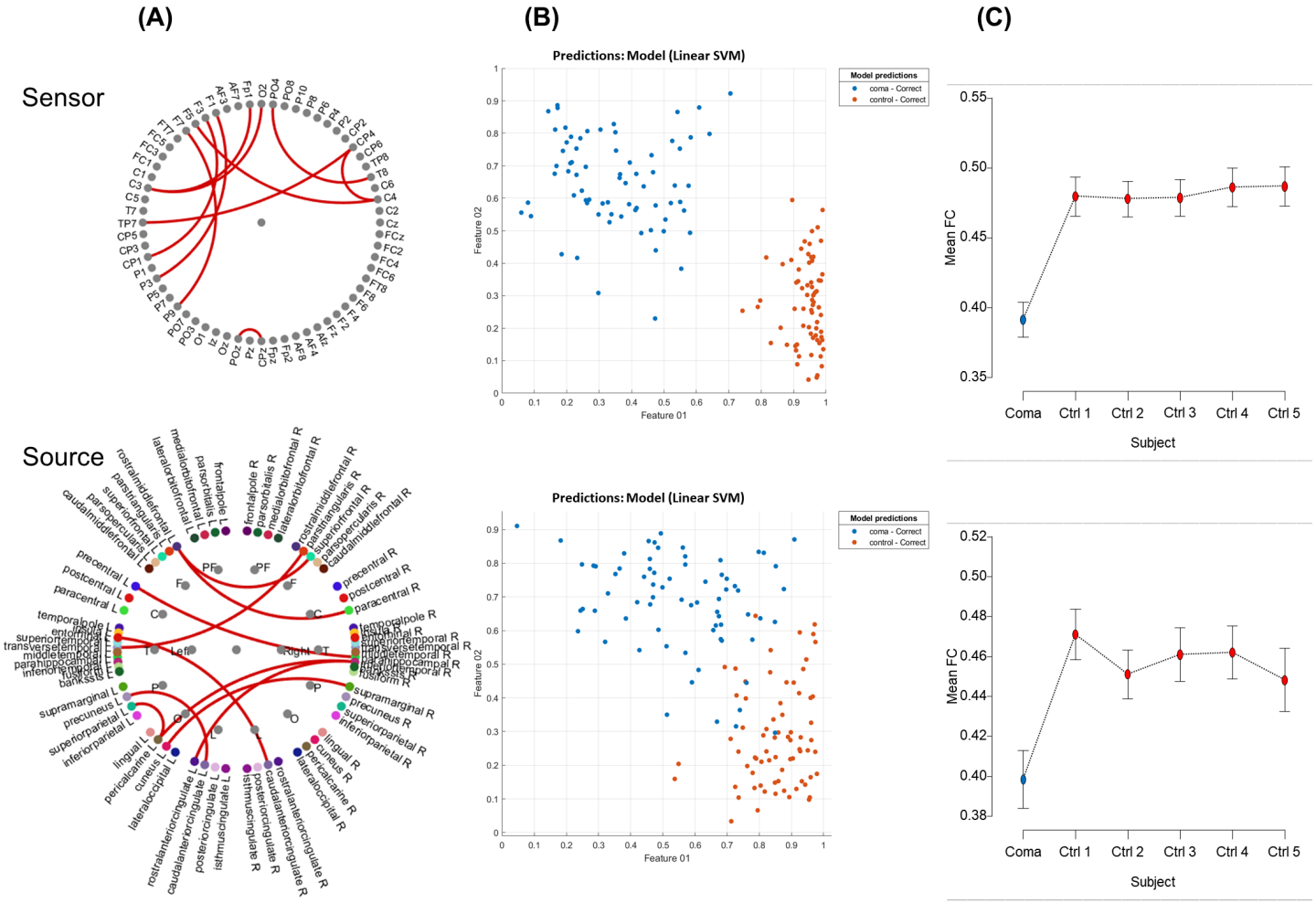

Figure 4.2: Functional connectivity between coma and controls in beta band at both the sensor and source levels. A) Most common discriminative FC features between coma and controls; B) Scatter plot projecting the first two main FC features for a linear SVM model prediction; C) Mean FC differences between the coma patient and each individual control.

4.3.2 Functional connectivity in resting state

Before conducting the ML procedure for discriminating changes in FC over time in resting state, we observed visual differences in the averaged FC matrices over time in the coma patient for all frequency bands, particularly in the theta band.

Figures 4.3 and 4.4 (panel A) display the averaged FC matrices across the RS periods in the comatose patient, a representative single control and the control group at sensor and source levels, respectively in theta band. Percentile thresholding was performed on the matrices by selecting the top 10% of the strongest connections (highest PLVs), while the remaining connections were set to zero. A circular graph (in panel B) displays an example of the top 10% FC connections in RS02.

As it can be observed at sensor level, FC seems to increase over time in the comatose patient, and the strongest connections are left lateralized in comparison to the controls, who showed both local (i.e., close electrodes are highly connected) and inter-hemispheric connections. Visual differences were not as obvious at the source level, but still a FC increase, especially in theta band, was observed during RS02 in the coma patient (see Figure 4.4). Here, the strongest connections (top 10%) were observed within frontotemporal, parietotemporal and frontolimbic regions, predominately in the left hemisphere. The rest of FC matrices corresponding to other frequency bands in the comatose patient are shown in Supplementary information II (Figures S2 and S3).

Our ML procedure achieved high classification when discriminating FC across the three RS periods within the coma patient. Figure 4.5 (panel A) shows the 10 discriminating FC in the theta band at both the sensor and source levels. As it can be observed in the scatter plot (panel B), two main features used as predictors were able to separate the three classes (RS01, RS02 and RS03), achieving 93.4% and 92.0% accuracies at the sensor and source levels, respectively when using a linear SVM classifier. Mean FC differences across the RS periods are displayed in panel C. See a summary of the classification performance for each classifier, and mean FC differences (one-way ANOVA at single-subject level) for the comatose patient in Table 4.2. Post-hoc comparison using a Bonferroni test revealed significant differences of mean FC among RS periods. At sensor level, greater mean FC was found during RS02 and RS03 in comparison to RS01; while at source level there was greater mean FC at RS02, which slightly decreased during RS03.

See the full list of the most discriminative FC features for both sensor and source levels in Supplementary information II (Tables S3 and S4).

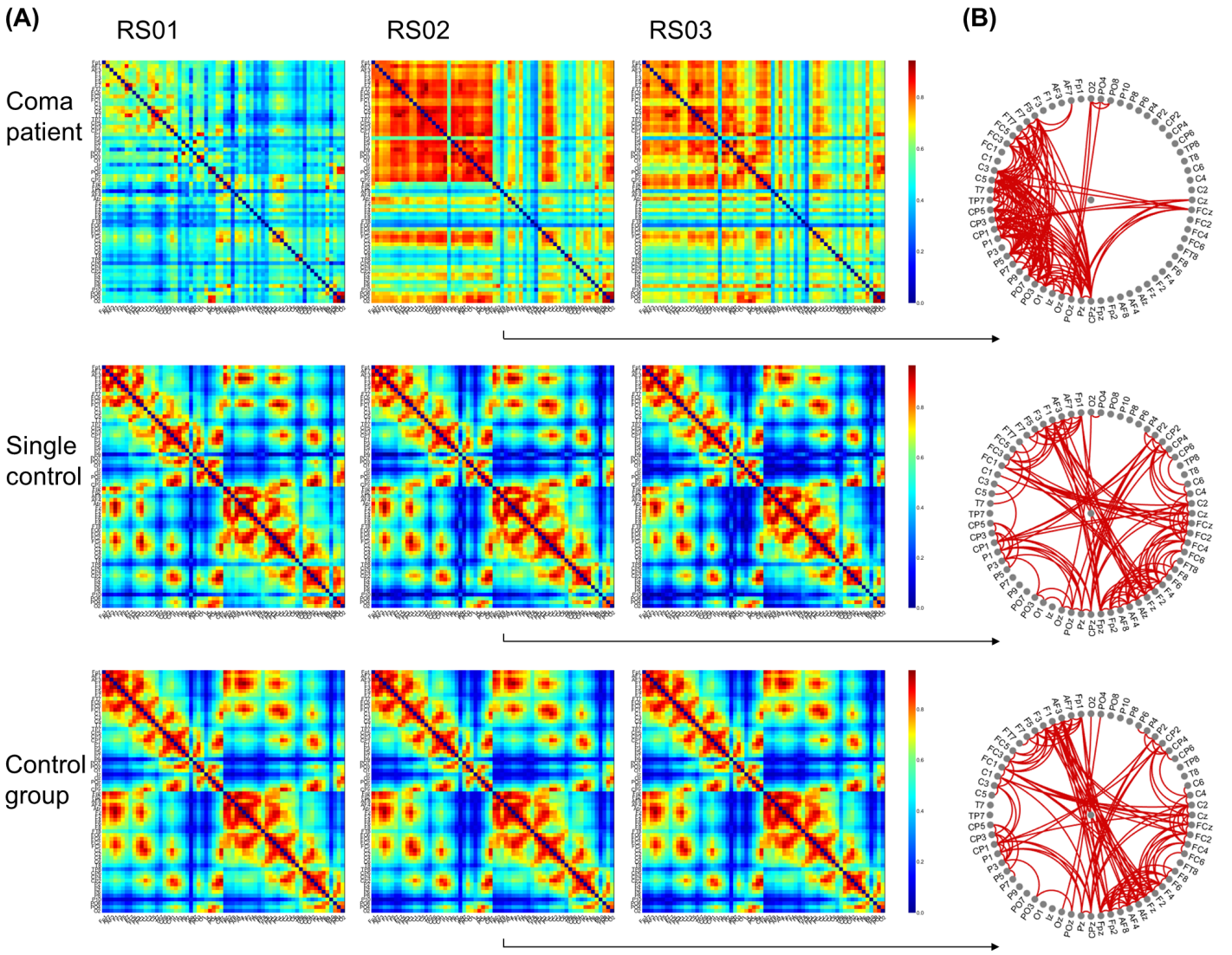

Figure 4.3: Sensor-level FC matrices across RS periods in the coma patient, a single control and the control group for the theta band, and top 10% of the strongest connections in RS02.

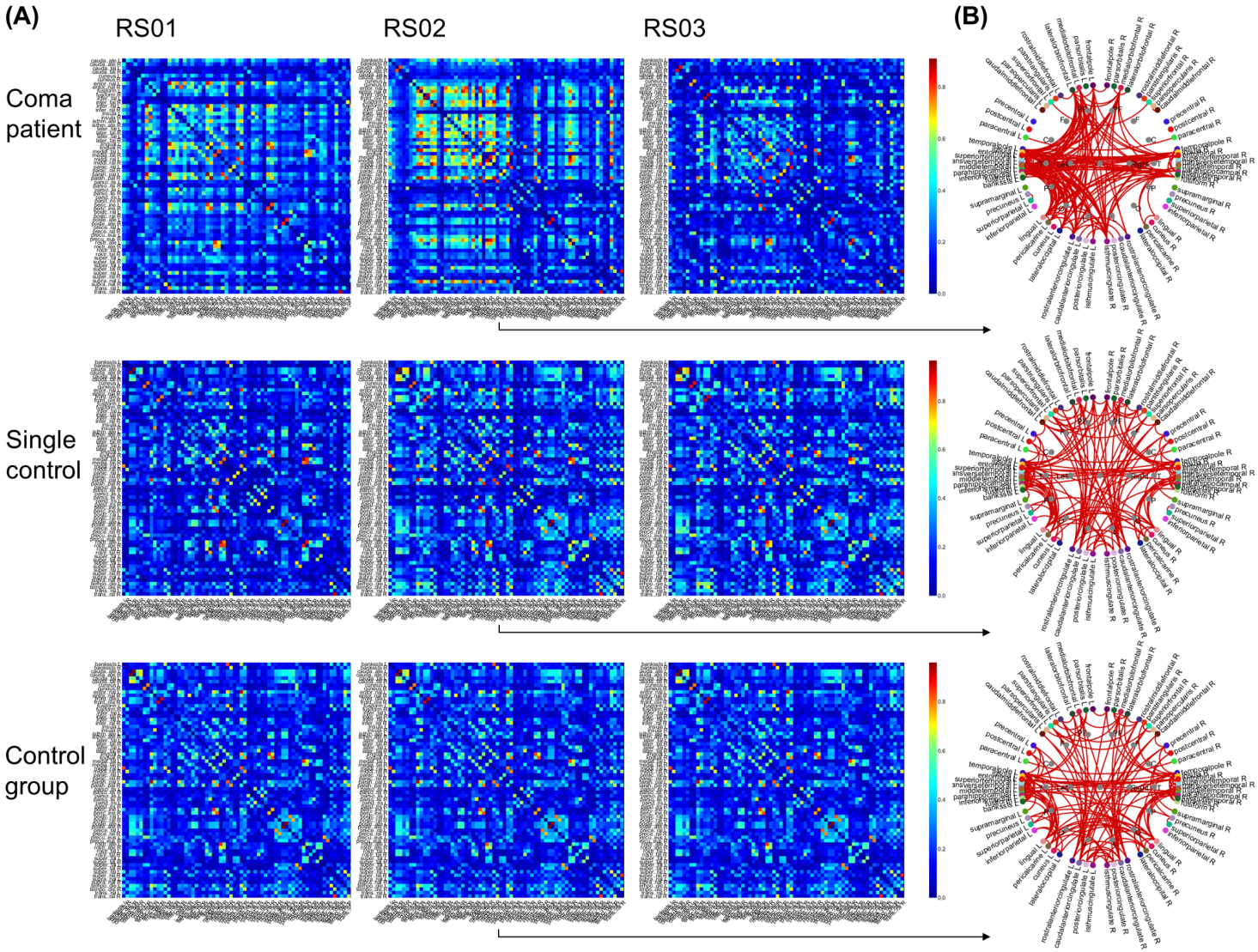

Figure 4.4: Source-level FC matrices across RS periods in the coma patient, a single control and the control group for the theta band, and top 10% of the strongest connections in RS02.

Table 4.2: Classification performance of several classifiers discriminating RS epochs within the coma patient, and mean differences at both the sensor and source levels for each frequency band.

		Classifiers					**One-way ANOVA**					**Post-hoc comparisons**			
		SVM	**LDA**	**NB**	**KNN**	**Tree**	**Condition**	**Mean**	**SD**	**F**	**p**	**Comparison**	**Mean diff.**	**t-value**	**pbonf**
SENSORS	Delta	**90.0**	83.3	84.0	84.1	78.9	RS01	0.629	0.05	22.4	< .001	RS01-RS02	-0.04	-5.70	< .001
							RS02	0.669	0.06			RS01-RS03	-0.04	-5.90	< .001
							RS03	0.671	0.07			RS02-RS03	0.00	-0.20	0.978
	Theta	**93.4**	**93.4**	**91.7**	**90.4**	89.0	RS01	0.477	0.06	90.95	< .001	RS01-RS02	-0.09	-10.63	< .001
							RS02	0.568	0.07			RS01-RS03	-0.11	-12.50	< .001
							RS03	0.584	0.08			RS02-RS03	-0.02	-1.87	0.186
	Alpha	**90.3**	89.0.1.1	82.6	79.2	73.3	RS01	0.481	0.066	7.397	< .001	RS01-RS02	-0.03	-3.83	< .001
							RS02	0.511	0.059			RS01-RS03	-0.01	-1.63	0.315
							RS03	0.493	0.068			RS02-RS03	-0.02	2.21	0.084
	Beta	**92.6**	**92.2**	**90.2**	89.0	84.1	RS01	0.457	0.05	4.68	< .05	RS01-RS02	-0.02	-0.28	1.00
							RS02	0.459	0.04			RS01-RS03	-0.02	-2.28	< .05
							RS03	0.472	0.05			RS02-RS03	-0.01	-2.50	< .05
SOURCES	Delta	**91.7**	**90.7**	**91.7**	**90.2**	81.4	RS01	0.478	0.05	4.494	< .05	RS01-RS02	-0.01	-1.20	0.69
							RS02	0.486	0.05			RS01-RS03	0.01	1.78	0.23
							RS03	0.467	0.05			RS02-RS03	0.02	2.98	< .01
	Theta	**92.0**	**91.2**	**91.2**	86.8	82.6	RS01	0.418	0.05	14.44	< .001	RS01-RS02	-0.03	-5.32	< .001
							RS02	0.452	0.06			RS01-RS03	-0.01	-1.97	0.15
							RS03	0.431	0.05			RS02-RS03	0.02	3.35	< .05
	Alpha	89.8	85.8	87.0	85.3	76.3	RS01	0.344	0.05	4.69	< .05	RS01-RS02	-0.02	-2.98	< .01
							RS02	0.360	0.04			RS01-RS03	-0.01	-0.86	1.00
							RS03	0.348	0.05			RS02-RS03	0.01	2.12	0.105
	Beta	**90.3**	**90.0**	89.6	89.6	88.7	RS01	0.252	0.042	3.895	< .05	RS01-RS02	-0.011	-2.791	< .05
							RS02	0.263	0.027			RS01-RS03	-0.006	-1.426	0.464
							RS03	0.257	0.028			RS02-RS03	0..005	1.365	0.519

SVM: Support Vector Machine; LDA: Linear discriminant analysis; NB: Naive Bayes; KNN: K-nearest neighbors; Tree: Decision trees; Mean diff: Mean difference; pbonf: p-value from Bonferroni post-hoc test. Accuracies $\geq$ 90% are displayed in bold.

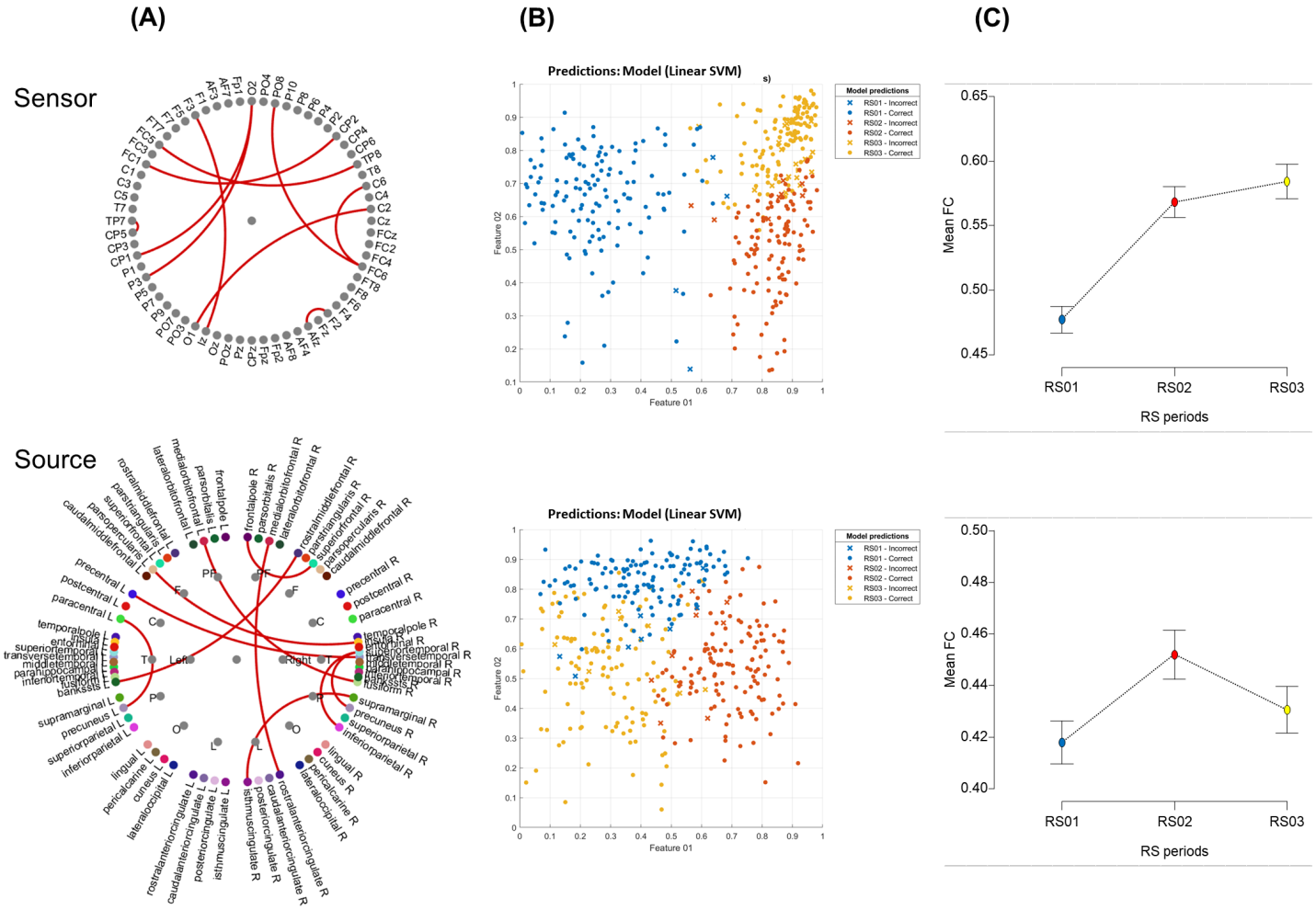

Figure 4.5: Functional connectivity in coma across RS periodos in theta band at both the sensor and source levels. A) Most discriminative FC features among RS periods in the coma patient; B) Scatter plot projecting the first two main FC features for a linear SVM model prediction; C) Mean FC differences among RS periods at single-subject level.

4.4 Discussion

This report makes a modest but important contribution at analyzing a phase-based measure of FC in response to auditory stimuli and resting state at both the sensor and source levels in a coma patient near death. Using a ML procedure, we sought to distinguish auditory responses from the dying coma patient vs. individual healthy controls, and track changes over time during resting state in coma.

4.4.1 Functional connectivity in response to auditory stimuli

Our ML procedure showed high classification performance when discriminating single-trial FC in response to auditory duration deviants between a comatose patient and healthy controls. Accuracies were above 90% across all frequency bands, with maximum scores in alpha and beta bands for both sensor and source-level analyses.

Marked connectivity differences have been reported between DOC patients and healthy controls in several studies, in which FC disruption tends to be more significant and proportional to the level of impairment in consciousness (Boly et al., 2009; Vanhaudenhuyse et al., 2010; Binder et al., 2017; Bodien et al., 2017). The specific hypothesis that neural synchronization in response to auditory sounds would reflect coma severity was recently evaluated by Alnes and colleagues in the alpha frequency band (Alnes et al., 2021). The authors found that FC, quantified by PLV between electrodes during the first day of acute coma, was significantly lower in non-survivor patients of cardiac arrest compared to both conscious controls and survivors. Interestingly, the PLV was also predictive of patients' outcome at 3 months, suggesting that preserved phase synchronization between EEG signals could be a necessary condition for the presence or return of consciousness. Similar alterations have been previously reported in sleep, showing decreased PLV to auditory stimuli in alpha and beta bands when subjects become unconscious (Lee et al., 2019). Changes in high-frequency connectivity, as suggested by Lee and colleagues, are an indicator of the disintegration of dynamic connectivity during the loss of consciousness (Lee et al., 2019). In the present study, the decreased FC in response to auditory deviant stimuli would be then an expected finding for a patient with a severe diffuse hypoxic-ischemic injury, who was particularly assessed in his last

hours of life in comparison to healthy controls. The fact that classification performance was found greater in the high-frequency bands, achieving perfect discrimination (100%) in beta band when compared to most controls, is consistent with previous work.

Furthermore, the main discriminative single-FC features or connections in relation to the controls were mainly distributed in frontocentral and frontoparietal regions. The discriminating source-level features varied across different frequency bands. Several brain structures within the frontal and posterior cingulate cortices, and others like insula, cuneus, precuneus, superiotemporal and parahippocampal cortices, which are believed to be important hubs for conscious information processing (Dehaene and Changeux, 2011; Laureys and Schiff, 2012; Holeckova et al., 2008; Boly et al., 2009), were commonly identified.

Since our coma patient died during the EEG session, only a single block of the auditory oddball paradigm was recorded. It remains to investigate the dynamics of FC trough different blocks over time at single-subject level as we did when analyzing RS periods.

4.4.2 Functional connectivity in resting state before the end of life

Single-subject analysis revealed RS connectivity changes over time in the coma patient before the end of life. Using discriminating FC features between the three RS periods, our ML framework was able to classify the epochs corresponding to each RS period, achieving accuracies up to 93.4% and 92.0% at sensor and source levels respectively. These findings provide evidence of increased FC in at least one of the last two RS periods closest to death. One may argue that the reduced FC observed in the first RS period (RS01) in our comatose patient, could be to the fact that this period was not preceded by any auditory task as the other periods (RS02 and RS03), which perhaps were affected as a result of previous auditory stimulation. In such a case, we should have observed similar results in healthy controls, who rather displayed stable patterns of connectivity across time.

Although a hypoactive brain with loss of anatomical and functional connections is generally assumed in brain-injured patients, hyperconnectivity is not rare in neurological

disorders. In fact, both hyper-and hypoconnectivity may coexist across different brain regions as fundamental responses to neurological disruption (see Hillary et al. (2015) for review). In a resting state-fMRI study, DiPerri and collegues found hyperconnectivity in limbic structures, including the orbitofrontal cortex, insula, hypothalamus, and the ventral tegmental area; with greater effects in UWS compared to MCS (Di Perri et al., 2013; Perri, 2014). The authors concluded that hyperconnectivity could be an indicator of persistent engagement of residual self-reinforcing neural loops, which could disrupt normal patterns of connectivity, included synchronized activity. While compensatory mechanisms (i.e., allocation of extra neural resources to compensate for injury/damage) have been the most common explanation for the hyperconnectivity responses documented in several brain insults like traumatic brain injury, multiple sclerosis, Alzheimer's disease and epilepsy (Hillary et al., 2014, 2015; Bharath et al., 2015), much additional work is needed to determine their functional role and underlying mechanisms.

There is also evidence demonstrating enhanced EEG brain activity and connectivity in the dying brain. For instance, Chawla and colleagues reported transient electrical spikes in critically ill patients immediately before cardiac arrest (Chawla et al., 2009, 2017). The exact cause of such responses, called end-of-life electrical surges (ELES), still remain unknown (Chawla et al., 2017). Moreover, an electrophysiological study showed a transient and global surge of synchronized gamma oscillations, exhibiting increased interregional connectivity, during cardiac arrests in rats (Borjigin et al., 2013). This latter study has been disseminated through mass media as establishing a hypothetical neurological explanation for the mental events known as "near-death experiences", which are considered conscious perceptual experiences (e.g., out-of-body experiences, deep feeling of peacefulness, entering a tunnel of bright light, etc), occurring in individuals during resuscitation after cardiac arrest or in other non-life threatening situations (Martial et al., 2020; Kondziella, 2020). However, more empirical evidence is still needed to explain such intriguing phenomenon, documented worldwide in multiple cultures.

Additionally, we also found left-lateralized FC in the comatose patient, a finding that was not observed in controls. These results are somehow consistent with previous fMRI and EEG studies that identified decreased interhemispheric FC in DOC patients (Ovadia-Caro et al., 2012; Demertzi et al., 2015; Cacciola et al., 2019). Very recently, Rizkallah and

colleagues demonstrated decreased EEG phase-based FC in brain network integration (i.e., communication between distant brain modules, reflecting global information) and increase in brain network segregation (i.e., communication within the same brain module) in DOC patients as compared to healthy controls (Rizkallah et al., 2019). In our patient, the increased FC across time, particularly during RS02 with a left-hemisphere preponderance, could perhaps be the result of a compensatory brain plastic mechanism, given the limited inter-hemispheric connections. However, this hypothetical explanation should be tested in further research.

4.4.3 Clinical significance and methodological considerations

This report, is to our knowledge, the first to assess EEG functional connectivity in a dying coma patient at both the sensor and source levels. Although spurious estimates of FC can still ocurr in source space as result of signal leakage[d], the inclusion of FC measures from source EEG signals is a step forward in reducing volume conduction effects. It could also serve as a first step for encouraging researchers to look for consistent information between sensor-and-source space analyses in the context of coma and DOC.

While further research with a greater number of comatose patients is ideal, our ML procedure can be easily applied in small sample sizes, as it distinguishes single-trial FC elicited by auditory stimuli of one patient with those of individual controls, and allows to determine FC changes under RS conditions at single-subject level. All this together has valuable clinical applications, since one of the most common questions from healthcare specialists and family members is whether a particular patient is actually responding to external stimuli and how the patient and her/his responses are evolving across time. With the advances in EEG technology, our procedure could be relatively easy to integrate in real time-EEG monitoring in DOC patients.

We acknowledge, however, certain limitations and methodological considerations. First, our analysis should be interpreted in the light of a single comatose patient with anoxic brain injury, suppressed EEG activity and poor outcome prognosis. Further research is necessary, since other etiologies and levels of consciousness are likely to

[d]Signal leakage refers to neighboring sources sharing some activity due to low spatial resolution of the data (Bruña et al., 2018)

reflect different connectivity features. Second, other phase synchronization measures, such as the weighted phase lag index (PLI) and the corrected imaginary PLV (ciPLV) Bruña et al. (2018) could be implemented, since they seem to be insensitive to zero-lag synchronization and therefore less prone to volume conduction and source leakage effects in comparison to PLV. Nevertheless, it is important to highlight that each connectivity measure has its own advantages and disadvantages, and similar to the source localization methods, there is no consensus on whether one outperforms the other. Also, there has been a growing interest in determining what is the best combination of inverse-source solution and connectivity method. In this regard, our choice was supported by two studies: one conducted by Hassan and colleagues (Hassan et al., 2017), which reported that wMNE/PLV performed better than other combinations of five inverse solution algorithms and four widely used connectivity measures; and the second study that recently used similar combination of wMNE/PLV in the context of DOC (Rizkallah et al., 2019).

Some may also argue that using a source template constructed from standard MRI images, instead of a subject-specific one, might be problematic when interpreting the results from a severely-injured patient. However, given that our results showed a relatively good match between sensor and source-based FC, we believe that the effects observed at the source level here, may more reliably reflect underlying neurophysiological changes in coma.

4.5 Conclusions

In conclusion, we found decreased single-trial FC in response to auditory stimuli in a comatose patient in comparison to controls, and identified FC changes over time during resting state in this patient before death. This case study is a further contribution to the neuroscience research focused on the neurophysiological mechanisms that may occur during the transition to death following severe brain damage.

References

Alnes, S. L., Lucia, M. D., Rossetti, A. O., and Tzovara, A. (2021). Complementary roles of neural synchrony and complexity for indexing consciousness and chances of surviving in acute coma. *Neuroimage*, 245:118638.

Armanfard, N., Komeili, M., Reilly, J. P., Mah, R., and Connolly, J. F. (2016). Automatic and continuous assessment of ERPs for mismatch negativity detection. *Proc. Annu. Int. Conf. IEEE Eng. Med. Biol. Soc. EMBS*, 2016-Octob:969–972.

Baillet, S., Mosher, J. C., and Leahy, R. M. (2001). Electromagnetic brain mapping. *IEEE Signal Process. Mag.*, 18(6):14–30.

Bharath, R. D., Munivenkatappa, A., Gohel, S., Panda, R., Saini, J., Rajeswaran, J., Shukla, D., Bhagavatula, I. D., and Biswal, B. B. (2015). Recovery of resting brain connectivity ensuing mild traumatic brain injury. *Front. Hum. Neurosci.*, 9(September):513.

Binder, M., Górska, U., and Griskova-Bulanova, I. (2017). 40 Hz auditory steady-state responses in patients with disorders of consciousness: Correlation between phase-locking index and Coma Recovery Scale-Revised score. *Clin. Neurophysiol.*, 128(5):799–806.

Blundon, E. G., Gallagher, R. E., and Ward, L. M. (2022). Resting state network activation and functional connectivity in the dying brain. *Clin. Neurophysiol.*, 135:166–178.

Bodien, Y. G., Chatelle, C., and Edlow, B. L. (2017). Functional Networks in Disorders of Consciousness. *Semin. Neurol.*, 37(5):485–502.

Boly, M., Tshibanda, L., Vanhaudenhuyse, A., Noirhomme, Q., Schnakers, C., Ledoux, D., Boveroux, P., Garweg, C., Lambermont, B., Phillips, C., Luxen, A., Moonen, G., Bassetti, C., Maquet, P., and Laureys, S. (2009). Functional connectivity in the

default network during resting state is preserved in a vegetative but not in a brain dead patient. *Hum. Brain Mapp.*, 30(8):2393–2400.

Borjigin, J., Lee, U. C., Liu, T., Pal, D., Huff, S., Klarr, D., Sloboda, J., Hernandez, J., Wang, M. M., and Mashour, G. A. (2013). Surge of neurophysiological coherence and connectivity in the dying brain. *Proc. Natl. Acad. Sci. U. S. A.*, 110(35):14432–14437.

Bruña, R., Maestú, F., and Pereda, E. (2018). Phase locking value revisited: Teaching new tricks to an old dog. *J. Neural Eng.*, 15(5):056011.

Brunner, C., Billinger, M., Seeber, M., Mullen, T. R., and Makeig, S. (2016). Volume Conduction Influences Scalp-Based Connectivity Estimates. *Front. Comput. Neurosci.*, 10:121.

Cacciola, A., Naro, A., Milardi, D., Bramanti, A., Malatacca, L., Spitaleri, M., Leo, A., Muscoloni, A., Cannistraci, C. V., Bramanti, P., Calabrò, R. S., and Anastasi, G. P. (2019). Functional brain network topology discriminates between patients with minimally conscious state and unresponsivewakefulness syndrome. *J. Clin. Med.*, 8(3):306.

Cao, C., Tutwiler, R. L., and Slobounov, S. (2008). Automatic classification of athletes with residual functional deficits following concussion by means of EEG signal using support vector machine. *IEEE Trans. Neural Syst. Rehabil. Eng.*, 16(4):327–335.

Carrasco-Gómez, M., Keijzer, H. M., Ruijter, B. J., Bruña, R., Tjepkema-Cloostermans, M. C., Hofmeijer, J., and van Putten, M. J. (2021). EEG functional connectivity contributes to outcome prediction of postanoxic coma. *Clin. Neurophysiol.*, 132(6):1312–1320.

Chawla, L. S., Akst, S., Junker, C., Jacobs, B., and Seneff, M. G. (2009). Surges of electroencephalogram activity at the time of death: A case series. *J. Palliat. Med.*, 12(12):1095–1100.

Chawla, L. S., Terek, M., Junker, C., Akst, S., Yoon, B., Brasha-Mitchell, E., and Seneff, M. G. (2017). Characterization of end-of-life electroencephalographic surges in critically ill patients. *Death Stud.*, 41(6):385–392.

Chennu, S., Annen, J., Wannez, S., Thibaut, A., Chatelle, C., Cassol, H., Martens, G., Schnakers, C., Gosseries, O., Menon, D., and Laureys, S. (2017). Brain networks predict metabolism, diagnosis and prognosis at the bedside in disorders of consciousness. *Brain*, 140(8):2120–2132.

Chennu, S., Finoia, P., Kamau, E., Allanson, J., Williams, G. B., Monti, M. M., Noreika, V., Arnatkeviciute, A., Canales-Johnson, A., Olivares, F., Cabezas-Soto, D., Menon, D. K., Pickard, J. D., Owen, A. M., and Bekinschtein, T. A. (2014). Spectral Signatures of Reorganised Brain Networks in Disorders of Consciousness. *PLoS Comput. Biol.*, 10(10).

Dehaene, S. and Changeux, J. P. (2011). Experimental and Theoretical Approaches to Conscious Processing. *Neuron*, 70(2):200–227.

Demertzi, A., Antonopoulos, G., Heine, L., Voss, H. U., Crone, J. S., De Los Angeles, C., Bahri, M. A., Di Perri, C., Vanhaudenhuyse, A., Charland-Verville, V., Kronbichler, M., Trinka, E., Phillips, C., Gomez, F., Tshibanda, L., Soddu, A., Schiff, N. D., Whitfield-Gabrieli, S., and Laureys, S. (2015). Intrinsic functional connectivity differentiates minimally conscious from unresponsive patients. *Brain*, 138(9):2619–2631.

Di Perri, C., Bastianello, S., Bartsch, A. J., Pistarini, C., Maggioni, G., Magrassi, L., Imberti, R., Pichiecchio, A., Vitali, P., Laureys, S., and Di Salle, F. (2013). Limbic hyperconnectivity in the vegetative state. *Neurology*, 81(16):1417–1424.

Friston, K. J. (2011). Functional and Effective Connectivity: A Review. *Brain Connect.*, 1(1):13–36.

Gramfort, A., Papadopoulo, T., Olivi, E., and Clerc, M. (2010). OpenMEEG: Opensource software for quasistatic bioelectromagnetics. *Biomed. Eng. Online*, 9(1):1–20.

Hassan, M., Benquet, P., Biraben, A., Berrou, C., Dufor, O., and Wendling, F. (2015). Dynamic reorganization of functional brain networks during picture naming. *Cortex*, 73:276–288.

Hassan, M., Dufor, O., Merlet, I., Berrou, C., and Wendling, F. (2014). EEG source connectivity analysis: From dense array recordings to brain networks. *PLoS One*,

9(8):e105041.

Hassan, M., Merlet, I., Mheich, A., Kabbara, A., Biraben, A., Nica, A., and Wendling, F. (2017). Identification of Interictal Epileptic Networks from Dense-EEG. *Brain Topogr.*, 30(1):60–76.

Hassan, M. and Wendling, F. (2018). Electroencephalography source connectivity: toward high time/space resolution brain networks. *arXiv prepr. arXiv1801.02549*.

He, B., Astolfi, L., Valdes-Sosa, P. A., Marinazzo, D., Palva, S. O., Benar, C. G., Michel, C. M., and Koenig, T. (2019). Electrophysiological Brain Connectivity: Theory and Implementation. *IEEE Trans. Biomed. Eng.*, 66(7):2115–2137.

Hillary, F. G., Rajtmajer, S. M., Roman, C. A., Medaglia, J. D., Slocomb-Dluzen, J. E., Calhoun, V. D., Good, D. C., and Wylie, G. R. (2014). The rich get richer: Brain injury elicits hyperconnectivity in core subnetworks. *PLoS One*, 9(8):e104021.

Hillary, F. G., Roman, C. A., Venkatesan, U., Rajtmajer, S. M., Bajo, R., and Castellanos, N. D. (2015). Hyperconnectivity is a fundamental response to neurological disruption. *Neuropsychology*, 29(1):59–75.

Holeckova, I., Fischer, C., Morlet, D., Delpuech, C., Costes, N., and Mauguière, F. (2008). Subject's own name as a novel in a MMN design: A combined ERP and PET study. *Brain Res.*, 1189(1):152–165.

Höller, Y., Thomschewski, A., Bergmann, J., Kronbichler, M., Crone, J. S., Schmid, E. V., Butz, K., Höller, P., Nardone, R., and Trinka, E. (2014). Connectivity biomarkers can differentiate patients with different levels of consciousness. *Clin. Neurophysiol.*, 125:1545–1555.

Kondziella, D. (2020). The Neurology of Death and the Dying Brain: A Pictorial Essay. *Front. Neurol.*, 11:736.

Lachaux, J. P., Rodriguez, E., Martinerie, J., and Varela, F. J. (1999). Measuring phase synchrony in brain signals. *Hum. Brain Mapp.*, 8(4):194–208.

Laureys, S. and Schiff, N. D. (2012). Coma and consciousness: Paradigms (re)framed by neuroimaging. *Neuroimage*, 61(2):478–491.

Lechinger, J., Wielek, T., Blume, C., Pichler, G., Michitsch, G., Donis, J., Gruber, W., and Schabus, M. (2016). Event-related EEG power modulations and phase connectivity indicate the focus of attention in an auditory own name paradigm. *J. Neurol.*, 263(8):1530–1543.

Lee, M., Baird, B., Gosseries, O., Nieminen, J. O., Boly, M., Postle, B. R., Tononi, G., and Lee, S. W. (2019). Connectivity differences between consciousness and unconsciousness in non-rapid eye movement sleep: a TMS–EEG study. *Sci. Rep.*, 9(1):1–9.

Martial, C., Cassol, H., Laureys, S., and Gosseries, O. (2020). Near-Death Experience as a Probe to Explore (Disconnected) Consciousness. *Trends Cogn. Sci.*, 24(3):173–183.

Masychev, K., Ciprian, C., Ravan, M., Reilly, J. P., and Maccrimmon, D. (2021). Advanced Signal Processing Methods for Characterization of Schizophrenia. *IEEE Trans. Biomed. Eng.*, 68(4):1123–1130.

Michel, C. M., Murray, M. M., Lantz, G., Gonzalez, S., Spinelli, L., and Grave De Peralta, R. (2004). EEG source imaging. *Clin. Neurophysiol.*, 115(10):2195–2222.

Ovadia-Caro, S., Nir, Y., Soddu, A., Ramot, M., Hesselmann, G., Vanhaudenhuyse, A., Dinstein, I., Tshibanda, J. F. L., Boly, M., Harel, M., Laureys, S., and Malach, R. (2012). Reduction in inter-hemispheric connectivity in disorders of consciousness. *PLoS One*, 7(5).

Peng, H., Long, F., and Ding, C. (2005). Feature selection based on mutual information: Criteria of Max-Dependency, Max-Relevance, and Min-Redundancy. *IEEE Trans. Pattern Anal. Mach. Intell.*, 27(8):1226–1238.

Perri, C. D. (2014). Measuring consciousness in coma and related states. *World J. Radiol.*, 6(8):589.

Rizkallah, J., Annen, J., Modolo, J., Gosseries, O., Benquet, P., Mortaheb, S., Amoud, H., Cassol, H., Mheich, A., Thibaut, A., Chatelle, C., Hassan, M., Panda, R., Wendling, F., and Laureys, S. (2019). Decreased integration of EEG source-space networks in disorders of consciousness. *NeuroImage Clin.*, 23.

Sawilowsky, S. S. (2009). Very large and huge effect sizes. *J. Mod. Appl. Stat. Methods*, 8(2):597–599.

Schoffelen, J.-M. and Gross, J. (2009). Source connectivity analysis with MEG and EEG. *Hum. Brain Mapp.*, 30(6):1857–1865.

Sitt, J. D., King, J. R., El Karoui, I., Rohaut, B., Faugeras, F., Gramfort, A., Cohen, L., Sigman, M., Dehaene, S., and Naccache, L. (2014). Large scale screening of neural signatures of consciousness in patients in a vegetative or minimally conscious state. *Brain*, 137(8):2258–2270.

Tadel, F., Baillet, S., Mosher, J. C., Pantazis, D., and Leahy, R. M. (2011). Brainstorm: A user-friendly application for MEG/EEG analysis. *Comput. Intell. Neurosci.*, 2011.

Tononi, G., Boly, M., Massimini, M., and Koch, C. (2016). Integrated information theory: from consciousness to its physical substrate. *Nat. Rev. Neurosci.*, 17(7):450–461.

Van de Steen, F., Faes, L., Karahan, E., Songsiri, J., Valdes-Sosa, P. A., and Marinazzo, D. (2019). Critical Comments on EEG Sensor Space Dynamical Connectivity Analysis. *Brain Topogr.*, 32(4):643–654.

Vanhaudenhuyse, A., Noirhomme, Q., Tshibanda, L. J., Bruno, M. A., Boveroux, P., Schnakers, C., Soddu, A., Perlbarg, V., Ledoux, D., Brichant, J. F., Moonen, G., Maquet, P., Greicius, M. D., Laureys, S., and Boly, M. (2010). Default network connectivity reflects the level of consciousness in non-communicative brain-damaged patients. *Brain*, 133(1):161–171.

Zubler, F., Steimer, A., Kurmann, R., Bandarabadi, M., Novy, J., Gast, H., Oddo, M., Schindler, K., and Rossetti, A. O. (2017). EEG synchronization measures are early outcome predictors in comatose patients after cardiac arrest. *Clin. Neurophysiol.*, 128(4):635–642.

Chapter 5

Summary and Conclusions

The present dissertation presented a series of studies in which several statistical methods (Chapter 2) and machine learning procedures (Chapter 3 and 4) were evaluated to determine whether auditory electrophysiological responses or states that are typically associated with coma emergence are transient over time, and can be objectively detected at single-subject level. Overall, our results replicate a number of findings and expand the utility of automated frameworks applied to EEG/ERP data to assess and track functional level in coma patients and potentially predict their outcomes.

Drawing reliable inferences at the individual level is challenging and cannot be made with similar confidence as at the group level. However, findings obtained from group level usually rely on some subjects exhibiting a strong effect, while others could exhibit little or even the opposite pattern of activity. In this dissertation, significant steps has been made in the identification of neurophysiological effects on a single-subject basis, which is essential for clinical applications that are likely to impact the diagnosis and prognosis in coma. This final chapter (5) will summarize our main findings, their contributions, limitations, as well as future research directions.

5.1 Summary of findings and contribution

5.1.1 Fluctuations in MMN detectability as a feature of coma

The MMN is a change-detection brain response, reflecting a predictive coding process that while automatic and independent of a person's conscious awareness, indicates the presence of a certain conscious state (Blain-Moraes et al., 2016; Dykstra et al., 2017; Tavakoli et al., 2019) that is necessary for other levels of consciousness to emerge. In Chapter 2, we have hypothesized, that the MMN's low sensitivity observed in previous work (Fischer et al., 1999, 2004; Naccache et al., 2005; Luauté et al., 2005) is attributable to its instability over time making it easily missed during a single assessment. Our results demonstrate for the first time the robust stability of the MMN over hours of continuous testing of healthy people; a result that contrasts with its waxing-and-waning cycling characteristic demonstrated recently in coma patients (Armanfard et al., 2018). Our results support the use of the MMN as a clinical tool for monitoring functional changes associated with coma awakening and potential return to consciousness. Findings in three coma patients, recorded over 24 hours provided further evidence that the MMN is present but transient in coma across hours.

Taken together, the results in Chapter 2 provide several guidelines for using the MMN as a neurophysiological predictor of coma emergence.

1.) First, it highlights that repeated assessments are extremely important to confirm the presence or absence of the MMN and related ERP components, given their occurrence rate is likely to vary over the course of hours within a day.

2.) Stimulus selection is crucial for accurate evaluation of the MMN during full conscious state and coma. Auditory duration deviants as in the multi-feature paradigm here used, are more suitable to elicit reliable MMNs over the course of several hours in comparison to other deviants. These results support the evidence that MMN to unexpected duration changes is highly reproducible and robustly identified in individual participants with high SNR (Michie et al., 2000; Recasens and Uhlhaas, 2017; O'Reilly and O'Reilly, 2021), promising greater clinical utility.

3.) Despite yielding significant differences on group level, if one selected method fails to distinguish significant effects at the single subject level, then their application for diagnostic purposes may be limited. Our findings revealed that Bayesian *t*-test analyses in contrast to other classic inference approaches (i.e., the permutation *t*-test), seem to be more sensitive in detecting reliable ERP responses and confirming visual inspection judgments on the presence of the MMN component.

It has been claimed for years that the MMN is not present in every healthy subjects (Lehembre, 2012); however, this statement could be somehow arguably. Perhaps a single assessment was acquired or other variables related with the design of the experimental paradigm, the stimuli selection, the number of trials collected, the placement of electrodes and signal quality, the statistical analysis and so on, could have prevented the confirmation of the MMN presence in such individuals. Our results revealed that some fluctuations in MMN detectability are certainly observed in some healthy subjects at single-subject level over an extended period of time, but depending on the deviant type within the multi-feature paradigm, and the statistical method performed. One possible explanation for the robust MMN responses to duration deviants across all the recording blocks, is that apparently duration changes in stimuli may also lead to a change in perceived intensity, suggesting that duration deviants in oddball paradigms might work in fact as double deviants (Michie et al., 2000; Jacobsen and Schröger, 2003).

5.1.2 Multivariate decoding is a feasible automatic tool for monitoring auditory discrimination in coma

In Chapter 3, it was demonstrated the feasibility of multivariate pattern analyses (MVPA) to track the temporal sequence of various levels of auditory information processing. Using the same dataset presented in Chapter 2, we found that single-trials responses elicited by duration deviants and standard sounds are robustly discriminated in healthy controls, with high decoding performance (maximum AUC scores ranging from 80 to 94%) during the latency intervals associated with either the MMN and the P3a components. We also showed preliminary evidence of the utility of MVPA for monitoring the functional level of some coma patients over time and predicting their chances to emerge from coma, either returning to conscious awareness or transitioning to other

post-comatose states. As expected, the decoding performance in the coma patients was lower in comparison to the healthy controls, but there were instances in which the patients, regardless of their final outcome, showed periods of classification performance above-chance level (50%) after stimulus onset, particularly during the second day of recording. The major contributions of this chapter are outlined below.

1.) Our results support the use of MVPA as a cost-efficient and automated technique for discriminating auditory neural responses that might be even difficult to detect by ERP/EEG experts at the single-subject level. This approach would allow clinicians to quantify the performance of individual patients in detecting auditory changes without no priori information about MMN or other related ERP components (Morlet and Fischer, 2014).

2.) Robust decoding performance was found with as few as 11 electrodes as with 64 electrodes. These sites are F3, Fz, F4, C3, Cz, C4, P3, Pz, P4, T7, T8 following the same 10/20 system. Achieving sufficient discriminative information of auditory responses with such reduced number of electrodes is extremely useful in intensive care, since a high-density EEG montage placed on severe-injured patients is not always feasible.

3.) The comatose patients reported in our study showed a slight increment in both classification performance (AUC) and behavioral scores (GCS and FOUR) during the second day of recording, suggesting that MVPA may predict the patient's clinical course. In fact, the patient who reached the highest decoding performance (AUC=80% in a single recording block), showed behavioral signals related with coma awakening that same day and a positive outcome after a year of rehabilitation. These findings provide further evidence of intact auditory discrimination in acute coma, as well as improvements in classification performance over time as predictors of coma outcome (Tzovara et al., 2013, 2016; Rossetti et al., 2014).

4.) MVPA is also able to capture automatically fluctuations of auditory discrimination in coma. Such instances of increases and decreases in decoding performance from a single block to another can help clinicians determine which time periods within a day are most suitable for conducting neurological evaluations that require the involvement of the patient's auditory system.

In summary, the multivariate decoding approach as here implemented could reveal how full conscious subjects and comatose patients differs in terms of information content they represent at each time point following the onset of a stimulus, and potentially serve as a method for online tracking of electrical brain activity associated with auditory deviance detection in DOC.

5.1.3 Functional connectivity in acute coma on the verge of death

Chapter 4 is a case study, in which a phase-based measure of FC in response to auditory stimuli and resting state was computed for the first time at both sensor and source levels in a comatose patient, who suddenly died during an EEG recording protocol. Using a machine learning procedure, the single-trials FC in response to auditory duration deviants between the patient and healthy controls were discriminated with accuracies above 90%, especially in alpha and beta bands for both sensor and source-level analyses. Interestingly, the coma patient showed at least a resting-state period of hyperconnectivity before dying, which seems to be a fundamental response to neurological disruption in traumatic brain injury and other disorders (Bharath et al., 2015; Hillary et al., 2015). Similar neurophysiological phenomenon of high activity and connectivity have been previously observed in dying brains of humans (Chawla et al., 2009, 2017) and mammals (Borjigin et al., 2013). The main contributions of this report are summarized below.

1.) First, our findings provide a machine learning approach that can be easily applied to evaluate comatose and other unresponsive patients in general, allowing to distinguish FC elicited by auditory sounds from those of healthy controls. This approach could be used in further research as a tool to distinguish among different levels of consciousness. For example, a comatose patient could be compared with other DOC patients rather than healthy subjects, helping clinicians to determine whether the patients have transitioned to either UWS or MCS.

2.) Changes in FC during resting state are identified in the coma patient even minutes before death; a finding that was not observed in healthy controls, who rather displayed stable patterns of connectivity across time. Although more evidence

is required, these findings suggest that FC during resting state, similarly to the MMN component, is also dynamic and fluctuating in acute coma.

3.) This report essentially supports the role of phase synchronization as a measure of FC that can reflect coma severity, and be used as reliable predictor of poor neurological outcome in coma patients after cardiac arrest (Zubler et al., 2017; Carrasco-Gómez et al., 2021; Alnes et al., 2021). It also constitutes an important effort to advance towards source-level connectivity analyses in coma research, since neighboring sensors on the scalp will always be correlated to a large extent due to EEG volume conduction.

5.2 Limitations and further directions

The present dissertation has several limitations that must be considered along with their contributions. The first and major shortcoming is the small sample size employed. Case series of comatose patients, rather than groups, were reported here. Our experience has shown that it is difficult to gather sufficient patients in acute coma from a single facility, since coma is a temporary state in which patients are likely to transition rapidly to other post-comatose states. Recruitment was essentially limited by high levels of sedation, family resistance to enrollment and rapid progression to other DOC or death. The COVID-19 pandemic also magnified these difficulties, by limiting clinical research in ICU for a prolonged time period during the development of this thesis. Future studies should recruit a sufficiently large number of patients to improve the generalizability of the results. This will be critical to deeply investigate whether the rate of waxing-waning cycles from either the MMN or other neural markers can better predict coma outcome than the simple presence of such markers.

It is important to highlight, however, that each independent study here followed single-subject designs to build towards a clinical tool for diagnosis and other assessments, accounting for the individual variability that has been extensively criticized in traditional group-level analyses. Accordingly, all the statistical methods and automated ML procedures were implemented to capture EEG/ERP effects on single-trials. Despite the reduced number of subjects in general, the amount of EEG data collected per each

healthy control and patient is relatively acceptable (a total of 78 EEG recordings collected from healthy subjects, and 48 EEG recordings from comatose patients only for evaluating the MMN component).

This large amount of data was the rationale, for example, behind the creation of superblocks (i.e., a set of single-recording blocks within a day that were concatenated) in Chapter 3. While analyzing superblocks as single subject datasets was convenient to compact information and reduce trial-to-trial variability, we must acknowledge that this step may not be necessary to evaluate comatose patients, given the MVPA was sensitive enough to provide significant above-chance performance in some single-recording blocks. Also, while the MMN was reliably detected by using a single oddball paradigm (Chapter 2), other MMN experimental tasks could be included in further research. For instance, it would be valuable to assess whether the MMN detectability vary with shorter stimuli durations or with other more complex sounds from real-life situations (e.g., speech, music and emotional stimuli). Additionally, other late ERP components, such as the P3b or the N400 were run and collected from the patients reported in this thesis, but they were not examined. The inclusion of these components could have provided other measures of higher-level processing and therefore a full picture of the brain cognitive function of the patients. Likewise, different etiologies, injury severity, age and other variables must be further investigated to identify their potential role in the neurophysiological fluctuations observed in coma.

5.3 Conclusion

In conclusion, we have demonstrated through different statistical and automated ML procedures that ERPs elicited by auditory deviant stimuli (particularly the MMN component), can fluctuate within hours in acute coma; and other EEG biomarkers of recovery of consciousness (FC) are also transient and dynamic even minutes before death. While the presence of such biomarkers in critically ill patients does not necessarily guarantee coma emergence with a positive functional outcome (return of conscious awareness), its

objective detection through repeated measurements shows promises to identify functional changes associated with cognitive function that could potentially impact diagnosis and medical decisions in the near future.

References

Alnes, S. L., Lucia, M. D., Rossetti, A. O., and Tzovara, A. (2021). Complementary roles of neural synchrony and complexity for indexing consciousness and chances of surviving in acute coma. *Neuroimage*, 245:118638.

Armanfard, N., Komeili, M., Reilly, J. P., and Connoly, J. (2018). A Machine Learning Framework for Automatic and Continuous MMN Detection with Preliminary Results for Coma Outcome Prediction. *IEEE J. Biomed. Heal. Informatics*, pages 1–1.

Bharath, R. D., Munivenkatappa, A., Gohel, S., Panda, R., Saini, J., Rajeswaran, J., Shukla, D., Bhagavatula, I. D., and Biswal, B. B. (2015). Recovery of resting brain connectivity ensuing mild traumatic brain injury. *Front. Hum. Neurosci.*, 9(September):513.

Blain-Moraes, S., Boshra, R., Ma, H. K., Mah, R., Ruiter, K., Avidan, M., Connolly, J. F., and Mashour, G. A. (2016). Normal Brain Response to Propofol in Advance of Recovery from Unresponsive Wakefulness Syndrome. *Front. Hum. Neurosci.*, 10:1–6.

Borjigin, J., Lee, U. C., Liu, T., Pal, D., Huff, S., Klarr, D., Sloboda, J., Hernandez, J., Wang, M. M., and Mashour, G. A. (2013). Surge of neurophysiological coherence and connectivity in the dying brain. *Proc. Natl. Acad. Sci. U. S. A.*, 110(35):14432–14437.

Carrasco-Gómez, M., Keijzer, H. M., Ruijter, B. J., Bruña, R., Tjepkema-Cloostermans, M. C., Hofmeijer, J., and van Putten, M. J. (2021). EEG functional connectivity contributes to outcome prediction of postanoxic coma. *Clin. Neurophysiol.*, 132(6):1312–1320.

Chawla, L. S., Akst, S., Junker, C., Jacobs, B., and Seneff, M. G. (2009). Surges of electroencephalogram activity at the time of death: A case series. *J. Palliat. Med.*, 12(12):1095–1100.

Chawla, L. S., Terek, M., Junker, C., Akst, S., Yoon, B., Brasha-Mitchell, E., and Seneff, M. G. (2017). Characterization of end-of-life electroencephalographic surges in critically ill patients. *Death Stud.*, 41(6):385–392.

Dykstra, A. R., Cariani, P. A., and Gutschalk, A. (2017). A roadmap for the study of conscious audition and its neural basis. *Phil. Trans. R. Soc. B*, 372(1714):20160103.

Fischer, C., Luauté, J., Adeleine, P., and Morlet, D. (2004). Predictive value of sensory and cognitive evoked potentials for awakening from coma. *Neurology*, 63(4):669–673.

Fischer, C., Morlet, D., Bouchet, P., Luaute, J., Jourdan, C., and Salord, F. (1999). Mismatch negativity and late auditory evoked potentials in comatose patients. *Clin. Neurophysiol.*, 110(9):1601–1610.

Hillary, F. G., Roman, C. A., Venkatesan, U., Rajtmajer, S. M., Bajo, R., and Castellanos, N. D. (2015). Hyperconnectivity is a fundamental response to neurological disruption. *Neuropsychology*, 29(1):59–75.

Jacobsen, T. and Schröger, E. (2003). Measuring duration mismatch negativity. *Clin. Neurophysiol.*, 114(6):1133–1143.

Lehembre, R. (2012). Electrophysiological investigations of brain function in coma, vegetative and minimally conscious patients. *Arch. Ital. Biol.*, 150:122–139.

Luauté, J., Fischer, C., Adeleine, P., Morlet, D., Tell, L., and Boisson, D. (2005). Late auditory and event-related potentials can be useful to predict good functional outcome after coma. *Arch. Phys. Med. Rehabil.*, 86(5):917–923.

Michie, P. T., Budd, T. W., Todd, J., Rock, D., Wichmann, H., Box, J., and Jablensky, A. V. (2000). Duration and frequency mismatch negativity in schizophrenia. *Clin. Neurophysiol.*, 111(6):1054–1065.

Morlet, D. and Fischer, C. (2014). MMN and novelty P3 in coma and other altered states of consciousness: A review. *Brain Topogr.*, 27(4):467–479.

Naccache, L., Puybasset, L., Gaillard, R., Serve, E., and Willer, J. C. (2005). Auditory mismatch negativity is a good predictor of awakening in comatose patients: A fast and reliable procedure [1]. *Clin. Neurophysiol.*, 116(4):988–989.

O'Reilly, J. A. and O'Reilly, A. (2021). A Critical Review of the Deviance Detection Theory of Mismatch Negativity. *NeuroSci*, 2(2):151–165.

Recasens, M. and Uhlhaas, P. J. (2017). Test–retest reliability of the magnetic mismatch negativity response to sound duration and omission deviants. *Neuroimage*, 157:184–195.

Rossetti, A. O., Tzovara, A., Murray, M. M., De Lucia, M., and Oddo, M. (2014). Automated auditory mismatch negativity paradigm improves coma prognostic accuracy after cardiac arrest and therapeutic hypothermia. *J. Clin. Neurophysiol.*, 31(4):356–361.

Tavakoli, P., Dale, A., Boafo, A., and Campbell, K. (2019). Evidence of P3a during sleep, a process associated with intrusions into consciousness in the waking state. *Front. Neurosci.*, 12:1028.

Tzovara, A., Rossetti, A. O., Juan, E., Suys, T., Viceic, D., Rusca, M., Oddo, M., and Lucia, M. D. (2016). Prediction of awakening from hypothermic postanoxic coma based on auditory discrimination. *Ann. Neurol.*, 79(5):748–757.

Tzovara, A., Rossetti, A. O., Spierer, L., Grivel, J., Murray, M. M., Oddo, M., and De Lucia, M. (2013). Progression of auditory discrimination based on neural decoding predicts awakening from coma. *Brain*, 136(1):81–89.

Zubler, F., Steimer, A., Kurmann, R., Bandarabadi, M., Novy, J., Gast, H., Oddo, M., Schindler, K., and Rossetti, A. O. (2017). EEG synchronization measures are early outcome predictors in comatose patients after cardiac arrest. *Clin. Neurophysiol.*, 128(4):635–642.

Appendix I

Supplementary information: Chapter 2

Table S1: Effect size of permutation *t*-test (Cohen's d) and Bayes factors (BF10) from the healthy control group across blocks.

		MMN		P3a	
Deviant	**Block**	**Cohen's d**	**BF10**	**Cohen's d**	**BF10**
Duration	1	1.29	> 100	2.02	> 100
	2	1.59	> 100	2.49	> 100
	3	1.43	> 100	2.48	> 100
	4	1.05	> 100	1.66	> 100
	5	1.04	> 100	2.62	> 100
Frequency	1	1.08	> 100	1.37	> 100
	2	0.70	> 100	1.58	> 100
	3	0.72	> 100	1.06	72.9
	4	0.76	> 100	1.51	> 100
	5	0.73	> 100	1.45	> 100
Intensity	1	1.12	> 100	1.42	> 100
	2	1.04	> 100	2.15	> 100
	3	1.26	> 100	1.38	> 100
	4	1.19	> 100	1.37	> 100
	5	1.13	> 100	1.24	50.41

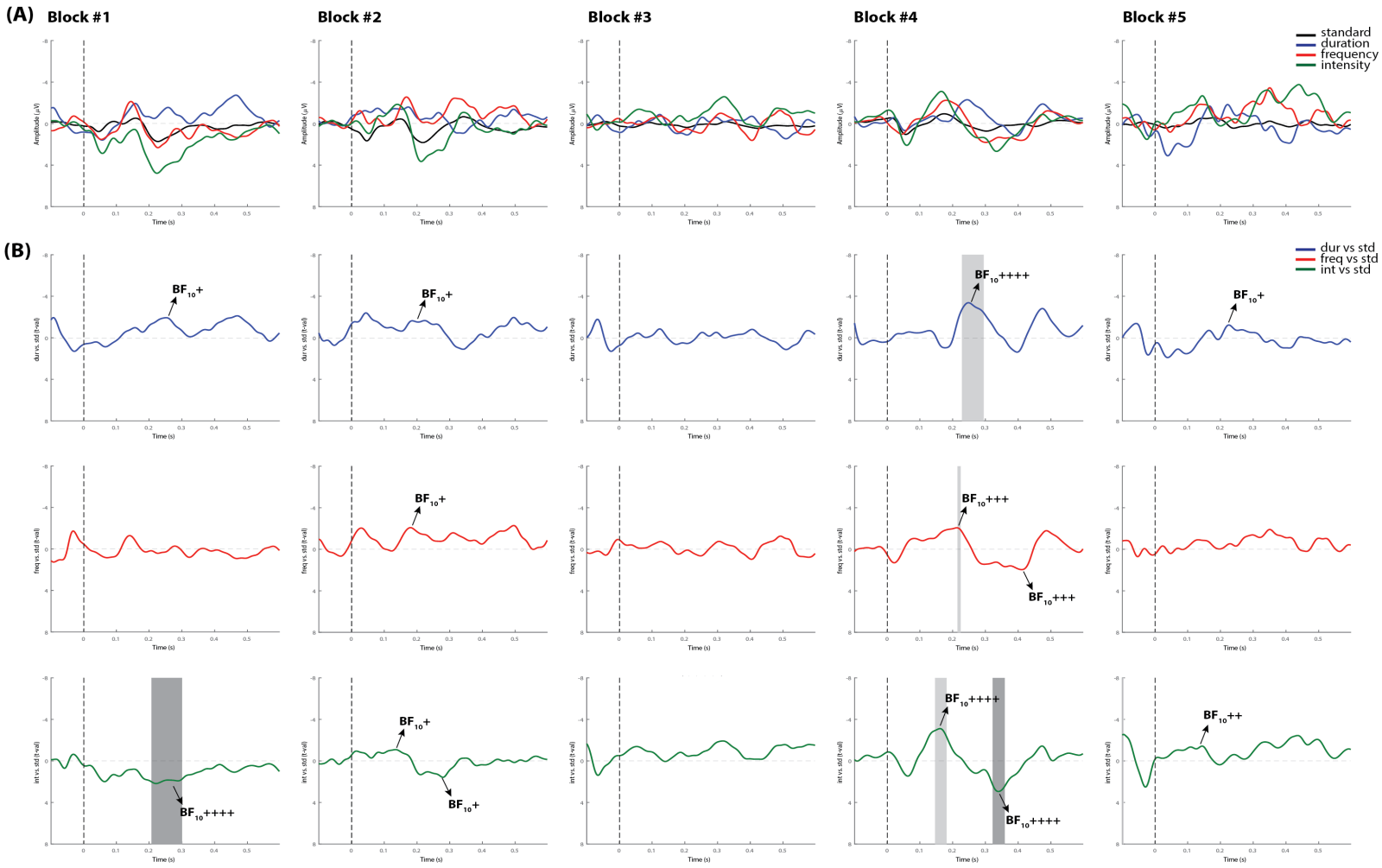

Figure S1: Individual ERPs and statistical findings of Patient 1 on day 0. (B) Time course of the difference between deviants and standard stimuli expressed in units of *t*-values. Significant intervals for negative components are denoted by a light gray area, and those for positive components are denoted by a dark gray area. Black arrows show the latency of maximum bayes factors and the strength of evidence for $H1$: + anecdotal; ++ moderate; +++ strong and ++++ very strong to extreme.

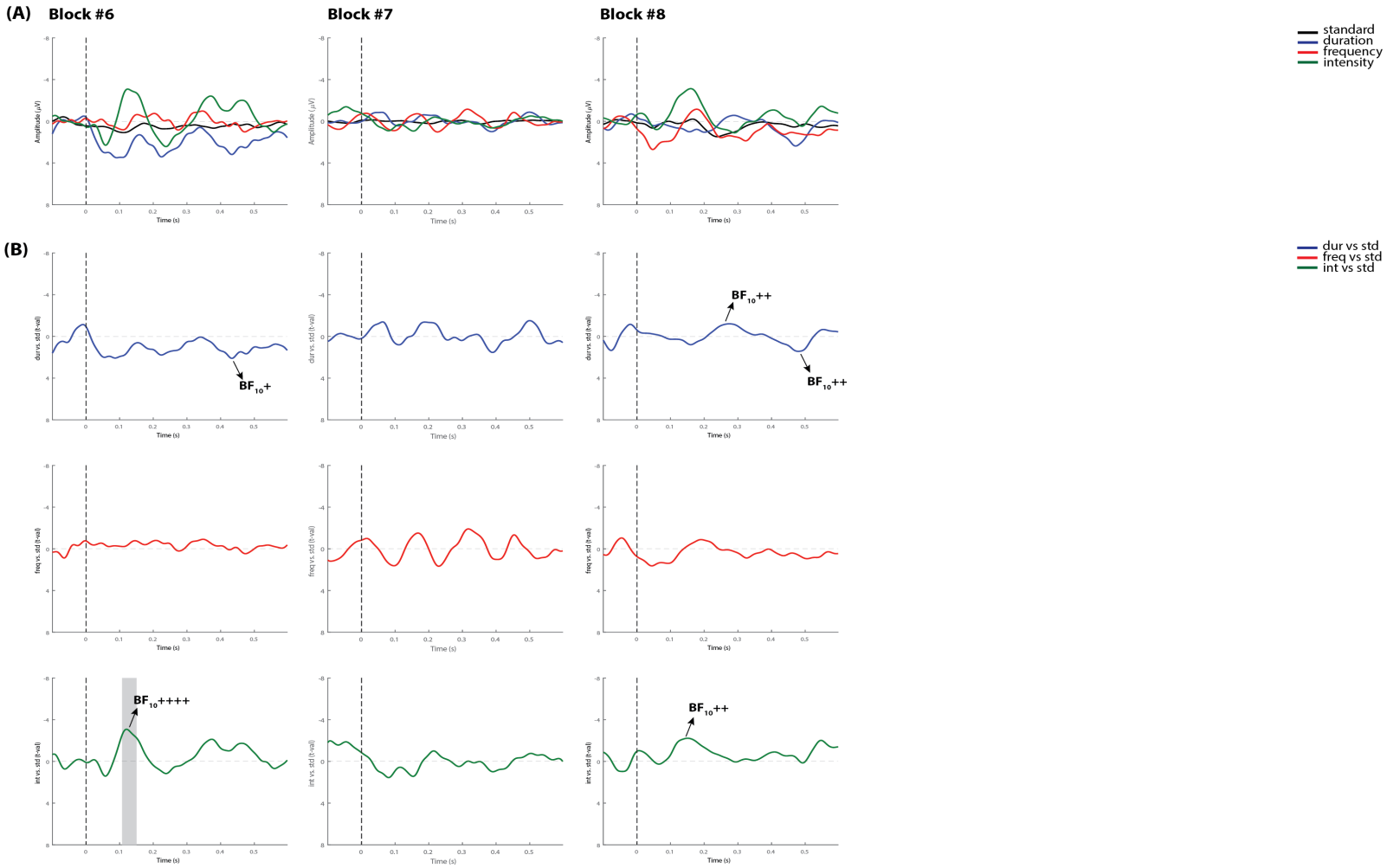

Figure S2: Individual ERPs and statistical findings of Patient 1 on day 0 (continuation). (B) Time course of the difference between deviants and standard stimuli expressed in units of *t*-values. Significant intervals for negative components are denoted by a light gray area, and those for positive components are denoted by a dark gray area. Black arrows show the latency of maximum bayes factors and the strength of evidence for $H1$: + anecdotal; ++ moderate; +++ strong and ++++ very strong to extreme.

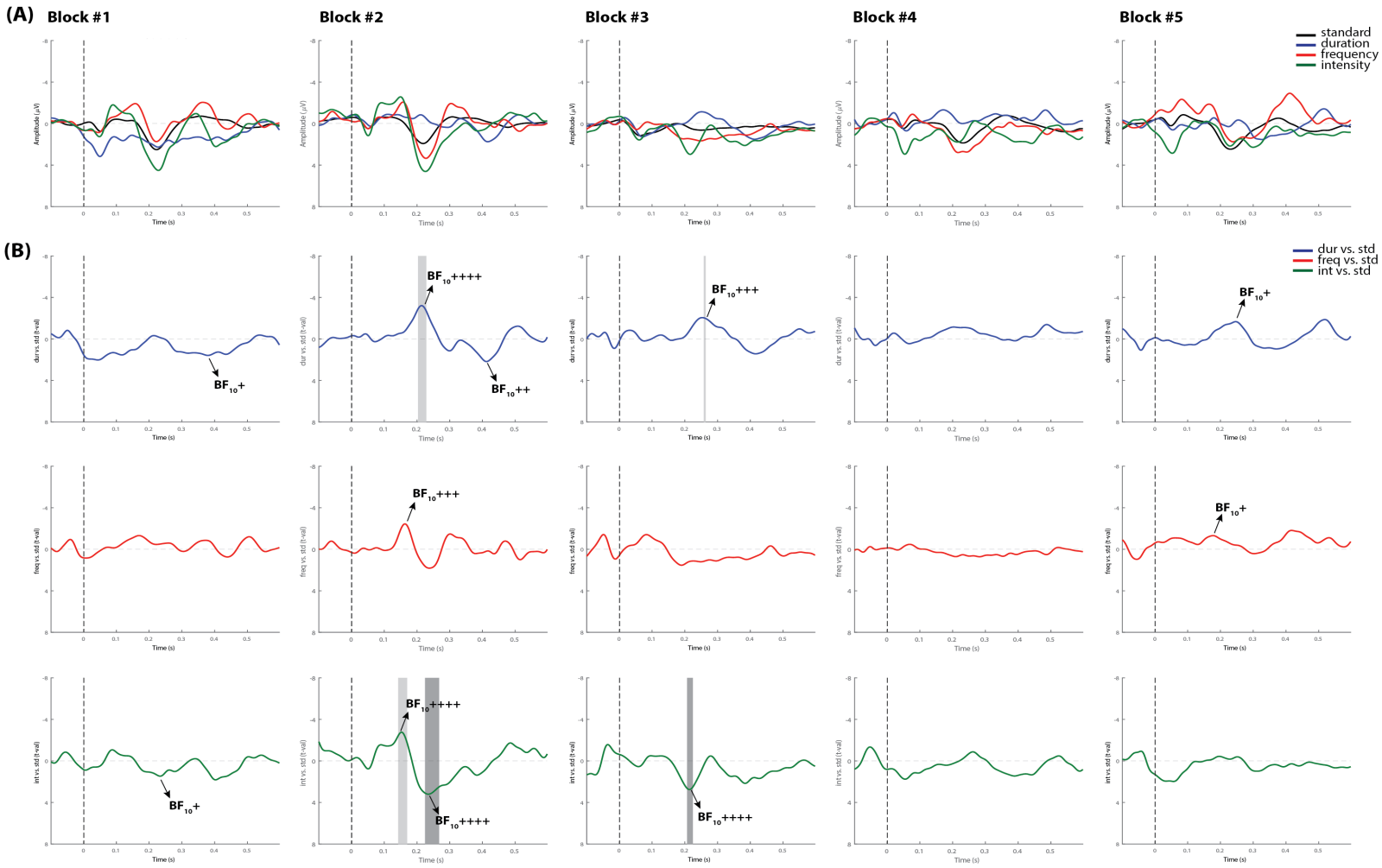

Figure S3: Individual ERPs and statistical findings of Patient 1 on day 3. (B) Time course of the difference between deviants and standard stimuli expressed in units of *t*-values. Significant intervals for negative components are denoted by a light gray area, and those for positive components are denoted by a dark gray area. Black arrows show the latency of maximum bayes factors and the strength of evidence for $H1$: + anecdotal; ++ moderate; +++ strong and ++++ very strong to extreme.

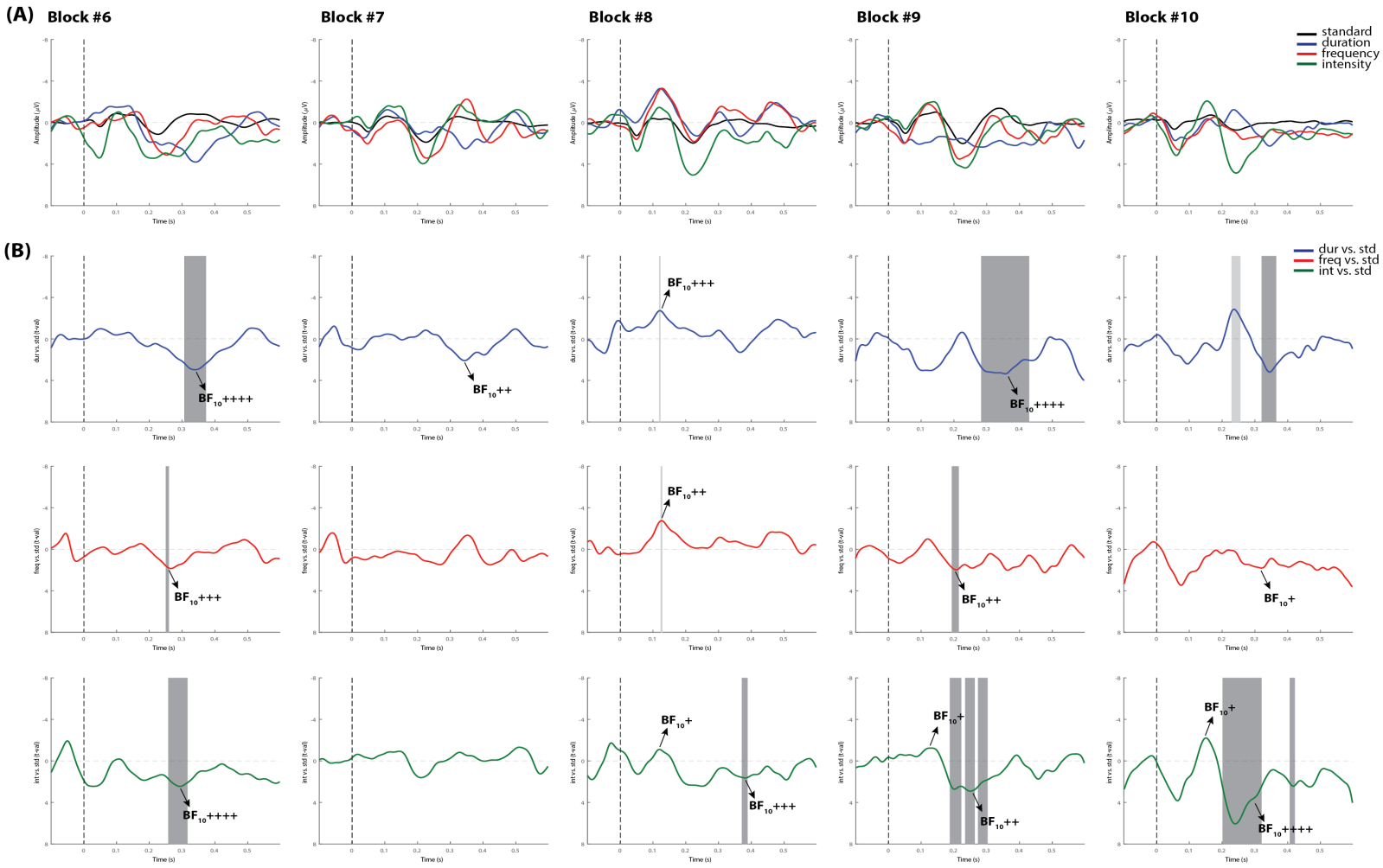

Figure S4: Individual ERPs and statistical findings of Patient 1 on day 3 (continuation). (B) Time course of the difference between deviants and standard stimuli expressed in units of *t*-values. Significant intervals for negative components are denoted by a light gray area, and those for positive components are denoted by a dark gray area. Black arrows show the latency of maximum bayes factors and the strength of evidence for $H1$: + anecdotal; ++ moderate; +++ strong and ++++ very strong to extreme.

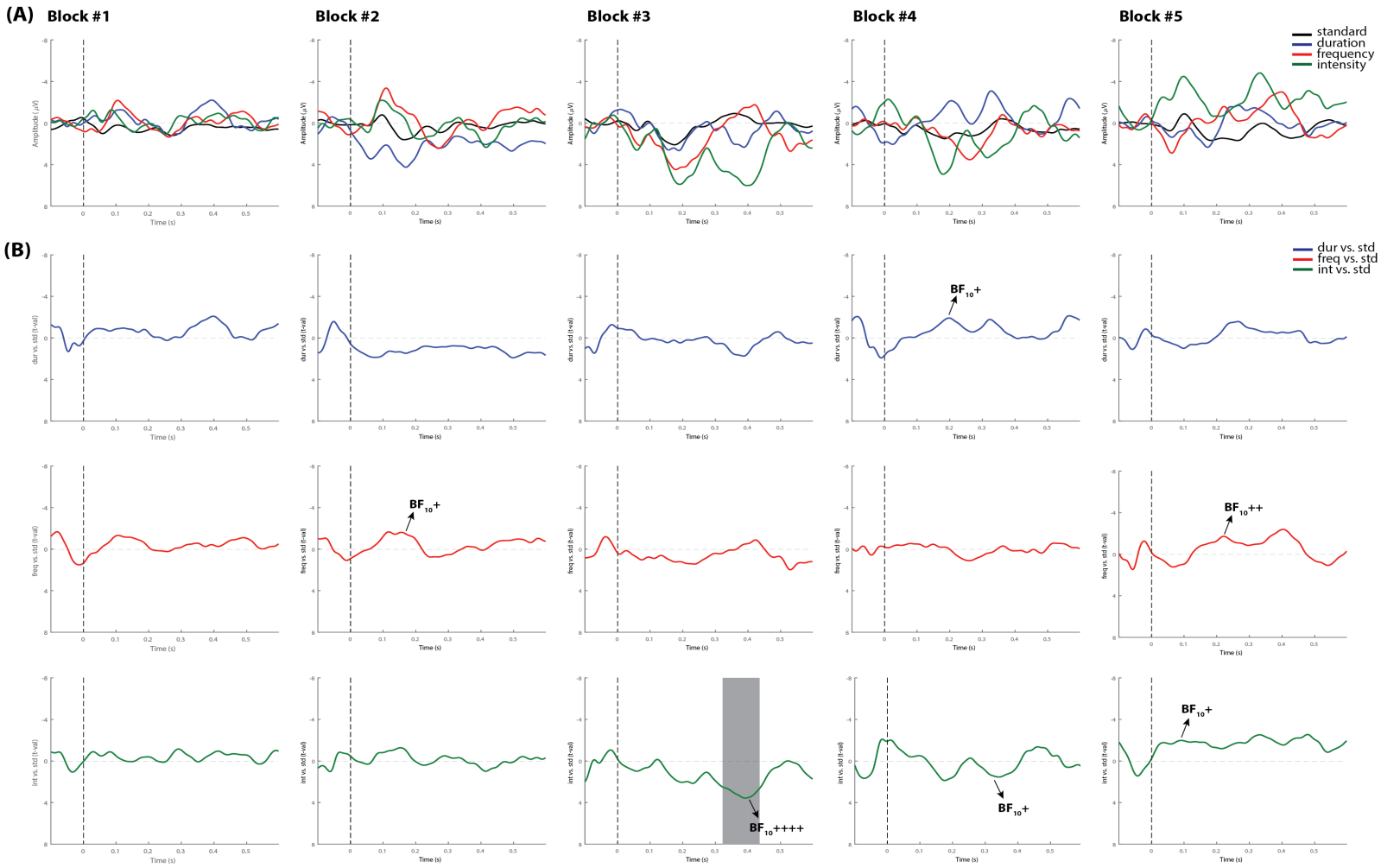

Figure S5: Individual ERPs and statistical findings of Patient 2 on day 0. (B) Time course of the difference between deviants and standard stimuli expressed in units of *t*-values. Significant intervals for negative components are denoted by a light gray area, and those for positive components are denoted by a dark gray area. Black arrows show the latency of maximum bayes factors and the strength of evidence for $H1$: + anecdotal; ++ moderate; +++ strong and ++++ very strong to extreme.

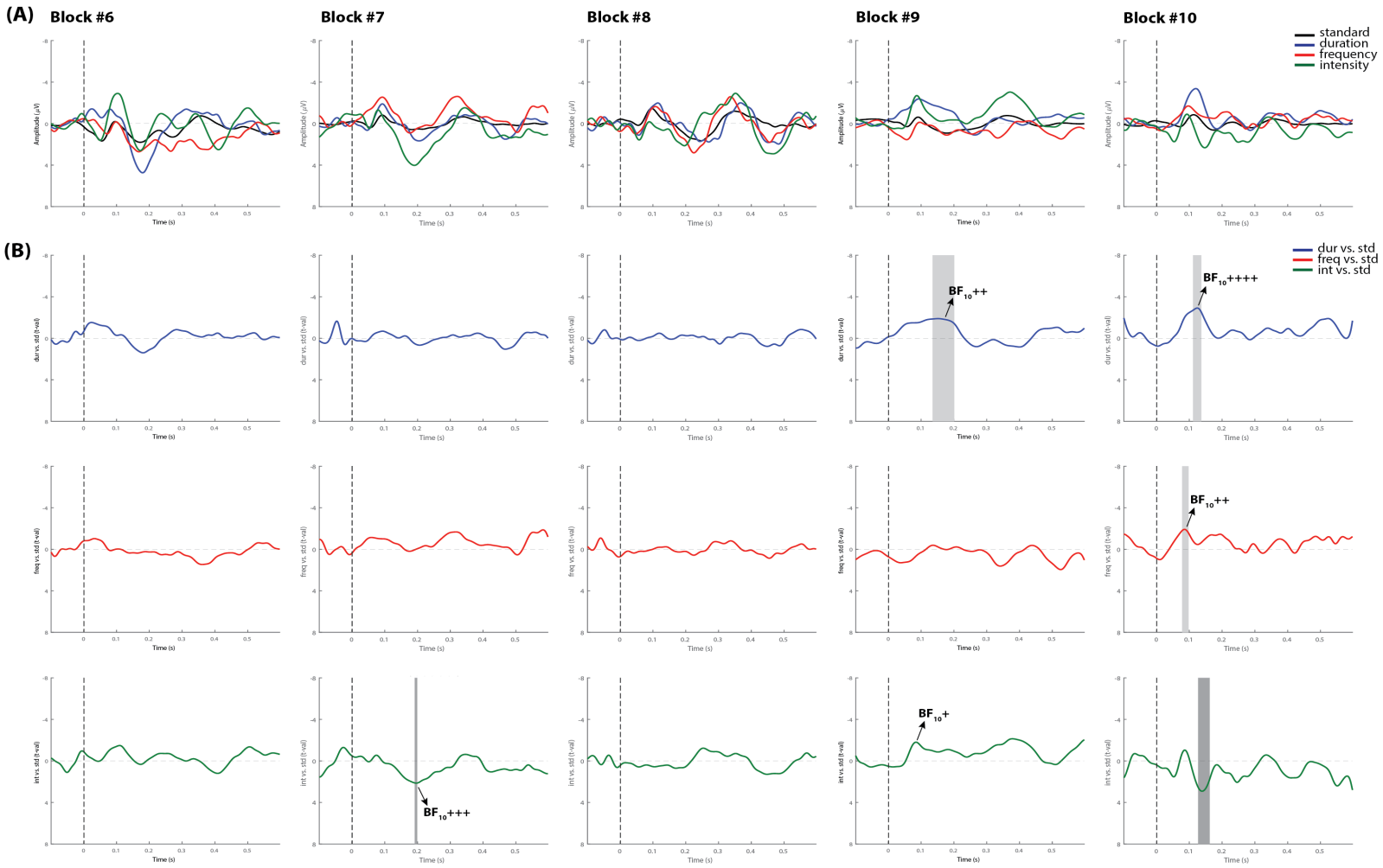

Figure S6: Individual ERPs and statistical findings of Patient 2 on day 0 (continuation). (B) Time course of the difference between deviants and standard stimuli expressed in units of *t*-values. Significant intervals for negative components are denoted by a light gray area, and those for positive components are denoted by a dark gray area. Black arrows show the latency of maximum bayes factors and the strength of evidence for $H1$: + anecdotal; ++ moderate; +++ strong and ++++ very strong to extreme.

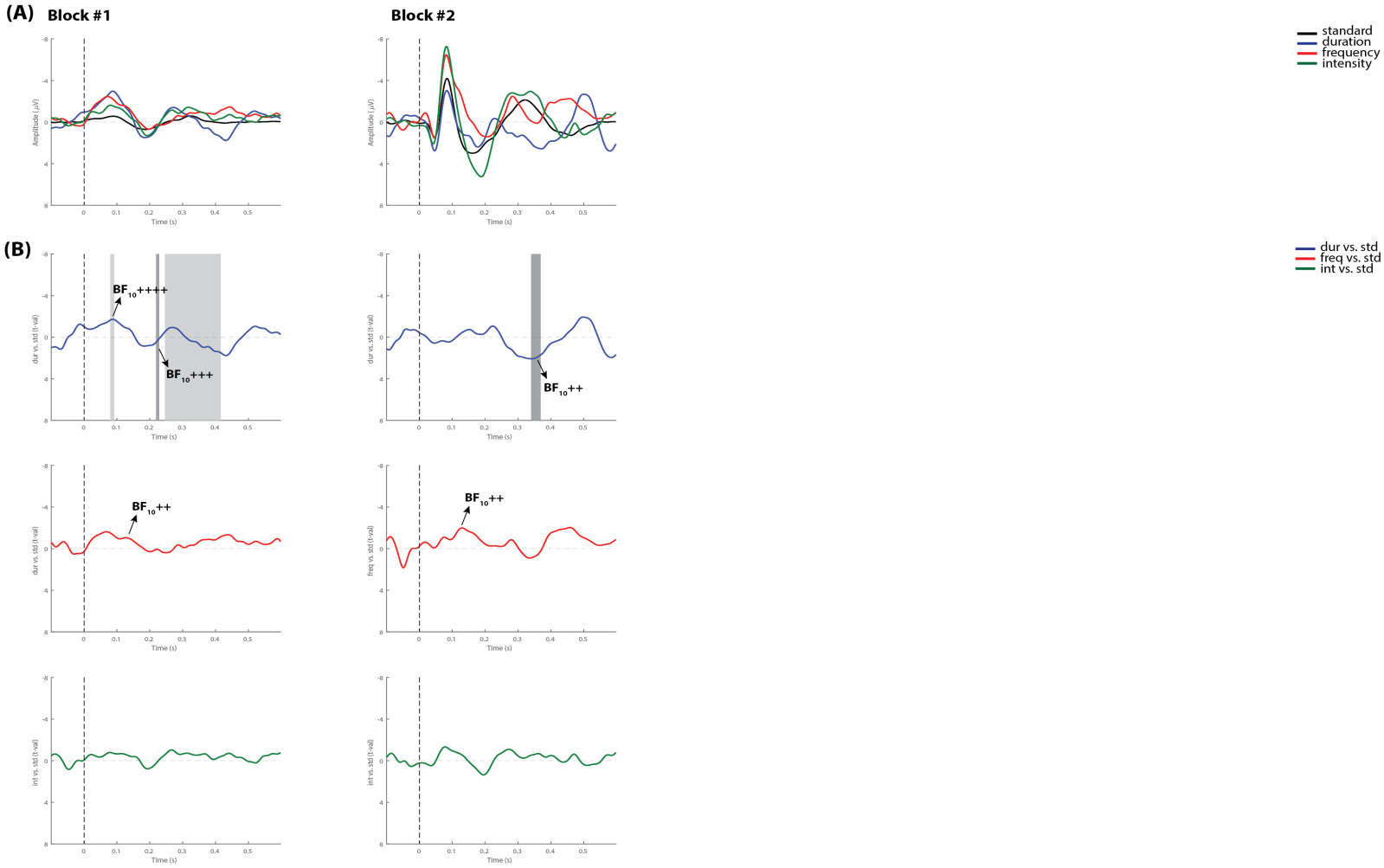

Figure S7: Individual ERPs and statistical findings of Patient 2 on day 3. (B) Time course of the difference between deviants and standard stimuli expressed in units of *t*-values. Significant intervals for negative components are denoted by a light gray area, and those for positive components are denoted by a dark gray area. Black arrows show the latency of maximum bayes factors and the strength of evidence for $H1$: + anecdotal; ++ moderate; +++ strong and ++++ very strong to extreme.

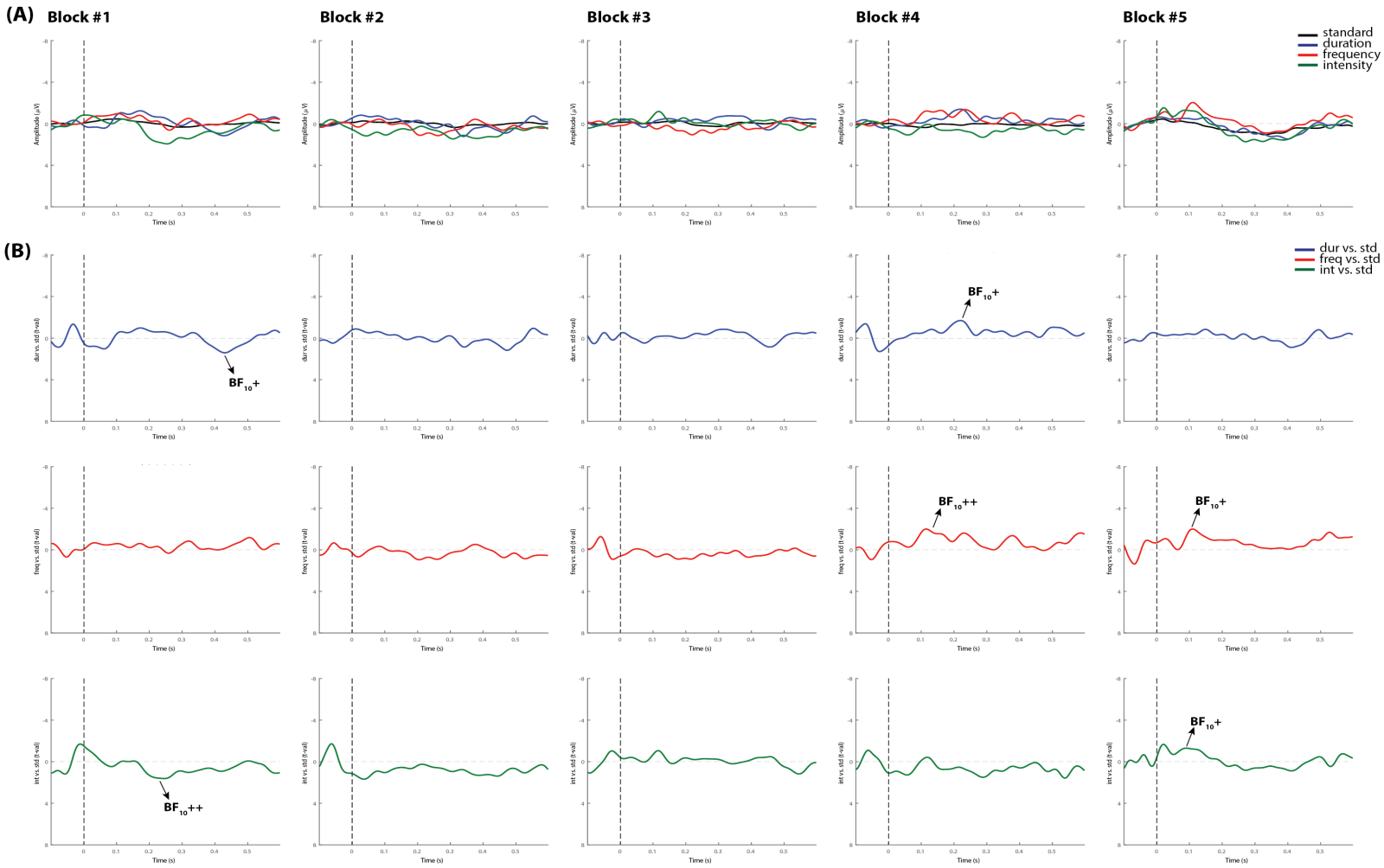

Figure S8: Individual ERPs and statistical findings of Patient 3 on day 0. (B) Time course of the difference between deviants and standard stimuli expressed in units of *t*-values. Significant intervals for negative components are denoted by a light gray area, and those for positive components are denoted by a dark gray area. Black arrows show the latency of maximum bayes factors and the strength of evidence for $H1$: + anecdotal; ++ moderate; +++ strong and ++++ very strong to extreme.

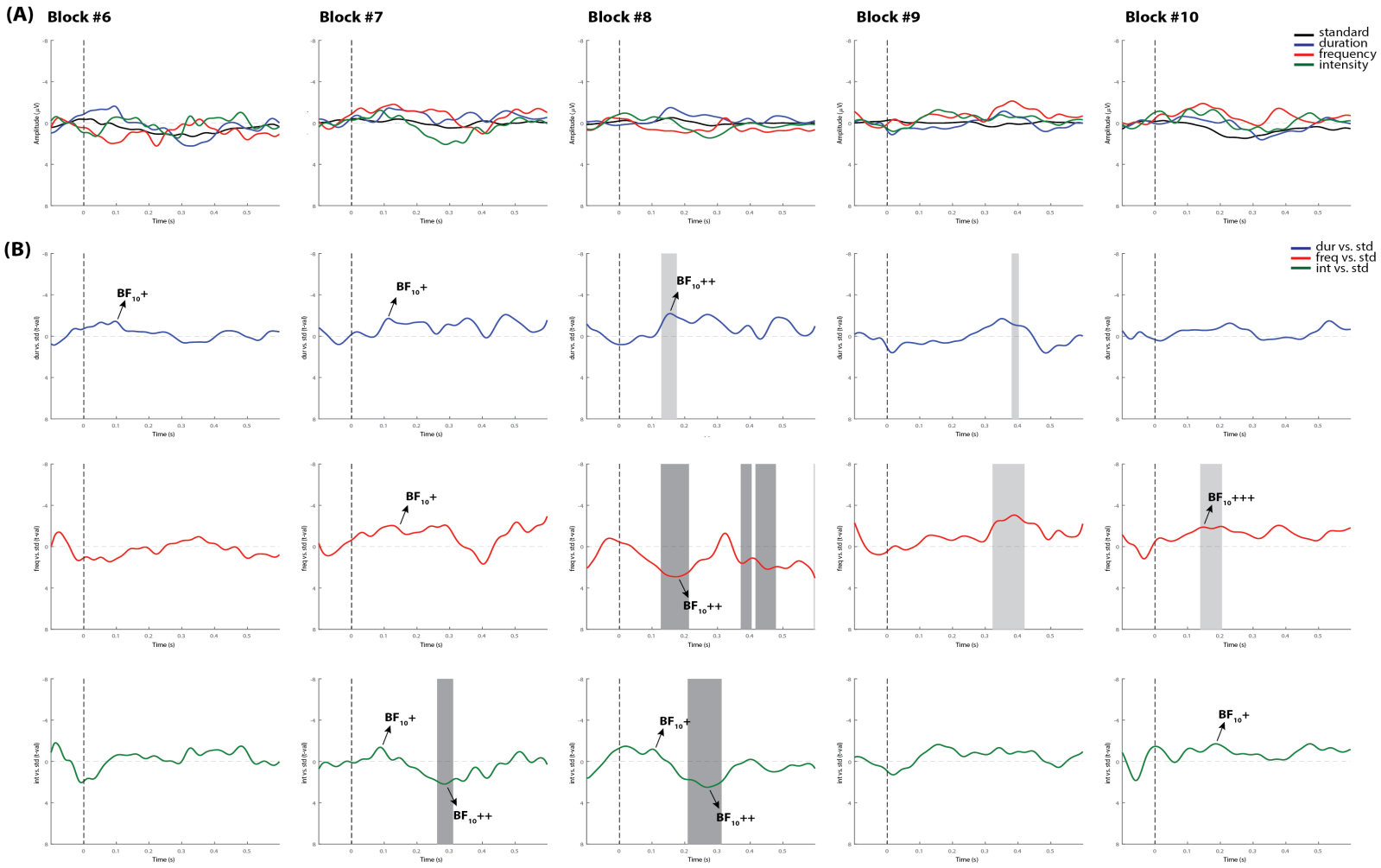

Figure S9: Individual ERPs and statistical findings of Patient 3 on day 0 (continuation). (B) Time course of the difference between deviants and standard stimuli expressed in units of *t*-values. Significant intervals for negative components are denoted by a light gray area, and those for positive components are denoted by a dark gray area. Black arrows show the latency of maximum bayes factors and the strength of evidence for $H1$: + anecdotal; ++ moderate; +++ strong and ++++ very strong to extreme.

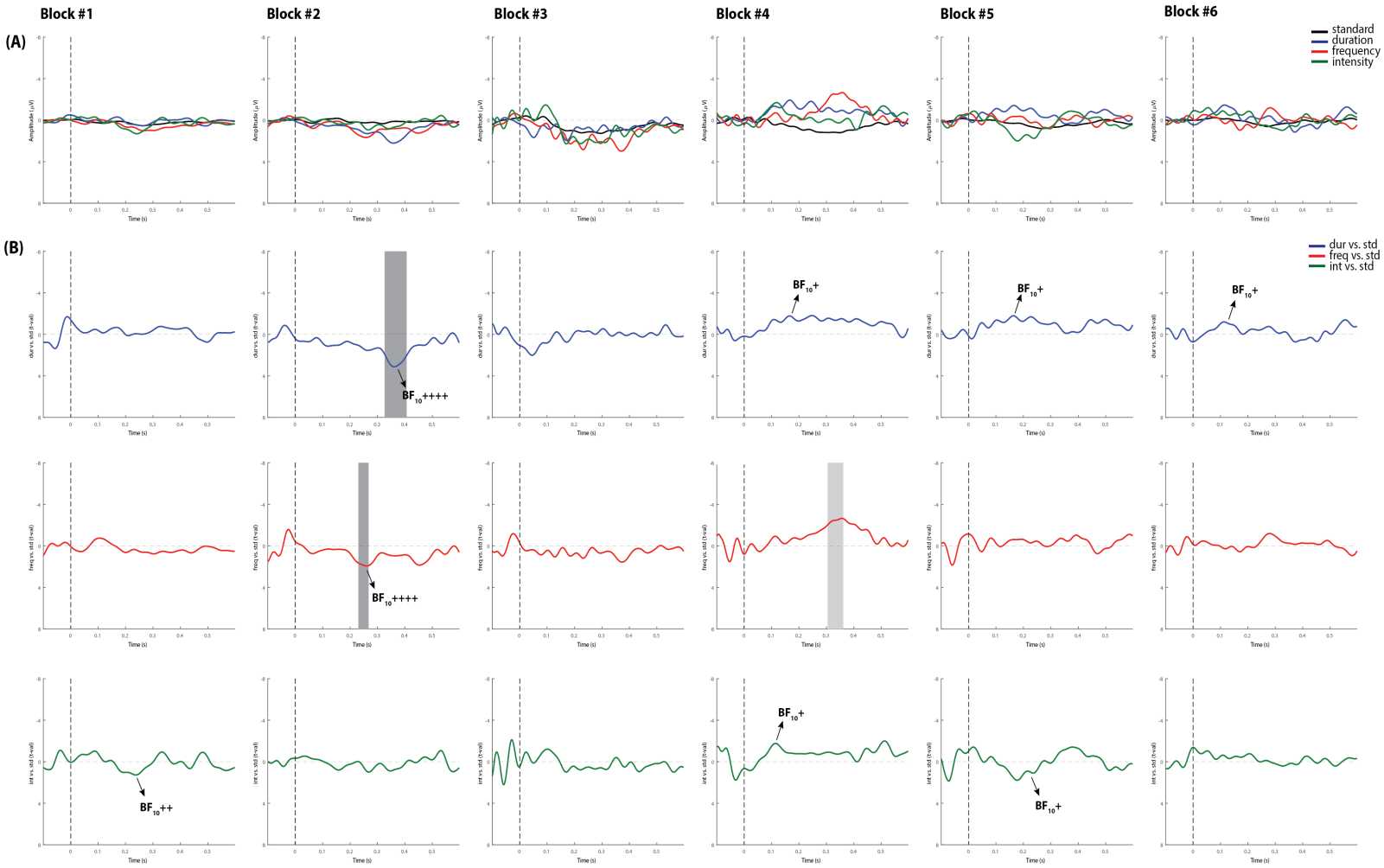

Figure S10: Individual ERPs and statistical findings of Patient 3 on day 3. (B) Time course of the difference between deviants and standard stimuli expressed in units of *t*-values. Significant intervals for negative components are denoted by a light gray area, and those for positive components are denoted by a dark gray area. Black arrows show the latency of maximum bayes factors and the strength of evidence for $H1$: + anecdotal; ++ moderate; +++ strong and ++++ very strong to extreme.

Table S2: Summary of the P3a results in Patient 1.

DAY 0		**DURATION**			**FREQUENCY**			**INTENSITY**		
Block	**Time**	**Visual**	**Perm. test**	**Bayes**	**Visual**	**Perm.test**	**Bayes**	**Visual**	**Perm.test**	**Bayes**
1	18:35 PM	-	-	-	-	-	-	+	+	++++
2	21:10 PM	+	-	-	-	-	-	+	-	+
3	22:49 PM	-	-	-	-	-	-	-	-	-
4	12:47 AM	-	-	-	+	-	+++	+	+	++++
5	06:26 AM	+	-	-	-	-	-	-	-	-
6	07:58 AM	+	-	+	-	-	-	+	-	-
7	10:08 AM	-	-	-	-	-	-	-	-	-
8	11:26 AM	+	-	++	+	-	-	-	-	-

DAY 3		**DURATION**			**FREQUENCY**			**INTENSITY**		
Block	**Time**	**Visual**	**Perm.test**	**Bayes**	**Visual**	**Perm.test**	**Bayes**	**Visual**	**Perm.test**	**Bayes**
1	18:20 PM	-	-	+	-	-	-	+	-	+
2	20:29 PM	+	+	++	+	-	-	+	+	++++
3	21:15 PM	+	-	-	+	-	-	+	+	++++
4	23:14 PM	-	-	-	+	-	-	-	-	-
5	01:05 AM	+	-	-	-	-	-	-	-	-
6	03:13 AM	+	+	++++	+	+	+++	+	+	++++
7	05:22 AM	+	-	++	+	-	-	+	-	-
8	06:09 AM	-	-	-	-	-	-	+	+	+++
9	07:56 AM	+	+	++++	+	+	++	+	+	++
10	10:11 AM	+	+	+++	+	-	+	+	+	++++

+ indicates a positive result, - a negative result. For Bayes column, + anecdotal evidence; ++ moderate evidence; +++ strong evidence and ++++ very strong to extreme evidence.

Table S3: Summary of the P3a results in Patient 2.

DAY 0		DURATION			FREQUENCY			INTENSITY		
Block	**Time**	**Visual**	**Perm. test**	**Bayes**	**Visual**	**Perm. test**	**Bayes**	**Visual**	**Perm. test**	**Bayes**
1	21:15 PM	-	-	-	-	-	-	-	-	-
2	12:14 AM	-	-	-	+	-	-	-	-	-
3	02:24 AM	+	-	-	+	-	-	+	+	++++
4	04:51 AM	-	-	-	+	-	-	+	-	+
5	07:00 AM	-	-	-	-	-	-	-	-	-
6	08:00 AM	+	-	-	+	-	-	-	-	-
7	10:09 AM	-	-	-	-	-	-	+	+	+++
8	11:48 AM	-	-	-	+	-	-	-	-	-
9	12:28 AM	+	-	-	+	-	-	-	-	-
10	02:37 PM	-	-	-	-	-	-	-	-	-

DAY 3		DURATION			FREQUENCY			INTENSITY		
Block	**Time**	**Visual**	**Perm. test**	**Bayes**	**Visual**	**Perm. test**	**Bayes**	**Visual**	**Perm. test**	**Bayes**
1	18:34 PM	+	+	+++	-	-	-	-	-	-
2	20:48 PM	+	+	++	-	-	-	+	-	-

+ indicates a positive result, - a negative result. For Bayes column, + anecdotal evidence; ++ moderate evidence; +++ strong evidence and ++++ very strong to extreme evidence.

Table S4: Summary of the P3a results in Patient 3.

DAY 0		DURATION			FREQUENCY			INTENSITY		
Block	**Time**	**Visual**	**Perm. test**	**Bayes**	**Visual**	**Perm. test**	**Bayes**	**Visual**	**Perm. test**	**Bayes**
1	14:52 PM	+	-	+	-	-	-	+	-	++
2	16:44 PM	-	-	-	+	-	-	+	-	-
3	18:46 PM	-	-	-	+	-	-	-	-	-
4	20:55 PM	-	-	-	-	-	-	+	-	-
5	21:36 PM	+	-	-	-	-	-	+	-	-
6	23:25 PM	+	-	-	-	-	-	-	-	-
7	01:34 AM	-	-	-	+	-	-	+	+	++
8	02:10 AM	-	-	-	+	+	++	+	+	++
9	05:24 AM	-	-	-	-	-	-	-	-	-
10	07:09 AM	-	-	-	-	-	-	-	-	-

DAY 3		DURATION			FREQUENCY			INTENSITY		
Block	**Time**	**Visual**	**Perm. test**	**Bayes**	**Visual**	**Perm. test**	**Bayes**	**Visual**	**Perm. test**	**Bayes**
1	20:46 PM	-	-	-	+	-	-	+	-	++
2	21:45 PM	+	+	++++	+	+	++++	-	-	-
3	23:29 PM	-	-	-	+	-	-	-	-	-
4	01:38 AM	-	-	-	-	-	-	-	-	-
5	04:33 AM	-	-	-	-	-	-	+	-	+
6	06:21 AM	-	-	-	-	-	-	-	-	-

+ indicates a positive result, - a negative result. For Bayes column, + anecdotal evidence; ++ moderate evidence; +++ strong evidence and ++++ very strong to extreme evidence.

Appendix II

Supplementary information: Chapter 4

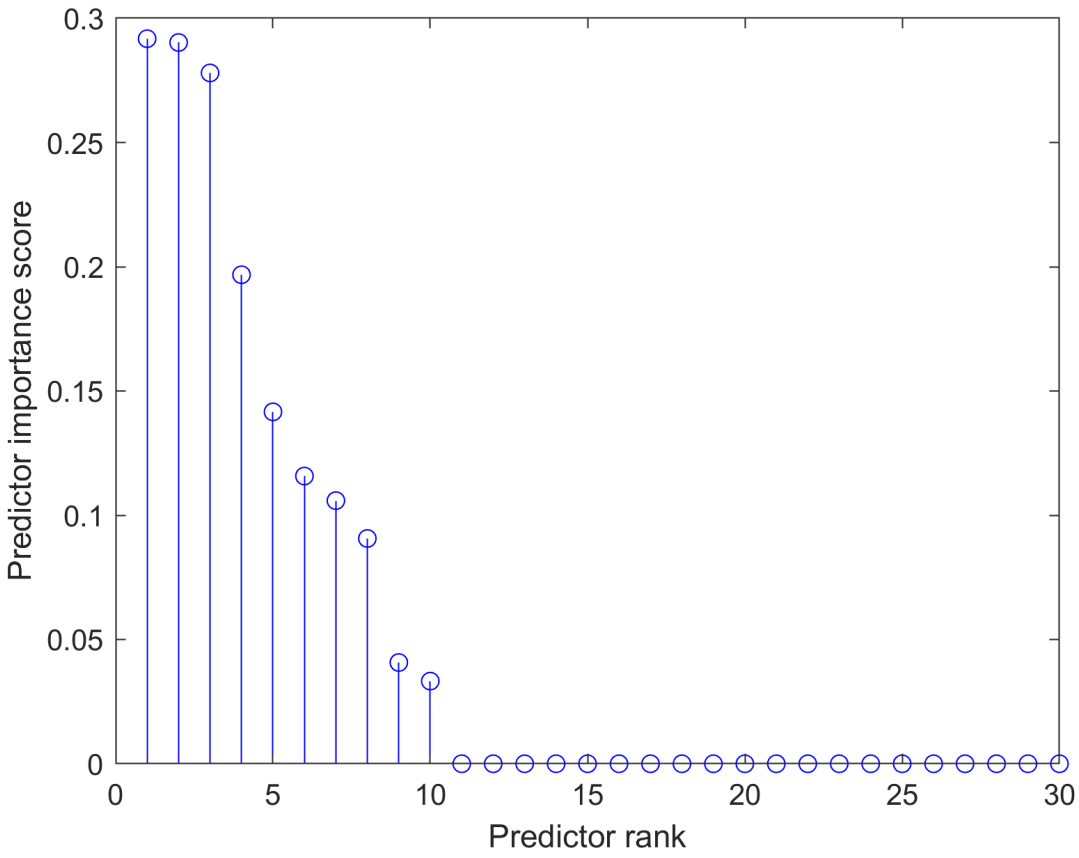

Figure S1: Example of the mRMR output for alpha frequency band at sensor level.

Table S1: Sensor-FC features to duration deviants that better distinguish coma vs. healthy controls for each frequency band.

	Delta			**Theta**		
#	**Features**	**Regions**	**Hemisphere**	**Features**	**Regions**	**Hemisphere**
1	F5-FC2	Frontocentral	Left	C3-PO4	Centroparietal	Both
2	TP7-Pz	Temporoparietal	Left	O1-O2	Occipital	Both
3	C3-O2	Centroccipital	Both	F1-Iz	Frontoccipital	Left
4	F1-CP2	Frontocentral	Both	CP3-O1	Centroparietoccipital	Left
5	Cz-P2	Centroparietal	Right	F3-FT8	Frontotemporal	Both
6	Fp1-C6	Frontocentral	Both	C1-FC6	Frontocentral	Both
7	F3-P2	Frontoparietal	Both	Cz-P4	Centroparietal	Left
8	FC5-AF4	Frontocentral	Both	Fp1-FC5	Frontocentral	Left
9	F5-P3	Frontoparietal	Left	AF8-C4	Frontocentral	Right
10	FC1-CP4	Frontocentroparietal	Both	FC1-CP4	Frontocentroparietal	Both
	Alpha			**Beta**		
#	**Features**	**Regions**	**Hemisphere**	**Features**	**Regions**	**Hemisphere**
1	C3-O2	Centroccipital	Both	C3-O2	Centroccipital	Both
2	Cz-P2	Centroparietal	Left	F3-CP1	Frontocentroparietal	Left
3	F7-Oz	Frontooccipital	Left	F1-P3	Frontoparietal	Left
4	F3-P6	Frontoparietal	Both	F7-P9	Frontoparietal	Left
5	F1-Iz	Frontoccipital	Left	Fp1-C3	Frontocentral	Left
6	O1-F4	Occitofrontal	Both	T8-PO4	Temporoparietal	Right
7	FC1-CP4	Frontocentroparietal	Both	C4-CP4	Centroparietal	Right
8	F2-CP4	Frontocentroparietal	Right	F5-C4	Frontocentral	Both
9	P7-FC6	Frontocentroparietal	Both	POz-CPz	Parietocentral	Both
10	CP1-Iz	Centroparietal	Left	TP7-CP4	Temporacentral	Both

Table S2: Source-FC features to duration deviants that better distinguish coma vs. healthy controls for each frequency band.

	Delta			**Theta**		
#	**Features**	**Regions**	**Hemisphere**	**Features**	**Regions**	**Hemisphere**
1	insulaR-postcentralR	Centrotemporal	Right	banksstsL-cuneusL	Temporoccipital	Left
2	paracentralL-superiortemporalL	Centrotemporal	Left	parahippocampalR-posteriorcingulateR	Temporolimbic	Both
3	inferiorparietalR-parsopercularisL	Frontoparietal	Both	caudalanteriorcingulateR-entorhinalL	Temporolimbic	Both
4	lateralorbitofrontalR-parahippocampalR	Frontotemporal	Right	middletemporalR-precentralL	Temporocentral	Both
5	lateralorbitofrontalL-posteriorcingulateR	Frontolimbic	Both	banksstsR-lingualL	Temporoccipital	Both
6	banksstsL-cuneusL	Temporoccipital	Left	lateralorbitofrontalR-rostralanteriorcingulateR	Frontolimbic	Right
7	entorhinalR- parahippocampalL	Temporal	Both	frontalpoleR-rostralmiddlefrontalR	Frontal	Right
8	caudalanteriorcingulateR-inferiorparietalL	Parietolimbic	Both	lateralorbitofrontalL-precentralL	Frontocentral	Left
9	lingualR-precuneusL	Parietoccipital	Both	postcentralR-rostralmiddlefrontalR	Frontal	Right
10	pericalcarineL-superiorparietalL	Occipitoparietal	Left	inferiorparietalR-superiortemporalR	Parietotemporal	Right

	Alpha			**Beta**		
#	**Features**	**Regions**	**Hemisphere**	**Features**	**Regions**	**Hemisphere**
1	insulaR-postcentralR	Temporocentral	Right	pericalcarineL-superiorparietalL	Occipitoparietal	Left
2	entorhinalL-supramarginalL	Paretotemporal	Left	parahippocampalR-precentralL	Temporocentral	Both
3	cuneusL-postcentralR	Occipitocentral	Both	cuneusL-supramarginalR	Occipitoparietal	Both
4	rostralanteriorcingulateL-superiortemporalR	Temporolimbic	Both	inferiortemporalR-pericalcarineL	Temporoccipital	Both
5	cuneusL-entorhinalL	Occipitotemporal	Left	caudalanteriorcingulateR-entorhinalL	Temporolimbic	Both
6	superiorparietalL-supramarginalR	Parietal	Both	RostralmiddlefrontalL-superiorfrontalR	Frontal	Both
7	entorhinalL-parsopercularisL	Frontotemporal	Left	caudalanteriorcingulateL-precuneusL	Parietolimbic	Left
8	isthmuscingulateL-isthmuscingulateR	Limbic	Both	parstriangularisR-transversetemporalL	Frontotemporal	Both
9	parstriangularisL-precuneusL	Frontoparietal	Left	paracentralR-rostralmiddlefrontalL	Frontocentral	Both
10	lateraloccipitalR-superiortemporalL	Temporoccipital	Both	inferiortemporalR-rostralanteriorcingulateL	Temporolimbic	Both

Table S3: Sensor-FC features that better distinguish three resting-state periods in coma for each frequency band.

	Delta			**Theta**		
#	**Features**	**Regions**	**Hemisphere**	**Features**	**Regions**	**Hemisphere**
1	FT7-P1	Frontoparietal	Left	F3-Iz	Frontoccipital	Left
2	FT7-P7	Frontotemporoparietal	Left	FC5-TP8	Frontocentrotemporal	Both
3	CP5-PO8	Centroparietoccipital	Both	P3-O2	Parietoccipital	Both
4	FC3-FC4	Frontocentral	Both	O1-C2	Centroccipital	Both
5	Fpz-FC2	Frontocentral	Right	TP7-CP5	Temporocentroparietal	Left
6	AF7-Afz	Frontocentral	Left	FC1-CP2	Frontocentroparietal	Both
7	FT8-C2	Frontocentral	Both	Afz-F2	Frontal	Right
8	FC5-CPz	Frontocentroparietal	Left	FC6-PO8	Frontocentroparietal	Right
9	CP3-P3	Centroparietal	Left	CP1-O2	Centroccipital	Both
10	C5-O2	Centrooccipital	Both	FC6-C6	Frontocentral	Right
	Alpha			**Beta**		
#	**Features**	**Regions**	**Hemisphere**	**Features**	**Regions**	**Hemisphere**
1	C4-CP6	Centroparietal	Right	P5-Fp2	Frontoparietal	Both
2	P7-F4	Frontoparietal	Both	FC5-TP8	Frontocentrotemporal	Both
3	P3-TP8	Temporoparietal	Both	F7-CP1	Frontocentroparietal	Left
4	TP7-TP8	Temporoparietal	Both	P3-Oz	Parietoccipital	Left
5	P3-Fpz	Frontoparietal	Left	P5-AF8	Frontoparietal	Both
6	C5-CP4	Centroparietal	Both	T7-F6	Frontotemporal	Both
7	FC1-T7	Frontotemporal	Left	F5-FCz	Frontocentral	Left
8	Fp2-PO8	Frontoparietal	Right	FC6-O2	Frontocentrooccipital	Right
9	FC6-FC2	Frontocentral	Right	P7-Pz	Parietal	Left
10	Fpz-FCz	Frontocetroparietal	Central	FC6-T8	Frontocentrotemporal	Right

Table S4: Source-FC features that better distinguish three resting-state periods in coma for each frequency band.

	Delta			**Theta**		
#	**Features**	**Regions**	**Hemisphere**	**Features**	**Regions**	**Hemisphere**
1	caudalanteriorcingulateL-precuneusL	Parietolimbic	Left	banksstsL-rostralmiddlefrontalR	Frontotemporal	Both
2	caudalanteriorcingulateLparsopercularisR	Frontolimbic	Both	inferiorparietalR-superiortemporalR	Parietotemporal	Right
3	caudalmiddlefrontalL-parsorbitalisR	Frontal	Both	medialorbitofrontalR-rostralanteriorcingulateR	Frontolimbic	Right
4	medialorbitofrontalR-transversetemporalR	Frontotemporal	Right	frontalpoleR-superiorfrontalR	Frontal	Right
5	caudalanteriorcingulateR-superiorparietalL	Parietolimbic	Both	precuneusR-superiortemporalR	Parietotemporal	Right
6	insulaL-superiorfrontalR	Frontotemporal	Both	insulaR-parsopercularisL	Frontotemporal	Both
7	fusiformL-parahippocampalR	Temporal	Both	paracentralL-precuneusL	Centroparietal	Left
8	superiorfrontalR-superiorparietal R	Frontoparietal	Right	isthmuscingulateR-supramarginalR	Parietolimbic	Right
9	cuneusL-parsorbitalisR	Frontoccipital	Both	precentralL-transversetemporalR	Centrotemporal	Both
10	postcentralL-temporalpoleR	Centrotemporal	Both	fusiformR-medialorbitofrontalL	Frontotemporal	Both

	Alpha			**Beta**		
#	**Features**	**Regions**	**Hemisphere**	**Features**	**Regions**	**Hemisphere**
1	superiorparietalR-transversetemporalL	Parietotemporal	Both	superiorparietalR-transversetemporalL	Parietotemporal	Both
2	rostralanteriorcingulateL-superiortemporalR	Temporolimbic	Both	caudalanteriorcingulateR-paracentralL	Centrolimbic	Both
3	medialorbitofrontalR-postcentralR	Frontocentral	Right	paracentralL-parsorbitalisL	Frontocentral	Left
4	caudalmiddlefrontalL-middletemporalL	Frontotemporal	Left	caudalmiddlefrontalL-lingualR	Frontooccipital	Both
5	caudalanteriorcingulateR-caudalmiddlefrontalL	Frontolimbic	Both	superiortemporalL-supramarginalR	Temporal	Both
6	rostralanteriorcingulateL-superiorfrontalR	Frontolimbic	Both	parahippocampalR-temporalpoleR	Temporal	Right
7	banksstsR-insulaR	Temporal	Right	lateralorbitofrontalL-postcentralL	Frontocentral	Left
8	banksstsR-transversetemporalL	Temporal	Both	insulaL-medialorbitofrontalL	Frontotemporal	Left
9	caudalmiddlefrontalL-inferiortemporalL	Frontotemporal	Left	lingualL-precuneusL	Parietoccipital	Left
10	insulaL-superiorparietalR	Parietotemporal	Both	lingualL-middletemporalR	Parietotemporal	Both

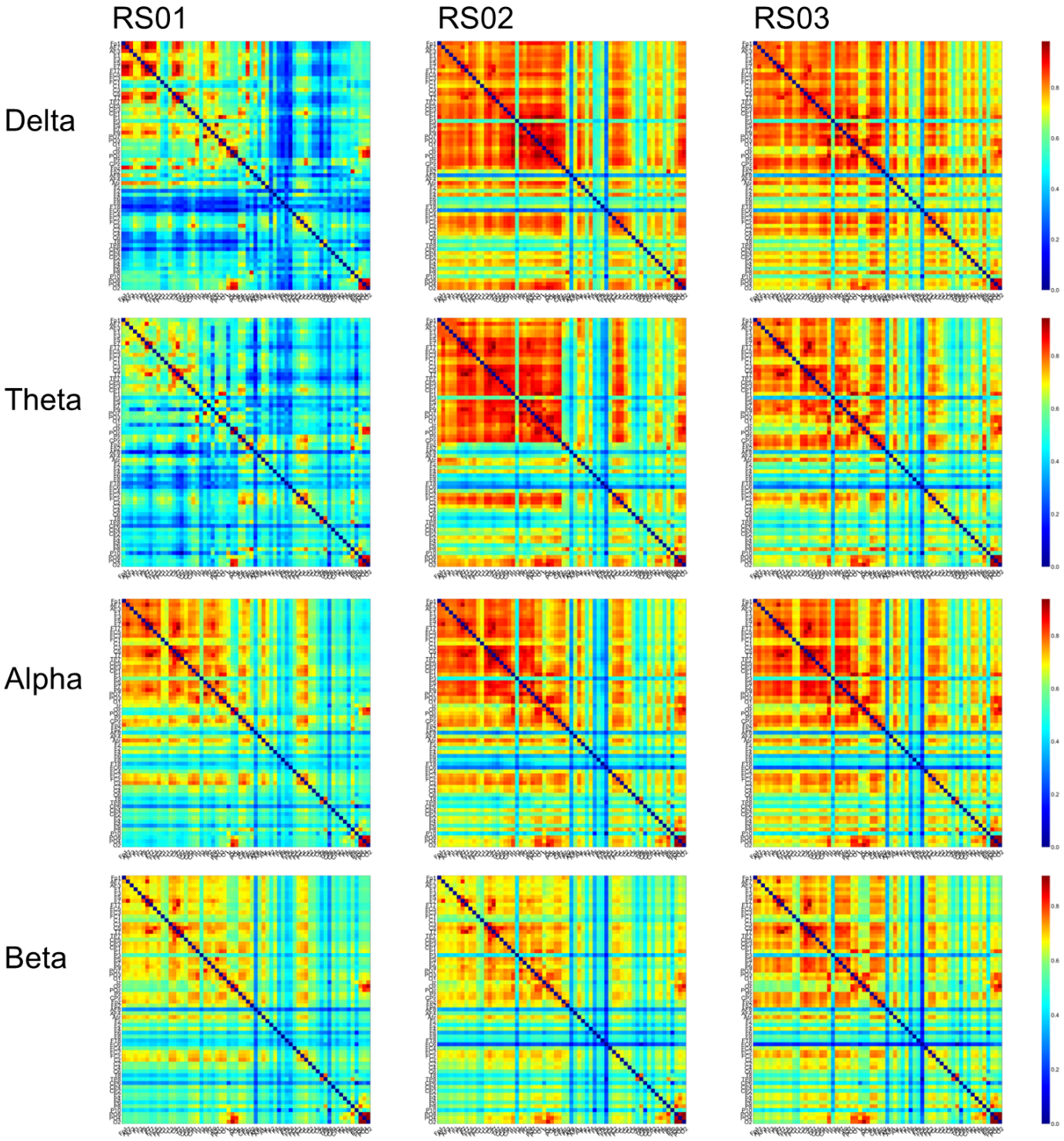

Figure S2: Sensor-level FC matrices across RS periods in the coma patient for each frequency band.

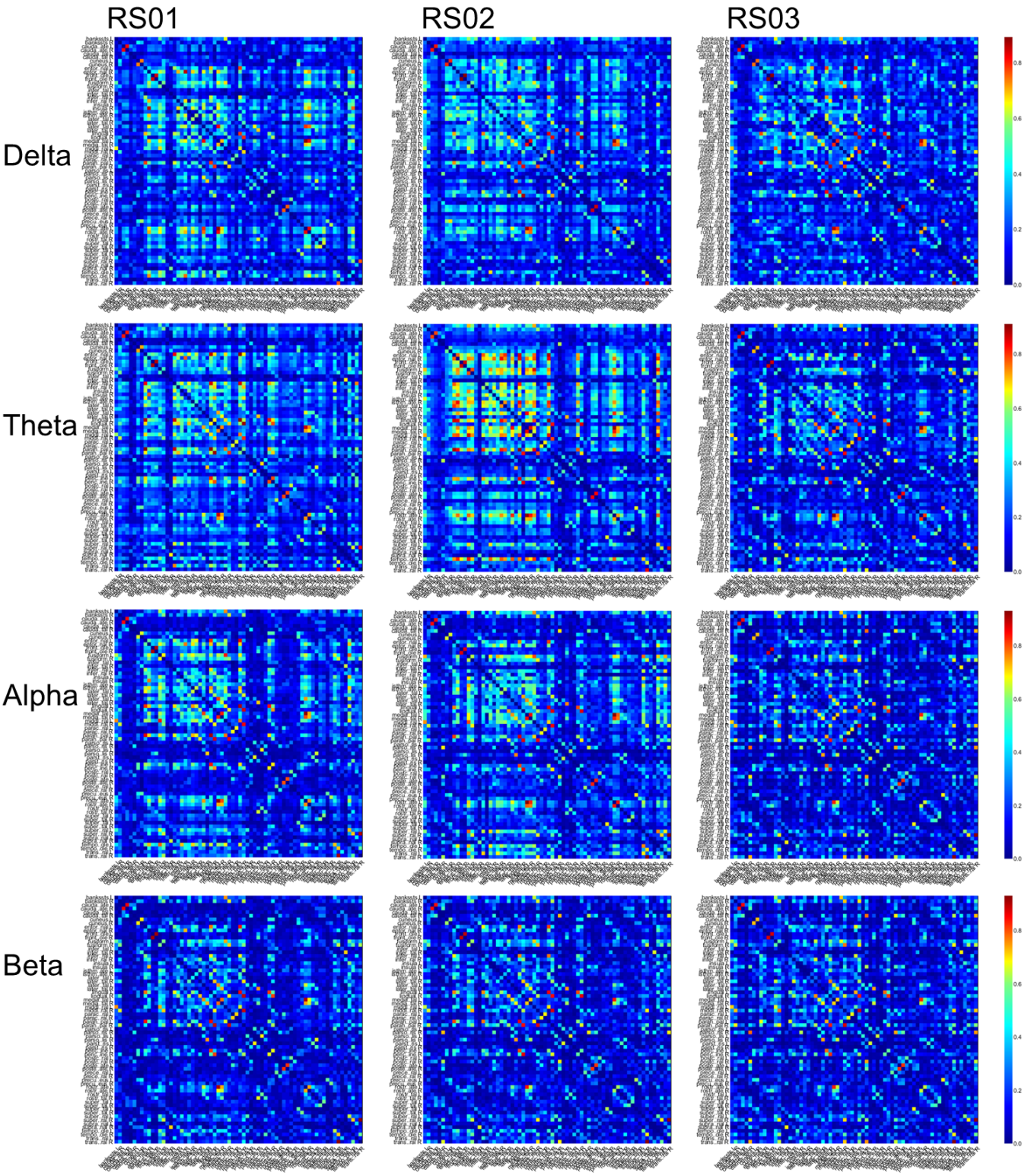

Figure S3: Source-level FC matrices across RS periods in the coma patient for each frequency band.